

**Integrated Experimental and Computational  
Analysis of Intercellular Communication with  
Application to Endometriosis**

by

Abby Shuman Hill

B.S., Georgia Institute of Technology (2011)

Submitted to the Department of Biological Engineering  
in partial fulfillment of the requirements for the degree of

Doctor of Philosophy

at the

MASSACHUSETTS INSTITUTE OF TECHNOLOGY

June 2018

© Massachusetts Institute of Technology 2018. All rights reserved.

**Signature redacted**

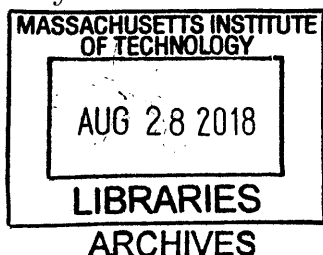
Author .....  
Department of Biological Engineering  
April 19, 2018

**Signature redacted**

Certified by .....  
Douglas A. Lauffenburger  
Ford Professor of Bioengineering  
Thesis Supervisor

**Signature redacted**

Accepted by .....  
Forest M. White  
Chair, Graduate Program Committee





# Integrated Experimental and Computational Analysis of Intercellular Communication with Application to Endometriosis

by

Abby Shuman Hill

Submitted to the Department of Biological Engineering  
on April 19, 2018, in partial fulfillment of the  
requirements for the degree of  
Doctor of Philosophy

## Abstract

Cell-cell communication is critically important to the function of the immune system, allowing a systems-level determination of the appropriate type of immune response to a perturbation. The immune system has at its disposal multiple types of responses, some beneficial and others harmful, all of which require coordination among immune cells and between the immune system and non-immune tissue cells.

In this thesis, we have explored the use of multiple experimental and computational methods to understand how intercellular communication shapes the immune response in health and disease. Applications of this work are primarily focused on endometriosis, a disease characterized by the presence of endometrial glands and stroma located outside of the uterus. Disease initiation (cell survival) and progression (including neovascularization and neurogenesis) are thought to depend on interactions with the immune system, particularly macrophages. We have investigated these interactions on several levels, using both clinical samples and 3D *in vitro* culture models. The model systems used here include endometrial stromal and epithelial cells as well as peripheral blood monocytes with which to study dynamic processes within either the eutopic endometrium or the endometriotic lesion environment.

Thesis Supervisor: Douglas A. Lauffenburger  
Title: Ford Professor of Bioengineering



# Acknowledgments

This work would not have been possible without contributions from many labmates and collaborators.

First and foremost, I would like to thank Doug Lauffenburger for scientific guidance and support throughout my time at MIT. My committee chair, Linda Griffith, has been a regular source of new ideas and contributed substantially to the overall direction of this thesis. Chris Love and Kevin Osteen both also contributed valuable scientific insights in the areas of immunology and endometriosis, respectively.

I would particularly like to thank Christi Cook, Sarah Schrier, Michael Beste, Emily Prentice, Johanna Frey Renggli, Julia Papps, Deborah Plana, Linda Stockdale, Hilde Jorgensen, and Keith Isaacson, all of whom have been close collaborators on the work shown here. Our lab manager, Hsinhwa Lee, was behind every successful experiment, as well as a source of encouragement throughout my time in the lab.

Early on in my time at MIT, I was fortunate to work with several experienced lab members who helped me get oriented in the lab and at MIT, including Melody Morris, Kelly Arnold, and Neda Bagheri.

Throughout my time in graduate school, it was often my office mates who made me excited to come into work in the morning: Samantha Dale Strasser, Marianna Sofman, Sepideh Dolatshahi, Alina Starchenko, Elizabeth Proctor, Christi Cook, Julia Papps, Mike Shockley, Martina DeGeus, Shannon Hughes, Emily Prentice, Michael Beste, Joel Wagner, and Brian Joughin.

I was fortunate to have many colleagues in the Lauffenburger and Griffith labs to have regular interesting and productive scientific discussions with, including Shannon Hughes, Brian Joughin, Alex Brown, Marianna Sofman, Allison Claas, Manu Kumar, and all of the Lauffenburger Lab Data Meeting group. Sepideh Dolatshahi and Annelien Zweemer were particularly helpful with project organization and writing. I also had the privilege of working with several talented undergraduate students: Deborah Plana, Sarah Bening, Paige Omura, and Chenuka Ratwatte.

I would like to thank the Koch Institute Swanson Biotechnology Center for tech-

nical support, specifically Eliza Vasile from Microscopy, Kathleen Cormier from Histology, Glenn Paradis from Flow Cytometry, and Charlie Whittaker and Stephen Goldman from Bioinformatics and Computing.

Thank you to Melody Morris and many collaborators at Novartis for the opportunity to gain industry experience and expand my computational skill set through my internship there in 2016.

Prior to my time at MIT, I was introduced to research by excellent undergraduate research mentors at Georgia Tech, Melissa Kemp and Catherine Rivet. If it had not been for the positive experiences I had working in Melissa's lab I would have never embarked on this journey.

My classmates were the first group of friends I had in Boston and were helpful with everything from problem sets to research dilemmas to making sure I ate lunch away from my desk on occasion. I was fortunate to live with roommates who also provided interesting scientific discussion, some of whom even became scientific collaborators: Sarah Schrier Hesse, Caroline Chopko Ahrens, Theresa Gipson Wasylenko, and Lily Xu. I would also like to thank friends outside of the lab, including Jackie Ohmura, Rachel Pei, and the fellow outdoorsy people I've met through the MIT Outing Club and all my paddling friends for encouraging me to get off campus and enjoy the many opportunities Boston and the greater New England area have to offer. Thanks to Chris Hopkins for ensuring that I was making steady progress on my writing over the past few months. Finally, I would like to thank my parents for their support and encouragement throughout my life and education.

This doctoral thesis has been examined by a Committee of the  
Department of Biological Engineering as follows:

Douglas A. Lauffenburger .....  
Thesis Supervisor  
Professor of Biological Engineering  
Massachusetts Institute of Technology

Linda G. Griffith .....  
Chair, Thesis Committee  
Professor of Biological Engineering  
Massachusetts Institute of Technology

J. Christopher Love .....  
Member, Thesis Committee  
Associate Professor of Chemical Engineering  
Massachusetts Institute of Technology

Kevin G. Osteen .....  
Member, Thesis Committee  
Professor of Obstetrics and Gynecology  
Vanderbilt University



# Contents

<b>1</b>	<b>Introduction</b>	<b>21</b>
1.1	Role of the immune system in diseases of chronic inflammation . . . .	21
1.2	Immune involvement in endometriosis . . . . .	22
1.3	Previous Efforts to Model Cell-Cell Communication . . . . .	24
1.3.1	Experimental Strategies . . . . .	24
1.3.2	Computational Strategies . . . . .	25
1.4	Thesis Objectives . . . . .	27
<b>2</b>	<b>A simplified in vitro system to identify effects of cell-cell communication on cytokine secretion</b>	<b>31</b>
2.1	Acknowledgments . . . . .	31
2.2	Introduction . . . . .	31
2.3	Methods . . . . .	32
2.3.1	Isolation of Monocytes and CD4+ T cells . . . . .	32
2.3.2	Experimental setup . . . . .	33
2.3.3	Viability measurements . . . . .	34
2.3.4	Cytokine measurements . . . . .	34
2.3.5	Self-organizing maps . . . . .	35
2.4	Results . . . . .	35
2.4.1	Cell isolation and viability . . . . .	35
2.4.2	Single cell-type behavior . . . . .	38
2.4.3	Identification of nonlinearities in monocyte-CD4+ T cell cytokine secretion . . . . .	40

2.4.4	Classification of cytokine behavior using self organizing maps . . . . .	41
2.5	Discussion and conclusions . . . . .	42
2.5.1	Follow-up work . . . . .	44
<b>3</b>	<b>Alteration of cytokine profiles in peritoneal fluid and endometrial biopsies from women with endometriosis</b>	<b>45</b>
3.1	Acknowledgments . . . . .	45
3.2	Introduction . . . . .	46
3.3	Materials and Methods . . . . .	47
3.3.1	Sample Collection . . . . .	47
3.3.2	Endometrial biopsy processing . . . . .	48
3.3.3	Measurement of cytokines and proteases . . . . .	48
3.3.4	Network Analysis . . . . .	49
3.4	Results . . . . .	50
3.4.1	Histology of previously frozen endometrial biopsies . . . . .	50
3.4.2	Development of a protocol for cytokine measurements in endometrial biopsies . . . . .	50
3.4.3	Cytokines in endometrial biopsies of infertile women with and without endometriosis . . . . .	52
3.4.4	Cytokines in peritoneal fluid of infertile women with and without endometriosis . . . . .	53
3.4.5	Comparison of endometrial biopsy and peritoneal fluid cytokines	54
3.4.6	Comparison of peritoneal fluid cytokines across patient cohorts	56
3.4.7	Network analysis of cytokines and proteases in peritoneal fluid samples . . . . .	57
3.5	Discussion and Conclusions . . . . .	61
3.5.1	Use of endometrial biopsies . . . . .	61
3.5.2	Peritoneal fluid cytokines across cohorts . . . . .	62
3.5.3	Network analysis . . . . .	62
3.5.4	Future work: <i>In vitro</i> models for time-dependent studies . . . . .	63

<b>4</b>	<b>Benchmarking of network modeling methods</b>	<b>65</b>
4.1	Acknowledgments . . . . .	65
4.2	Introduction . . . . .	65
4.3	Methods . . . . .	66
4.3.1	Network algorithms . . . . .	66
4.3.2	Data sets . . . . .	69
4.3.3	Networks . . . . .	70
4.3.4	Crossvalidation and target validation . . . . .	70
4.3.5	Empirical null distributions . . . . .	71
4.4	Results . . . . .	72
4.4.1	Overview of algorithm workflow . . . . .	72
4.4.2	Algorithms differ in ranking of start nodes . . . . .	73
4.4.3	Algorithms differ in preference for node degree . . . . .	75
4.4.4	Algorithm sensitivity and specificity found through crossvalidation . . . . .	77
4.4.5	Use of algorithms for target identification using Connectivity Map . . . . .	79
4.4.6	Comparison of network sources . . . . .	79
4.4.7	Empirical significance determined using random input lists . . . . .	83
4.4.8	Algorithm choice for different tasks . . . . .	83
4.5	Discussion and Conclusions . . . . .	85
4.5.1	Algorithm selection depends on desired outcomes. . . . .	85
4.5.2	Effects of network size and confidence on results . . . . .	86
4.5.3	Biases inherent in gold standard input lists . . . . .	86
<b>5</b>	<b>Development of a hydrogel tri-culture system to study intercellular interactions in endometrial tissue</b>	<b>89</b>
5.1	Acknowledgments . . . . .	89
5.2	Introduction . . . . .	89
5.2.1	Normal endometrial function . . . . .	89

5.2.2	Endometriosis and adenomyosis . . . . .	90
5.2.3	Immune-endometrial crosstalk . . . . .	90
5.2.4	Hydrogel models . . . . .	90
5.3	Methods . . . . .	91
5.3.1	Endometrial cell isolation . . . . .	91
5.3.2	Cell culture . . . . .	92
5.3.3	Monocyte isolation . . . . .	93
5.3.4	Gel synthesis . . . . .	93
5.3.5	Imaging . . . . .	96
5.3.6	Cytokine Measurements . . . . .	96
5.3.7	Principal Components Analysis . . . . .	97
5.3.8	Mixed effects model . . . . .	97
5.4	Results . . . . .	98
5.4.1	Monocytes survive, invade, and differentiate into macrophages in endometrial hydrogels. . . . .	98
5.4.2	Cytokine secretion is stable over time . . . . .	102
5.4.3	Apical and basal cytokine environments differ . . . . .	103
5.4.4	Cytokine profiles are cell-type dependent . . . . .	103
5.4.5	Evidence of cell-cell communication in cytokine signaling . . . . .	107
5.4.6	Cell lines vs. primary cells . . . . .	107
5.5	Discussion and Conclusions . . . . .	110
5.5.1	Importance of multicellular interactions in representing tissue biology . . . . .	110
5.5.2	Alternative methods for model selection . . . . .	110
5.5.3	Primary endometrial cells differ from cell lines in cytokine se- cretion . . . . .	110
5.5.4	Confounding effects complicate use of transwell system for study- ing cell-cell communication . . . . .	111
5.5.5	Methods for more physiological addition of monocytes . . . . .	111

<b>6</b>	<b>Development of an endometriosis/adenomyosis lesion model</b>	<b>113</b>
6.1	Introduction . . . . .	113
6.1.1	Endometriosis . . . . .	113
6.1.2	Dysregulation of signaling in endometriosis . . . . .	114
6.1.3	Prior use of <i>in vitro</i> hydrogel models . . . . .	115
6.1.4	Prior use of multicellular <i>in vitro</i> systems . . . . .	116
6.2	Methods . . . . .	116
6.2.1	Endometrial cell isolation . . . . .	116
6.2.2	Monocyte isolation . . . . .	117
6.2.3	Triculture hydrogels . . . . .	118
6.2.4	Hormonal stimulation and inhibitor treatment . . . . .	119
6.2.5	LDH assays . . . . .	120
6.2.6	Prolactin and IGFBP-1 ELISAs . . . . .	120
6.2.7	Cytokine measurements . . . . .	122
6.2.8	Network modeling . . . . .	123
6.3	Results . . . . .	123
6.3.1	Cell survival in primary triculture hydrogels . . . . .	123
6.3.2	Primary triculture hydrogels respond to hormone stimulation .	127
6.3.3	IL-1 $\beta$ -induced inflammation decreases hormone response, and hormone responsiveness is not rescued by JNK or Akt inhibitor treatment . . . . .	127
6.3.4	Cytokine communication profiles . . . . .	127
6.3.5	Network model of disease . . . . .	130
6.4	Discussion and conclusions . . . . .	130
6.4.1	Cytokine response in model system recapitulates some aspects of clinical phenotypes . . . . .	130
6.4.2	Death of primary cells in hydrogels . . . . .	133
6.4.3	Identification of additional drug targets and/or treatment pro- tocols . . . . .	133
6.4.4	Use of model system to study cell-cell communication . . . . .	134

6.4.5	Phenotype and activity of myeloid cells in lesion model . . . .	134
6.4.6	Use of lesion model for personalized medicine applications . .	135
6.4.7	Intercellular network models . . . . .	136
<b>7</b>	<b>Conclusions and Future Work</b>	<b>137</b>
7.1	Summary of findings and impact on field . . . . .	137
7.1.1	Multicellular Interactions . . . . .	137
7.1.2	<i>In Vitro</i> Model Systems . . . . .	138
7.1.3	Patient Stratification in Endometriosis . . . . .	139
7.2	Future work . . . . .	139
7.2.1	Characterization of Endometriotic Lesion Model . . . . .	139
7.2.2	Macrophage differentiation and activation in lesion model . . .	140
7.2.3	Intercellular communication in lesion model . . . . .	140
7.2.4	In-gel measurement of cytokines . . . . .	141
7.2.5	Experimental methods for multicellular interactions . . . . .	141

# List of Figures

2-1	Generation of a self-organizing map. . . . .	36
2-2	Staining for CD4 (T cells) and CD14 (monocytes) shows composition of whole PBMCs and purity of isolated CD4+ T cells and monocytes. . . . .	37
2-3	Cell viability was assessed in each fractional population and PBMCs after 24 hours at rest in assay conditions. . . . .	38
2-4	Cytokine secretion by single cell types follows expected patterns in terms of response to stimuli and cell type-specific cytokine secretion. . . . .	39
2-5	Relationships between cytokine concentrations and fractional cell compositions range from roughly linear to highly non-linear. . . . .	40
2-6	Self-organizing map separates patterns of cytokine communication responses in CD4+ T cell/monocyte cocultures. . . . .	43
3-1	Comparisons among data sets. . . . .	47
3-2	FFPE sample. . . . .	51
3-3	Frozen sample histology. . . . .	51
3-4	PCA on all cytokine concentrations normalized endometrial biopsy cytokines. Samples are color-coded by disease stage (A) or whether they achieved spontaneous pregnancy by 12 months of follow-up (B). . . . .	54
3-5	GRO $\alpha$ and SDF-1 $\alpha$ were significantly different in luteal phase but not follicular phase endometrial biopsies. . . . .	55
3-6	PCA on separated Luteal and Follicular phase normalized endometrial biopsy cytokines. . . . .	56

3-7	No cytokines were strongly correlated between endometrial biopsies and peritoneal fluid samples across the Oslo patient cohort. . . . .	57
3-8	Cytokine-protease correlation network. . . . .	58
3-9	Cytokine-protease partial correlation network. . . . .	60
4-1	Overview of use of network algorithms. . . . .	72
4-2	Algorithms differ in ability to add non-start nodes. . . . .	74
4-3	Algorithms differ in preference for high-degree nodes. . . . .	76
4-4	Algorithm performance was quantified by the fraction of data sets for which the algorithms ranked in the top 3 best algorithms by cross-validation AUC. . . . .	78
4-5	As an alternative performance metric, algorithms were ranked by the fraction of Connectivity Map datasets for which they ranked in the top 3 by target identification AUC. . . . .	80
4-6	Different network sources were compared by crossvalidation AUC using DisGeNET datasets. . . . .	82
4-7	Cumulative distributions of ranks with random input lists vary by node degree and algorithm used. . . . .	84
4-8	Algorithm selection can be guided by AUC, preference for high-degree nodes, and preference for start nodes. . . . .	85
5-1	Schematic of triculture hydrogel experimental setup. . . . .	95
5-2	Monocytes survive, migrate into the gel, and differentiate in the presence of endometrial cells. . . . .	99
5-3	Monocytes are retained in culture over time in the presence of endometrial cells. . . . .	100
5-4	Monocytes differentiate into macrophages and express CD206 in the presence of endometrial cells. . . . .	101

5-5	Apical cytokine concentrations are stable over time. Each cytokine is centered at the mean of three replicate gels of three monocyte donors each, with error bars representing standard deviations. A two-fold (or half-fold) change is indicated by dashed lines. . . . .	102
5-6	Apical and basal concentrations may be affected by diffusion, binding within the gel, dilution effects, and polarized secretion. Dotted lines represent roughly equal concentrations in apical and basal medium, corresponding to free/fast diffusion across the gel. Dashed lines represent roughly 6-fold higher concentrations in the apical medium, as would be expected from dilution effects if diffusion was negligible and production of cytokines was constant across the gel volume. . . . .	104
5-7	Monocytes are retained in culture over time in the presence of endometrial cells. . . . .	105
5-8	Ishikawa cells are the predominant factor in determining cytokine environment in tHESC/Ishikawa/Monocyte triculture hydrogels. . . . .	106
5-9	Coefficients for terms in mixed effects model indicate substantial effects of three-cell interactions. . . . .	108
5-10	Primary cells secrete more cytokines than cell lines. . . . .	109
6-1	Addition of cells to syringe gels. . . . .	119
6-2	Cell death in syringe gels over time and treatment condition. . . . .	125
6-3	Cell death is higher in gels with LAP as the photoinitiator vs. Irgacure under the same UV conditions. . . . .	126
6-4	Decidualization response in triculture gels. . . . .	128
6-5	Cytokines under decidualization and IL-1 $\beta$ -induced inflammation. . . . .	129
6-6	Cytokines for which AKT and/or JNK inhibitor(s) rescued decidualization response. . . . .	131
6-7	Network related to inflammatory cytokines and hormone response. . . . .	132



# List of Tables

3.1	Error associated with lysis preparation and normalization methods. . .	52
3.2	Subject characteristics by presence of endometriosis, shown as mean (range). . . . .	53
3.3	Cytokine significance across three cohorts. . . . .	59
3.4	Density of subsets of the full and partial correlation networks. . . . .	61
4.1	Network Algorithms . . . . .	67
4.2	Algorithm parameters . . . . .	69
4.3	Data sets used for algorithm benchmarking . . . . .	70
4.4	Input network properties . . . . .	71
6.1	Gel formulations and overall gel quality. . . . .	124
6.2	Comparison of endometrial vs. lesion hydrogel systems. . . . .	124



# Chapter 1

## Introduction

### 1.1 Role of the immune system in diseases of chronic inflammation

The human immune system is responsible for defending the body from foreign pathogens and also plays a key role in repairing tissue damage after an insult. The innate immune system recognizes molecular patterns that indicate certain types of threats, including microbial, parasitic, and viral pathogens, as well as sterile injury. While the adaptive immune response has historically been considered a second step activated upon failure of the innate immune response to clear a pathogen, it is clear now that cytokine communication between these two branches of the immune system is crucial to shaping the response of each. In addition, interactions between the immune system and non-immune tissue cells are critical to determining the appropriate immune response and repairing tissue after an insult [108].

An appropriate and successful immune response depends heavily on network-level decision making with input from both immune and non-immune cell types. Our understanding of how the network reaches a decision is limited by both the number of interactions and the logical complexity of the system. As such, it is necessary to gain an improved understanding of the flow of information throughout the intercellular communication network in order to find the source of a defect that gives rise to an

inadequate or inappropriate immune response.

When the immune system encounters a particular molecular pattern, it must decide whether the pattern is indicative of danger and, if so, what type of response would be most effective. As many patterns encountered will originate from normal, healthy tissue throughout the body, it is essential that the resulting immune response is to remain inactivated or to produce anti-inflammatory factors. For this reason, both T cells and macrophages must be able to adopt anti-inflammatory phenotypes in the absence of a foreign pathogen, or to return to homeostasis once a pathogen has been cleared. In the case of an infection, however, the appropriate response is to activate a killing program appropriate for the type of pathogen detected. If injury occurs in the absence of a pathogen, the immune system is able to respond by secreting factors that will encourage tissue growth and angiogenesis [116].

## 1.2 Immune involvement in endometriosis

Endometriosis, characterized by the growth of endometrial stroma and epithelial tissue outside of the uterus, is a primary cause of pelvic pain and infertility, affecting 6-10% of women of reproductive age [60]. According to Sampson's hypothesis, proposed in 1927, endometriotic lesions originate from shed endometrial tissue that travels in a retrograde direction through the fallopian tubes and into the peritoneal cavity during menstruation [152, 41]. However, this process of retrograde menstruation occurs in approximately 90% of women, and it is not well understood why a subset of these women develop endometriosis while others do not [17]. The quantity of refluxed tissue does not appear to be different in women who develop endometriosis, although it is likely that defects in eutopic endometrial tissue contribute to disease development [156, 15, 29].

Evidence suggests that endometriosis develops as a result of a complex set of interactions between cells of the immune system, shed endometrial tissue, and tissue cells native to the peritoneal cavity. One focus of this thesis will be the differences in how the immune cells, particularly macrophages, process and respond to cues from

this complex environment. Ectopic and eutopic endometrial stromal cells are known to secrete RANTES, a macrophage chemoattractant that may partially explain the increase in macrophages present in the peritoneal fluid of endometriosis patients [70]. Additionally, RANTES expression is increased in response to  $\text{TNF}\alpha$ , which is secreted by macrophages, suggesting a positive feedback loop between macrophages and endometrial stromal cells present in the peritoneal environment of endometriosis [71].  $\text{IL-1}\beta$  is another cytokine secreted by macrophages which also increases expression of RANTES in endometrial stromal cells, in addition to promoting angiogenesis, which is necessary for survival and invasion of endometriotic lesions [166, 70].

In a normal menstrual cycle, immune cell populations, particularly macrophages, increase just prior to menstruation. Macrophages and other leukocytes secrete proteases that contribute to ECM breakdown and inflammatory factors that induce apoptosis in stromal and epithelial cells [151]. Apoptosis has been shown to be reduced in both eutopic endometrial cells and shed endometrium from patients with endometriosis compared to tissue from controls [42, 68]. This finding provides a possible explanation for how refluxed endometrial tissue is able to survive in some women but not others. Additionally, apoptotic cells generally induce an anti-inflammatory immune response; macrophages will respond to clear dying cells and debris, but will not secrete pro-inflammatory cytokines or chemoattractants [95]. Conversely, if refluxed endometrial cells fail to undergo apoptosis, they will either establish themselves in a suitable environment, if they are able to obtain sufficient oxygen and nutrients, or undergo necrosis. Necrotic cells, often found in sites of injury, release damage-associated molecular patterns (DAMPs) such as high mobility group box 1 (HMGB1), heat shock proteins, ATP, and DNA and RNA and tend to induce a wound-healing response [163].

Bruner-Tran et al. have developed an ovariectomized  $\text{rag2}\gamma(c)$  mouse model which has convincingly shown the role of immune cells in the growth of endometriotic lesions [14]. Endometriosis was induced in mice by injection of human endometrium with or without injection of autologous human leukocytes. Mice that received human leukocytes were more likely to clear endometrial fragments and tended to develop

smaller lesions than mice that were lacking functional immune cells [14].

There is increasing evidence that macrophages are a key population of immune cells in the development and progression of endometriosis. In addition to increased prevalence in the peritoneal cavity of women with endometriosis, macrophages in endometriosis patients do express markers associated with alternative macrophage activation, and alternatively activated macrophages increase lesion growth in mice [4]. This wound healing phenotype is necessary for angiogenesis in endometriotic lesions [22]. Previous work from our lab has used unsupervised clustering to classify subjects based on peritoneal fluid cytokines [9]. Many of these cytokines are secreted primarily by macrophages, providing further evidence that macrophage activation may play a key role in endometriosis. Cytokines which are known to be secreted by macrophages also appear to affect endometrial cell attachment and invasion into a mesothelial monolayer in an *in vitro* model, although studies thus far have been limited in the complexity of the cue environment to only a few cytokines [127, 82]. Non-endometriotic cells of the peritoneum have also been found to have increased mRNA expression of some cytokines and proteases, including  $TGF\beta$ , IL-6, and MMP-3, in women with endometriosis compared to controls, providing further evidence that peritoneal cells both respond to and contribute to the inflammatory environment of the peritoneal cavity [50].

## 1.3 Previous Efforts to Model Cell-Cell Communication

### 1.3.1 Experimental Strategies

A major difficulty in studying multicellular systems is isolating signals from each of the contributing cell types. One commonly employed method for determining which cell type in multicellular systems is responsible is to simply separate cell type across a transwell membrane or other divider, including microfabricated systems [159]. These types of methods allow for recovery of pure populations of each cell type as well

as exchange of soluble signaling molecules across the membrane, but also cause local accumulation of signals within each compartment, with a lower concentration reaching the other cell type(s) of interest.

An alternative method which allows for more proximal interaction among cell types involves labelling the proteins of each cell type by culturing the cells in heavy or light medium, then measuring proteins by mass spectrometry [84]. Recently, a method has been developed to allow similar labeling of proteins in cell lines continuously, so the time period over which communication can be studied is extended [165, 164]. These methods require relatively larger numbers of cells, so that sufficient protein can be obtained for the mass spectrometry [84] and as such are challenging for use with primary cells.

### 1.3.2 Computational Strategies

To better understand the immune and immune-tissue cell interaction networks, one would ideally aim both to make the network topology tractable and to assign quantitative transfer functions between nodes. Incorporating multiple cell types into the network also requires the network to include two types of nodes, or nodes and "meta-nodes" representing cytokines and cells, where cytokines are secreted by specific cell types and then act to affect specific signaling pathways within specific cell types. Previous efforts to model immune cell interaction networks have been very difficult to interpret because of the complexity of the network [157, 54]. In order to make the network more interpretable, we must first identify the most important cells and cytokines (nodes) to include in the network.

Enrichment score-based methods, such as gene set enrichment analysis and the Connectivity Map approach allow specific functions, pathways, cell types, or molecules to be identified as important distinctions between two populations [103, 161]. Enrichment scores may also be used with measurements that are relative, rather than quantitative, since they depend only on ranks of analytes measured, which may make this approach particularly useful for cytokines that have wide concentration ranges, possibly outside of the range of a standard curve but still within the detection limits of

an assay such as Luminex. Enrichment scores have previously been used successfully by Bolen et al. to identify PBMC subsets based on gene expression data using the Immune Response in Silico (IRIS) database [10, 2]. In addition, Beste et al. used a similar approach to infer which immune populations were active in the peritoneal fluid of endometriosis subjects, with the major modification of comparing gene expression databases to secreted cytokine protein levels rather than gene expression levels [9]. The use of enrichment scores thus provides a method to identify cell types of interest to be included as nodes, in addition to the cytokines identified directly from Luminex results.

Previously, deconvolution has also been used to identify subsets of immune cells that are active in a mixed population. An early example was the application of expression deconvolution first to identify cell populations present in a mixture of immune cell lines and then to discover activated cell populations present in different proportions in systemic lupus erythematosus [1]. An extension of this method which is of particular interest is the comparison by Qiao et al. of algorithms that include (1) reference populations only, (2) reference populations plus additional unknown profiles, and (3) reference profiles adjusted to account for environmental conditions [141]. Deconvolution-based methods could therefore provide several alternatives to enrichment scores for identifying activated cell populations.

Principal components analysis (PCA) has been used extensively in the past to reduce the dimensionality of data collected on complex cell phenotypes in an unsupervised manner. Partial least squares discriminant analysis (PLSDA) is an alternative method frequently used to distinguish between classes of samples, for example, diseased vs. control, and identify factors most important for differentiating between the classes [81, 106]. Both PCA and PLSDA are useful for prediction and classification tasks, but are not able to infer any information about network structure.

Several groups have previously attempted to use computational strategies to infer information about cell-cell communication or multi-cell systems from ligand-receptor pairs [146, 7]. By combining receptor-ligand interactions with gene expression data, cell type-specific interactions can be inferred [146]. Combined with intracellular sig-

naling prior knowledge, cells could be defined as "meta-nodes" containing their respective intracellular signals, with "meta-edges" representing cytokines or other soluble signals involved in receptor-ligand interactions among the cell types of interest.

## 1.4 Thesis Objectives

Previous work has shown that endometriosis is an extremely common cause of pelvic pain and infertility affecting up to 10% of women. While the disease is defined by endometrial glands and stroma located outside of the uterus, it is additionally characterized by an inflammatory environment conditioned by immune cells, including macrophages. Interactions among these cell types are key to the initiation and progression of the disease, yet this remains an understudied area. In this thesis, I have aimed to apply computational methodologies to understand intercellular communication in physiologically relevant *in vitro* systems, with a focus on inflammatory signaling in endometriosis.

I began with a simplified *in vitro* system of easily obtainable primary cells that could be cultured in suspension, CD4+ T cells and monocytes, to investigate interactions between the innate and adaptive immune system and characterize cytokine behavior using self-organizing maps (Chapter 2, published in [154]).

I simultaneously began a project investigating cytokine and protease concentrations in clinical samples (peritoneal fluid and lysed endometrial biopsies) from two patient cohorts, Boston and Oslo (Chapter 3; partially published in [85]). This study was closest to the clinic, but, due to the nature of the samples, it did not allow for the development of a robust system for perturbing the cells and obtaining time-dependent measurements. The clinical studies thus motivated the further development of an *in vitro* system that could be manipulated over time.

To gain more computational expertise, I did a 6-month internship at Novartis, working on benchmarking various network modelling methods (Chapter 4). While these methods were developed largely for gene expression data, we further tested their use with a variety of other data types (functional genomics screens, KEGG and

Reactome pathways, genetic association data, and gene expression from the Connectivity Map[102]) as well as multiple network sources. I independently extended these methods in some preliminary tests using multi-cell networks as would apply to my remaining thesis work.

I then proceeded to a more physiological and dynamic 3D model system representing eutopic endometrium, with which we performed preliminary investigations of interactions between monocytes and endometrial cells (Chapter 5). We found that monocytes differentiate into macrophages in the presence of endometrial cells, but fail to adhere to the gel in the absence of other cell types. We additionally characterized cytokine secretion of each of the three cell types alone and in combination, applying methods from Chapter 2 to the same disease area as Chapter 3 (partially published in [34]).

Finally, I have combined aspects from each of the previous chapters to develop a 3D culture model of an endometriotic lesion. By encapsulating primary endometrial stromal and epithelial cells and monocytes into a functionalized PEG hydrogel and stimulating with IL-1b, we were able to impair hormone responsiveness of cells in a way that mimics endometriosis. Using network modeling methods to incorporate prior knowledge of intracellular signaling, we then aimed to predict potential drug targets that may reduce inflammation and restore hormone responsiveness in this disease-like state (Chapter 6). In the future, this system could be customized to include all three cell types from an individual patient, to test responsiveness to a panel of drugs in a personalized lesion model.

The overall impact of this work has two aspects: experimental methods and data analysis. The development of a synthetic hydrogel lesion model that allows for the use of primary cells should advance understanding of endometriosis pathogenesis and treatment. Additionally, the application of existing computational methods (self-organizing maps, network models) to multi-cell systems will expand our ability to understand the function of complex tissues. While this work has focused on endometriosis, methods applied here could also be used to further understand other diseases of chronic inflammation in which immune and non-immune tissue cells inter-

act, such as cancer or autoimmune disease.



# Chapter 2

## A simplified in vitro system to identify effects of cell-cell communication on cytokine secretion

### 2.1 Acknowledgments

Work in this chapter was conceived of and performed in collaboration with Sarah Schrier Hesse. Follow-up work described in the Discussion was done by Sarah Schrier Hesse and Deborah Plana. This work has been published in [154].

### 2.2 Introduction

The innate immune system, the older of the two arms of the immune system, is shared across animal species. More recent in evolutionary terms, the adaptive immune system allows for more precise response to specific pathogens. Communication between these two branches occurs by both direct cell-cell contacts and through soluble factors and is critical for an appropriate immune response. Cytokine signaling, a major mode of soluble factor communication, allows for coordination between these two branches as well as among cells of different or the same type within each branch.

Cytokine profiles have been studied in human serum, plasma, and other fluids in

many disease states, including specifically immune disorders, such as arthritis [183, 69], lupus [96], and ulcerative colitis [36], as well as diseases of other systems that also involve chronic inflammatory processes, such as cancer [181, 90], cardiovascular disease [122, 137], and endometriosis [9]. Since the introduction of TNF $\alpha$  antibody infliximab (Remicade) in the 1990's for the treatment of colitis and arthritis [45], many drugs have been developed for the treatment of chronic inflammatory conditions which target either cytokines themselves (e.g. ustekinumab for psoriasis and Crohn's disease [147, 6], secukinumab for psoriasis [73], mepolizumab for asthma [184], and ixekizumab for psoriasis [118]) or other proteins such as cytokine receptors that are critical to cytokine signaling (e.g. benralizumab for asthma [128] and sarilumab for rheumatoid arthritis [58]).

Peripheral blood provides easily accessible cells from both branches of the immune system. We have elected here to use monocytes as a representative innate immune cell and CD4+ T cells as a representative adaptive immune cell, as both cells are populous in the peripheral blood (roughly 10% of peripheral blood mononuclear cells) and secrete numerous cytokines involved in communication between the two cell types.

## 2.3 Methods

### 2.3.1 Isolation of Monocytes and CD4+ T cells

Freshly collected peripheral blood was purchased (Research Blood Components, Boston, MA). Peripheral blood mononuclear cells were isolated using Lymphoprep (StemCell Technologies, Cambridge, MA, cat #07811) according to the manufacturer's instructions. Briefly, blood was diluted 1:1 in PBS 2% FBS. 30 mL diluted blood was layered slowly on top of 15 mL Lymphoprep in a 50 mL conical tube without mixing. Blood fractions were separated by centrifuging 20 minutes at room temperature and 800g with the brake off. The buffy coat layer was collected using a Pasteur pipette, then rinsed twice with PBS.

CD4+ T cells and monocytes were each isolated by negative enrichment (Stem-

Cell Technologies, Cambridge, MA, cat #19058 and #14052, respectively). PBMCs were resuspended at  $50 \times 10^6$ /mL in EasySep buffer (StemCell Technologies #20144), then incubated with either CD4+ T cell or monocyte enrichment antibody cocktails followed by incubation with magnetic particles. EasySep buffer was added up to 2.5 mL, and cells were placed in an EasySep magnet (StemCell Technologies #18000) for 2.5 minutes, then inverted so that cells that were not bound to magnetic beads (CD4+ T cells or monocytes) could be collected in a second tube. Live cells were counted using trypan blue and a hemocytometer.

Cells were thawed and stained for CD4 and CD14 to validate CD4+ T cell and monocyte enrichment. Cells were incubated in PBS 1% BSA 0.1% tween-20 (PBS-TB) for 1 hour to block, then resuspended with FITC anti-CD4 (BD Pharmingen) and PerCP-Cy5.5 anti-CD14 (BD Pharmingen) and incubated overnight at 4C. The following day cells were washed 3x in PBS-TB and analyzed using an Accuri C6 flow cytometer (Becton Dickinson). Results were analyzed in FlowJo software (FlowJo).

### 2.3.2 Experimental setup

Cells were cultured 24 hours in a 96 well U-bottom plate with cell compositions of 100,000 CD4+ T cells; 75,000 CD4+ T cells and 25,000 monocytes; 25,000 CD4+ T cells and 75,000 monocytes; or 100,000 monocytes. PMBCs were seeded at a density of 100,000 total cells per well. Mixtures of cells came from the same subject. Cells were unstimulated or stimulated with  $2.5 \mu\text{L}$ /well anti-CD3/CD28 beads (TCR; Dynabeads, Thermo-Fisher) to stimulate T cells; 20 ng/well lipopolysaccharide (LPS, Sigma), to stimulate monocytes; or 1:500 diluted PMA/ionomycin cocktail (PI; Cell Stimulation Cocktail, eBioscience), to stimulate both cell types. Conditioned medium was collected at 24 hours post stimulation, clarified by centrifugation 15 min at 15,000 RPM and immediately used in Luminex assays. Each condition was performed in technical triplicate (3 wells for each stimulation condition) and biological triplicate (3 separate human donors). Cell culture was performed in RPMI media supplemented with 10% FBS.

In addition to conditioned medium, plasma from the same subjects was collected

from one 10mL tube of blood. One 10mL vial from each subject was centrifuged for 15 minutes at 2000 g at 4°C. Plasma was collected from the supernatant and frozen at -80°C until use.

### **2.3.3 Viability measurements**

Viability was measured using cells from one subject after 24 hours of mono- or co-culture using propidium iodide (BioLegend). Cells and medium were collected after 24 hours of incubation, and wells were rinsed with PBS and rinsate collected to retrieve remaining cells from the bottom of the well. Propidium iodide was immediately added to cells at a 1:200 dilution. Cells were analyzed using an Accuri C6 flow cytometer (Becton Dickinson), and gating was performed manually.

### **2.3.4 Cytokine measurements**

Cytokines in undiluted conditioned medium and plasma were measured by Luminex (BioPlex 27-plex and 21-plex cytokine kits) immediately following each experiment, without freezing. Protocols provided by the manufacturer were adapted to allow the assay to be performed in a 384 well plate to avoid introducing batch effects. Eight-point standard curves plus blanks (medium) were included for quantification and prepared according to manufacturers instructions.

For each cytokine, 5-parameter logistic curves were fit to the standards, including the blanks using MATLAB (MathWorks) and the L5P function [23]. Curves were used to calculate concentrations for each sample replicate. Median fluorescence intensities for the samples below the lower asymptote or above the upper asymptote of the standard curve were imputed to be either the MFI of minimum asymptote or 99% of the MFI of the maximum asymptote, respectively. Lower limit of quantification was calculated for each cytokine as the lowest standard concentration that could be distinguished from (at least three standard deviations above) the media-only blank for that cytokine. One cytokine, IL-7, was excluded from further analyses because measurements for all subjects and conditions fell below the background, which was

taken to be equal to the blank plus 3 standard deviations.

### **2.3.5 Self-organizing maps**

Self-organizing maps were used to identify patterns of cytokine communication between CD4+ T cells and monocytes. Self-organizing maps allow for unsupervised clustering of data into lower-dimensional space, frequently selected to be 1- or 2-dimensions for visualization purposes.

Cytokine concentrations across different donors and stimuli were considered as a function of cell composition (100% monocytes, 75% monocytes with 25% CD4+ T cells; 25% monocytes with 75% CD4+ T cells; 100% CD4+ T cells) and were normalized to be between 0 and 1 across the 4 cell fractions. Cytokine-conditions that were zero across all 4 fractions were omitted. The SOM was generated using the neural network toolbox in MATLAB 2015b (The MathWorks, Natick, MA). The map was initialized with a 2-dimensional 4x4 square grid, resulting in 16 clusters, and the algorithm was allowed to continue for  $10^7$  iterations, with an initial neighborhood size of 4. The number of clusters ( $2^4$ ) was selected to allow for clusters of high or low values for each of the 4 cell fractions, although varying the number of clusters did not affect the overall conclusions (Fig. 2-1).

## **2.4 Results**

### **2.4.1 Cell isolation and viability**

PBMCs and isolated CD4+ T cells and monocytes were stained for CD4 (CD4+T cell-specific) and CD14 (monocyte-specific). PBMCs (excluding neutrophils) without any isolation steps were roughly 20% CD4+ T cells and 35% monocytes, compared to >90% CD4+ T cells after CD4+ T cell isolation and 70% monocytes in the isolated monocyte population.

It is unknown exactly how cell death would affect conditioned medium levels of each cytokine. Thus we wanted to ensure that cell death was comparable across

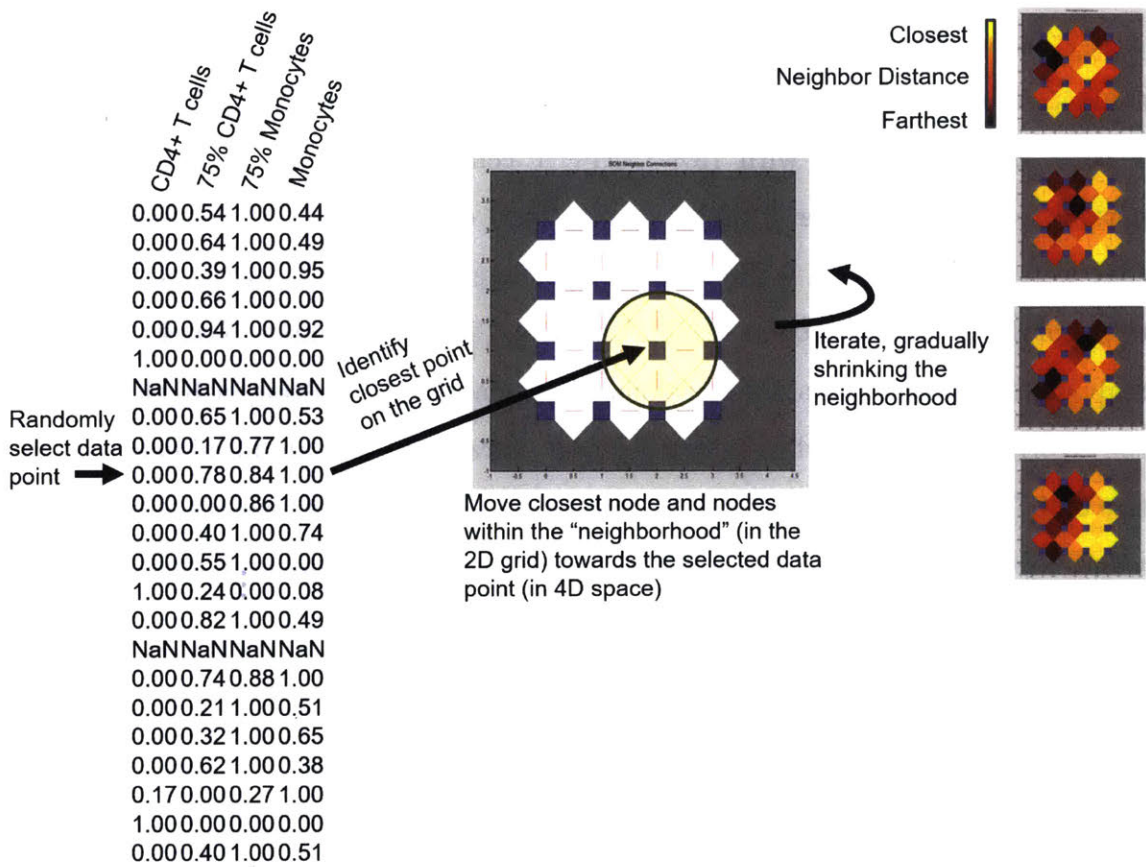
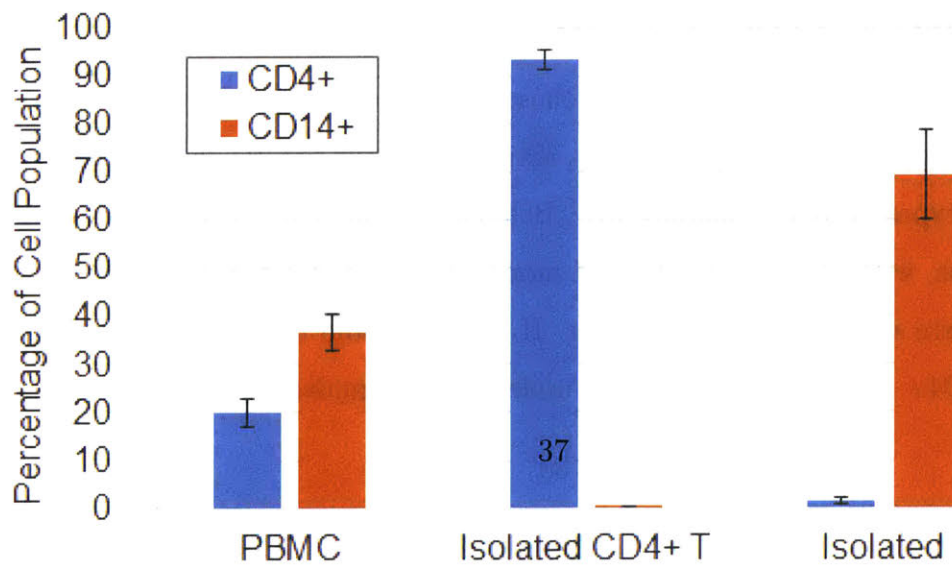
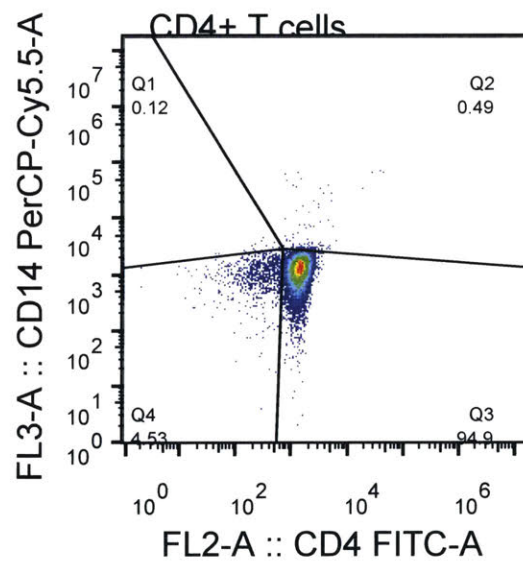
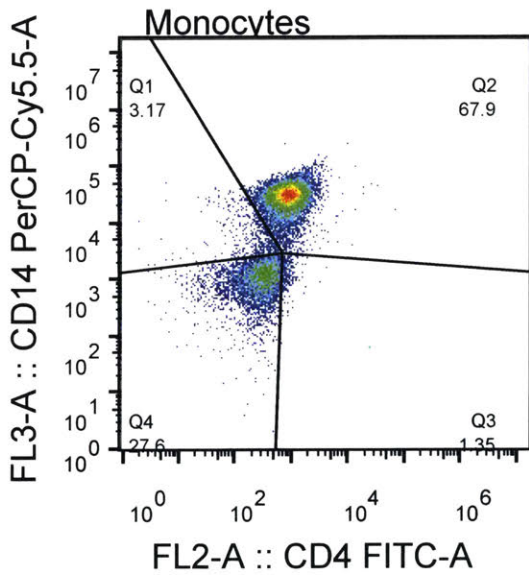
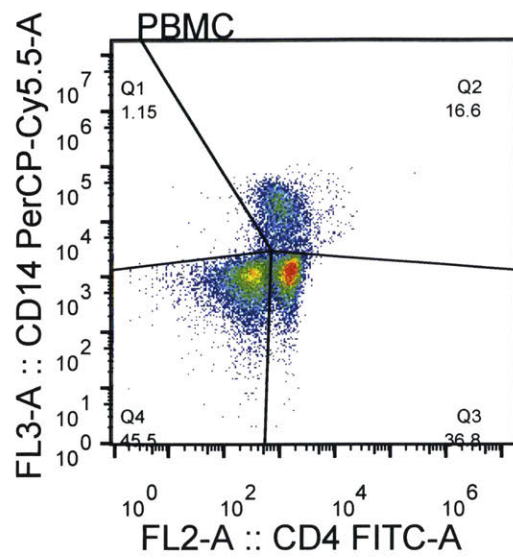
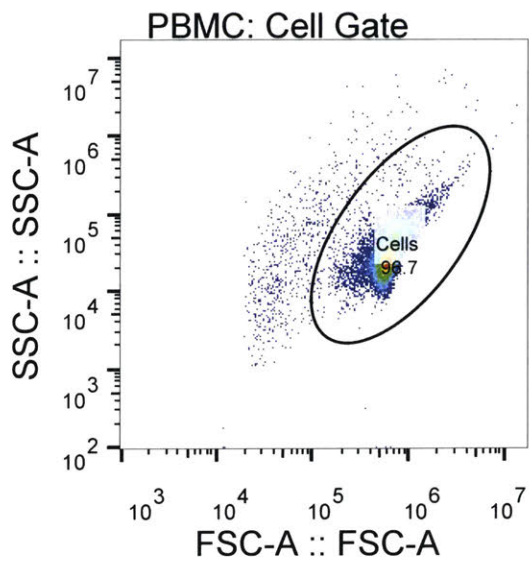


Figure 2-1: Generation of a self-organizing map.



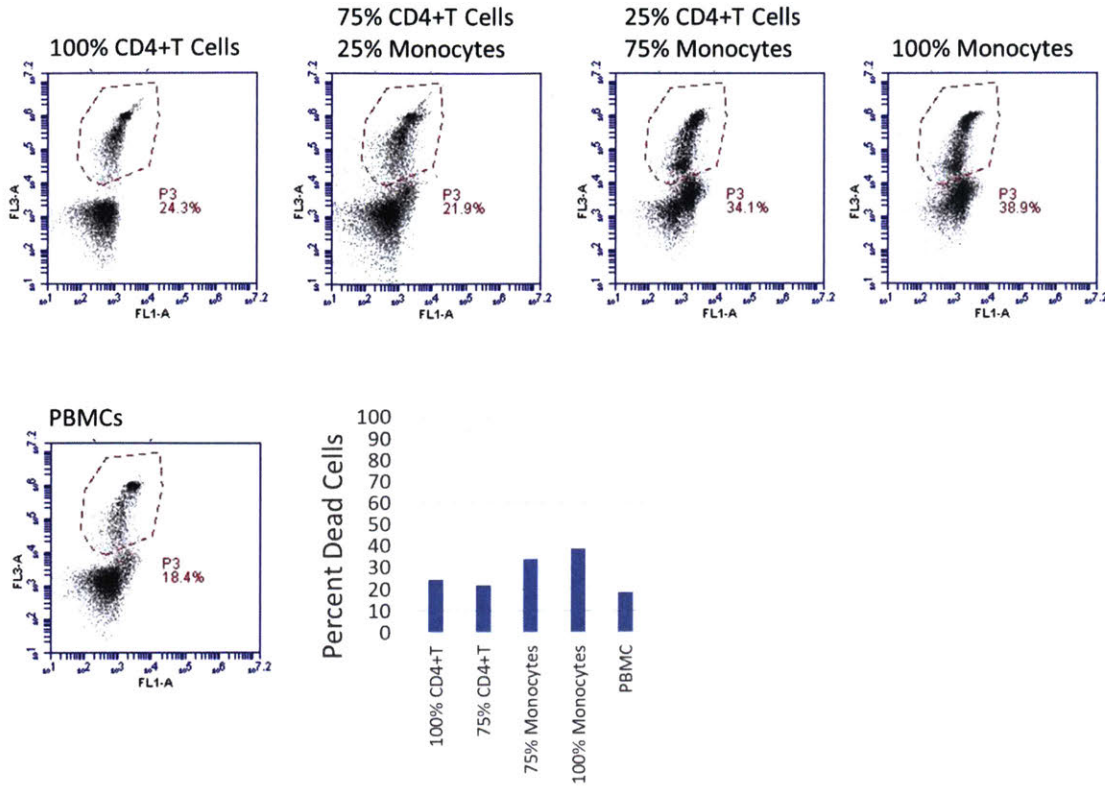


Figure 2-3: Cell viability was assessed in each fractional population and PBMCs after 24 hours at rest in assay conditions.

cell compositions. Due to sample limitations, viability staining was performed on cells from one donor only, in the resting condition. The percent of dead cells was lowest in whole PBMCs (18.4%) and highest in monocytes only (38.9%) (Fig. 2-3). Of particular importance for this study, interactions between CD4+ T cells and monocytes did not appear to increase cell death.

## 2.4.2 Single cell-type behavior

Stimulation conditions in this work were chosen to capture both cell types at rest (no stimulation), activated monocytes (LPS), activated T cells (TCR) or dual activation of both cell types (PMA + ionomycin). Behavior of the single cell types reflected these patterns, with strong activation of monocyte-secreted cytokines present when monocytes were stimulated with LPS (e.g. IL-1 $\alpha$  and  $\beta$  and IL-6) [37] and activation of known CD4+ T cell-secreted factors under TCR stimulation (e.g. IL-2 and IL-

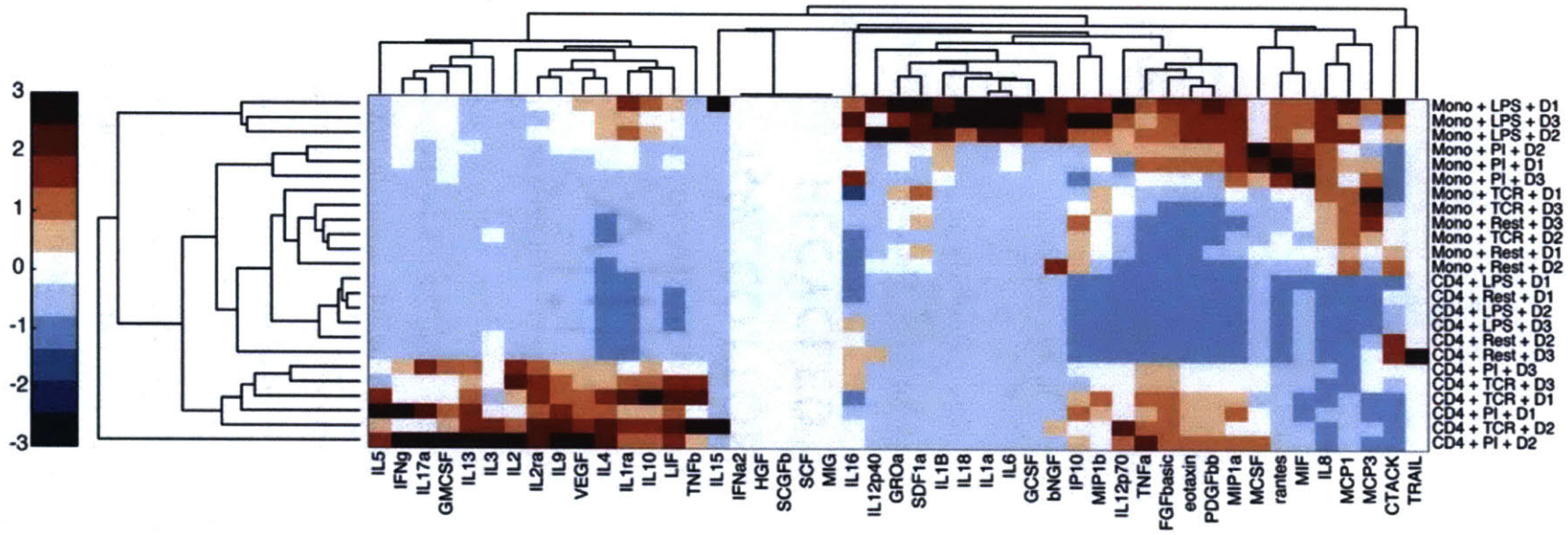


Figure 2-4: Cytokine secretion by single cell types follows expected patterns in terms of response to stimuli and cell type-specific cytokine secretion.

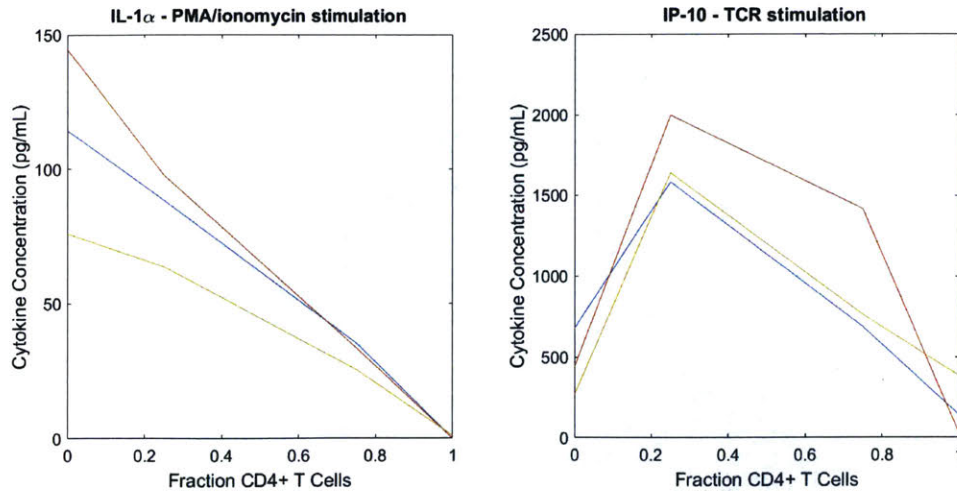


Figure 2-5: Relationships between cytokine concentrations and fractional cell compositions range from roughly linear to highly non-linear.

4). Similarly, CD4+ T cells behaved similarly under LPS stimulation as at rest, consistent with a lack of response to LPS. Monocytes had only a limited response to TCR stimulation beads, possibly due to an ability to phagocytose particles rather than the actual molecular TCR stimulus.

### 2.4.3 Identification of nonlinearities in monocyte-CD4+ T cell cytokine secretion

Some cytokines are secreted primarily by one cell type without substantial effects due to communication between the two cell types, and concentrations of such cytokines in conditioned medium were roughly proportional to the fraction of the secreting cell type. An example of this type of behavior is IL-1 $\alpha$  under PMA/ionomycin stimulation (Fig. 2-5A); IL-1 $\alpha$  within the immune system is secreted mainly by myeloid cells, and the concentration measured decreases as the fraction of monocytes decreased.

On the other hand, many cytokines exhibited highly non-linear relationships to the fractional composition of the cells. IP-10, for example, was detected at relatively low levels in either 100% monocytes or 100% CD4+ T cells but at much higher levels in cell mixtures (Fig. 2-5B). We can thus infer that IP-10 is affected in some way by interactions between the two cell types.

## 2.4.4 Classification of cytokine behavior using self organizing maps

We were interested in classifying the types of linear and, more interestingly, non-linear relationships between fractional cell composition and cytokine concentrations measured in the conditioned medium. We were interested in patterns that occur in any stimulation condition or in any individual donor, across any of the 47 cytokines detected above background, so data used consisted of a matrix of 564 cytokine-conditions by 4 fractional compositions.

Self-organizing maps were used to identify these patterns of secretion resulting from CD4+ T cell-monocyte communication (Fig. 2-6). Self-organizing maps are an unsupervised clustering technique that allows multi-dimensional data to be mapped into clusters in a lower-dimensional space, frequently in one or two dimensions to allow for visualization, where similar clusters appear close together [98, 182]. For each cytokine and stimulation condition, the three donors were generally clustered into the same or neighboring clusters, with the median (0.667) of the mean distances between assigned clusters for the three donors for a given cytokine and stimulus resulting from two donors being in one cluster and the third being in a neighboring cluster. Only four conditions had a mean donor-to-donor cluster distance of greater than 2, two of which were resting (MCP-3 and SCGF-b), indicating possible differences in baseline activation of each cell population across subjects.

The algorithm identified a natural organization of the data by clustering together cytokines secreted primarily by monocytes (Fig. 2-6, cluster 1) or by CD4+ T cells (cluster 16) as well as cytokines enhanced (cluster 4) or depleted (cluster 13) due to communication between the two cell types. As expected, 10 out of 12 conditions in cluster 1 were stimulated with LPS (blue), inducing strong monocyte activation, and all conditions in cluster 16 were stimulated with either TCR (green) or PI (red). While few cytokines were observed to decrease due to interactions between the cell types, many cytokines were increased. Of particular interest, cluster 4 included measures of IP-10, MIG, and IL-16 from all three subjects, indicating a consistently elevated

response due to interactions between the cell types. Cluster 8 also included cytokines elevated in both mixture conditions relative to individual populations, including TCR-stimulated IL-1 $\beta$  and MIP-1 $\beta$  from all three donors. In the case of IL-1 $\beta$ , TCR stimulation of CD4+ T cells induces IFN $\gamma$ , which in turn induces monocyte secretion of IL-1 $\beta$ . IL-1 $\beta$  and MIP-1 $\beta$  are also known to induce secretion of each other in multiple cell types, suggesting positive feedback regulation among cytokines in this cluster. IFN $\gamma$ , a possible effector of these and other observed communication events, appears in clusters nine and seven in the absence of T cell stimulation and clusters 12, 14, 15, and 16 under TCR or PI. IL-10, a well-studied example of an anti-inflammatory cytokine, appears in clusters associated with either monocyte or CD4+T cell secretion under stimulation of those individual cell types (LPS or TCR, respectively) but is one of the few cytokines to be decreased due to communication under resting (cluster 9) or PI (cluster 14) stimulation. It is likely that other less well-studied cytokines in these clusters, such as CTACK (CCL27), may have an inhibitory role under some conditions.

## 2.5 Discussion and conclusions

In the CD4+ T cell-monocyte co-culture experimental setup described here, we observed that secretion of most cytokines differs in co-culture from what would be expected based on a linear combination of mono-culture cytokine responses. Therapeutics targeting the function of specific populations of immune cells are currently of great clinical interest, and this work indicates that understanding how such interventions affect not only the cell type of interest but interactions with other immune cell populations is critical.

Clustering using SOM allowed us to identify key features of secretion patterns. For example, we could ascertain whether, under a given stimulation condition, a cytokine is secreted primarily by CD4+ T cells or by monocytes, and whether a cytokine is increased or decreased due to interaction between the two cell types. More cytokines were increased due to communication between cell types than decreased, as might be

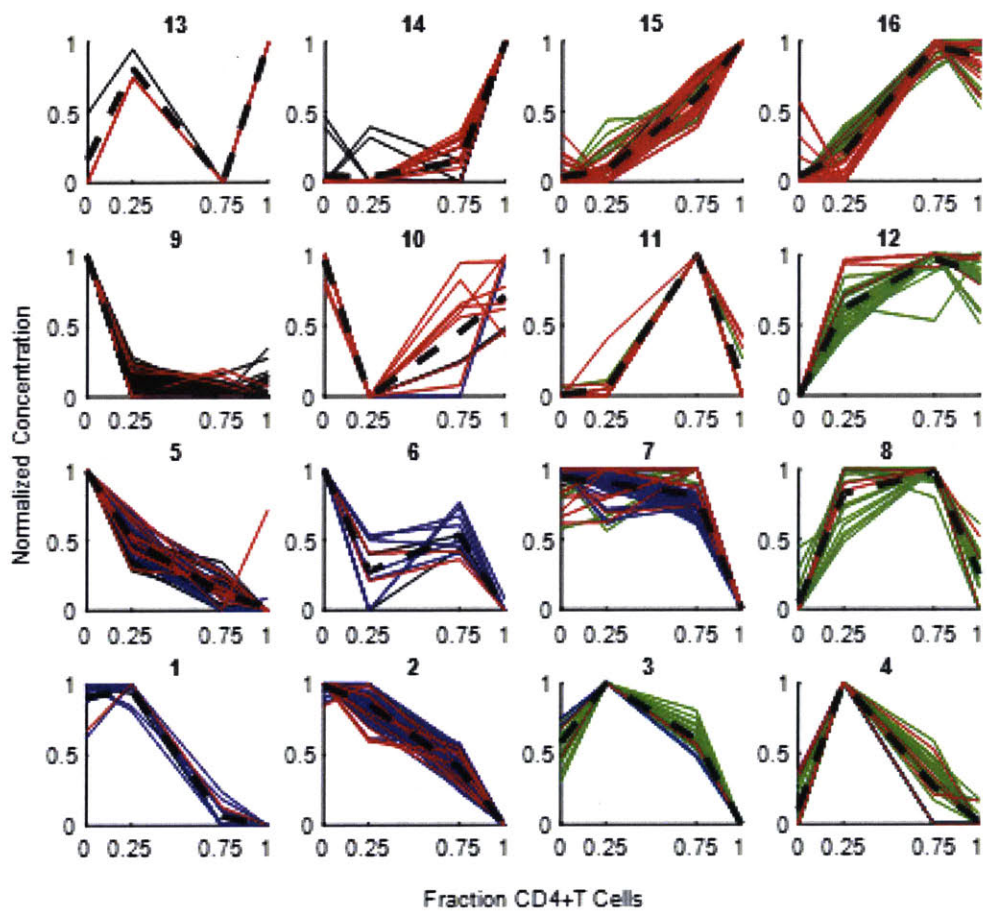


Figure 2-6: Self-organizing map separates patterns of cytokine communication responses in CD4+ T cell/monocyte cocultures.

expected given the known ability of innate immune cells to activate adaptive immune cells, and increasing evidence that adaptive immune cells also influence the innate immune response [57]. As appropriate functioning of the immune system is dependent on coordination of many branches of a complex network of cell types and proteins, understanding this interplay between cells can potentially impact many studies of disease biology. In fact, the immune system plays a role in many acute and chronic diseases, and improved understanding of the inflammatory environment conditioned by interactions between the immune and non-immune tissue cells using similar types of co-culture assays is likely to improve our understanding of many disease states.

### **2.5.1 Follow-up work**

In this chapter, we identified many examples of intercellular communication effects on cytokine signaling, but this observational design did not allow us to directly elucidate mechanisms behind the observed interaction effects. Combined with published data, however, we could use this information to hypothesize mechanisms for follow-up. As shown in Schrier et al. [154], one such example is the high level of IP-10 (IFN $\gamma$ -inducible protein) observed in 75% monocyte 25% CD4+ T cell condition under TCR stimulation, despite being low in either individual cell population. IP-10 is induced in monocytes under stimulation with IFN $\gamma$ , which is in turn induced by TCR stimulation of CD4+ T cells. Thus, the production of IP-10 is not expected in the absence of intercellular communication. It was observed that conditioned medium from TCR-stimulated (but not resting) CD4+ T cells was sufficient to induce IP-10, indicating that the effect is due to communication via soluble factors rather than cell-cell contact.

# Chapter 3

## Alteration of cytokine profiles in peritoneal fluid and endometrial biopsies from women with endometriosis

### 3.1 Acknowledgments

Data in this chapter was collected by myself, Michael Beste, Hilde Jorgensen, Amelia Bailey, Christi Cook, and Miles Miller. Work would not have been possible without the contributions of our clinical collaborators: Keith Isaacson, Stephanie Morris, Megan Loring, Stina Salazar, Marron Wong, and Valencia Miller. Some data and samples used here are from [9] and [121], and part of this work has been published in [85]. Histology samples were prepared in collaboration with Kathleen Cormier at the Koch Core Facility.

The authors would like to thank Emily Prentice and the surgical staff at Newton-Wellesley Hospital for assistance in sample collection, Paige Omura for experimental assistance, and Christi Cook, Aaron Meyer, Miles Miller, and Joel Wagner for helpful discussions. Funding was provided by the National Institute of Allergy and Infectious

Diseases (1U19AI089992), the Institute for Collaborative Biotechnologies through grant W911NF-09-0001 from the U.S. Army Research Office, the MIT Center for Gynepathology Research, and Newton-Wellesley Hospital.

## 3.2 Introduction

Endometriosis, or growth of endometrial glands and stroma outside of the uterus, is a common cause of pelvic pain and infertility affecting up to 10% of women. Current first-line therapy is hormonal medications, which may treat pain but are counter-productive for fertility and often have unpleasant side effects; definitive treatment requires hysterectomy.

The most commonly held hypothesis for the pathogenesis of the disease, proposed by Sampson in 1927, is retrograde menstruation, whereby endometrial tissue shed during menstruation is transported in a reverse direction through the fallopian tubes and deposited into the peritoneal cavity [152]. It is thought that over 90% of women have evidence of retrograde menstruation, however, and the mechanisms of disease initiation and progression are unclear. Alternative hypotheses include (1) that lesions are of Mullerian origin and (2) aberrant differentiation into endometrial-like cells *in situ* [19], and it is likely that these alternatives explain some subset of cases of endometriosis.

In the case of retrograde menstruation, immune cells and the inflammatory environment of the peritoneal cavity may play a key role in determining whether displaced tissue is cleared or able to develop into endometriotic lesions. If shed endometrial tissue was undergoing apoptosis, the tissue should release signals instructing nearby macrophages to phagocytose the cells, in which case macrophages are stimulated towards more of an anti-inflammatory phenotype. In contrast, if shed tissue is undergoing necrosis, the tissue is more likely to promote more of a wound-healing macrophage phenotype, which promotes tissue growth and angiogenesis. In the lesion microenvironment (similar to a tumor microenvironment) these alternatively activated macrophages can thus promote survival, growth, and invasion by lesions

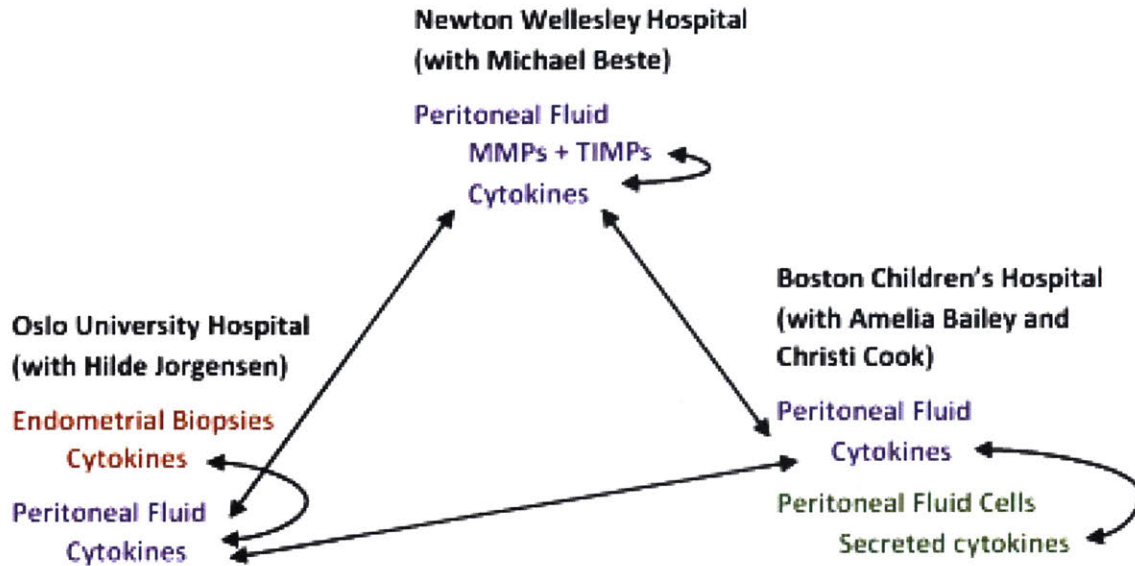


Figure 3-1: Comparisons among data sets.

[4].

Previous work from our lab and others has shown that inflammatory cues in the peritoneal fluid may be related to the presence of endometriosis or to disease severity [9, 86]. In this chapter, we investigate cytokines and proteases in peritoneal fluid and endometrial biopsies from three cohorts of patients (Fig. 3-1).

### 3.3 Materials and Methods

#### 3.3.1 Sample Collection

Peritoneal fluid samples were collected from pre-menopausal women who were undergoing surgery for benign gynecological conditions. Peritoneal fluid was aspirated at the beginning of surgery, then centrifuged 5 min at 330g to separate cells and fluid. The cells were resuspended in PBS, and the samples were transported on ice to the laboratory.

Endometrial biopsies were similarly taken from pre-menopausal women undergoing surgery for benign gynecological conditions. Biopsies were taken using a 3mm

Pipelle, with up to 3 biopsies/patient. Biopsies were expelled into cryovials and flash frozen in either a dry ice-ethanol slurry (NWH) or liquid nitrogen (Oslo University). Biopsies were then stored at  $-80^{\circ}\text{C}$  until use. Biopsies collected in Oslo were shipped to MIT on dry ice.

### **3.3.2 Endometrial biopsy processing**

Initially, endometrial biopsies were processed in several ways, and the most consistent method was selected for further analysis across all samples. Because biopsies consist of varying amounts of solid tissue, blood, and mucus, protocol tests were done with tissues either not rinsed, rinsed with PBS to remove blood, or rinsed with both PBS and dithiothreitol (DTT) to dissolve mucus prior to cell lysis. Biopsies were lysed by addition of  $250\mu\text{L}$  lysis buffer (10 mM Tris-HCl, 150 mM NaCl, 2 mM EDTA, 1% NP40 substitute, and 10% glycerol in DI water, with cOmplete mini protease inhibitor (Roche) and phosphatase inhibitor cocktail II (Boston Bioproducts)), followed by tissue disruption using a pellet pestle (Kimble Kontes), then addition of  $750\mu\text{L}$  additional lysis buffer and incubation at  $4^{\circ}\text{C}$  for 30 minutes. Lysates were clarified by centrifugation 15 minutes at  $16,100\times g$  and  $4^{\circ}\text{C}$ . Supernatant was collected and stored at  $-80^{\circ}\text{C}$  until use.

For actual data collection, biopsies were divided into three sections each, with one section lysed, one section re-frozen, and the third section used for histology. Samples for histology were prepared in two ways: formalin-fixed paraffin embedded (FFPE) or frozen in optimal cutting temperature (OCT) compound. FFPE samples were placed in a bag inside of a cassette and fixed for 6 hours at room temperature on a plate rotator.

### **3.3.3 Measurement of cytokines and proteases**

Concentrations of cytokines and proteases were measured in neat peritoneal fluid, conditioned medium, and clarified lysates using multiplexed bead-based immunoassays (human cytokine panels I and II, BioRad; human MMP and TIMP luminex panels,

R&D systems). The concentrations of 48 different cytokines, chemokines, and growth factors in the PF were measured with the BioPlex FLEXMAP 3D system (Bio-Rad Laboratories), and data were collected with xPONENT version 4.2 (Luminex Corporation). The cytokines were all included in human cytokine panels I and II from Bio-Rad. The samples were assayed in triplicate of undiluted PF samples. The mean of median fluorescence intensity (MFI) in 10 parallel aliquots of standard diluents was used to establish the background MFI. The lowest limit of detection was defined as the background +2 SD. Average MFI from three parallels of PF samples were converted to absolute concentrations above the lowest limit of detection via calibration to ninepoint standard curves using the L5P function [23] in MATLAB R2015b (The Mathworks).

### 3.3.4 Network Analysis

As both cytokine signalling and protease activity are known to play roles in endometriosis, we aimed to find relationships between these two systems. We combined cytokine MFI data from [9] and protease (concentration) MFI measurements from the same peritoneal fluid samples. For each analyte, technical replicates were averaged, and Spearman correlations were found for each other analyte in the assays. Correlations were included in a network model if Benjamini-Hochberg  $FDR < 0.025$ . Correlation networks are highly susceptible to artifacts from confounding effects [105]. To account for this and further investigate relationships between individual analytes, a partial correlation network was generated from the same data. Partial correlations are found by regressing one analyte "A" against all but one "B" of the remaining analytes, then finding the Spearman correlation of "B" with the residuals from the regression of "A" against the other analytes. Edges were included if  $p < 0.025$ , without multiple hypothesis correction.

## **3.4 Results**

### **3.4.1 Histology of previously frozen endometrial biopsies**

Only one third of each biopsy vial was used for cytokine measurements, so we aimed to use some of the remaining tissue for histology. Endometrial biopsies used for diagnostic purposes are typically formalin fixed in the operating room, then paraffin embedded; however, all endometrial biopsies from this study were previously flash-frozen in the OR in order to preserve cytokine levels. We thus attempted two methods of sample preparation, either formalin-fixed, paraffin embedded (FFPE) or frozen in optimal cutting temperature (OCT) compound. While OCT-frozen samples did not retain much glandular structure, epithelial glands and stroma were visible in the H&E-stained FFPE sample (Fig. 3-3).

### **3.4.2 Development of a protocol for cytokine measurements in endometrial biopsies**

Test biopsies were collected from Newton-Wellesley Hospital hospital and split into three cryotubes before freezing. On three separate days, one cryotube per biopsy was thawed and divided into three sections. Biopsies were processed in three ways prior to lysis: (1) without rinsing, (2) rinsing with PBS to remove blood, or (3) rinsing with both PBS and DTT to remove blood and mucus. In addition, both total protein and DNA were measured as a method of normalizing to either amount of tissue (including mucus) or number of cells. This process was repeated two additional times on different days to determine reproducibility. In general, both median coefficient of variation (CV) across the measured cytokines and mean squared error were lowest for unrinsed biopsies (Table 3.1). While rinsing was intended to remove components of the samples that would confound tissue cytokine measurement, the extra processing steps added additional sources of variability.

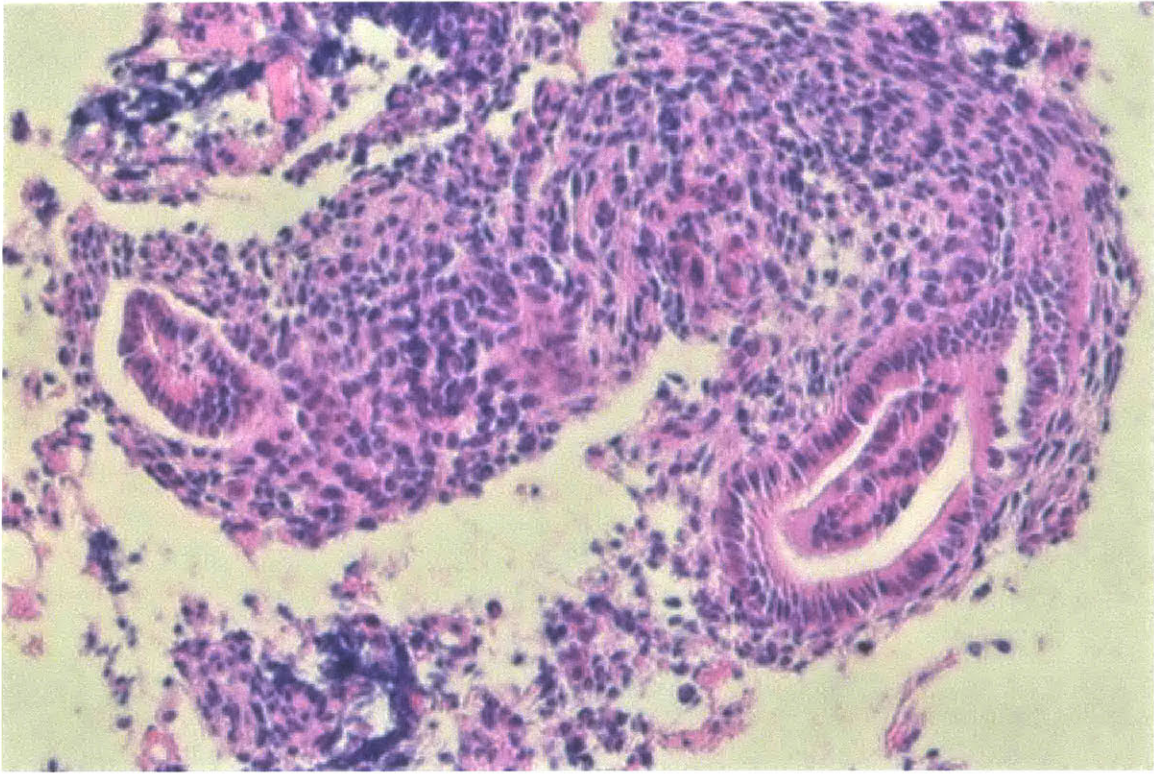


Figure 3-2: FFPE sample.

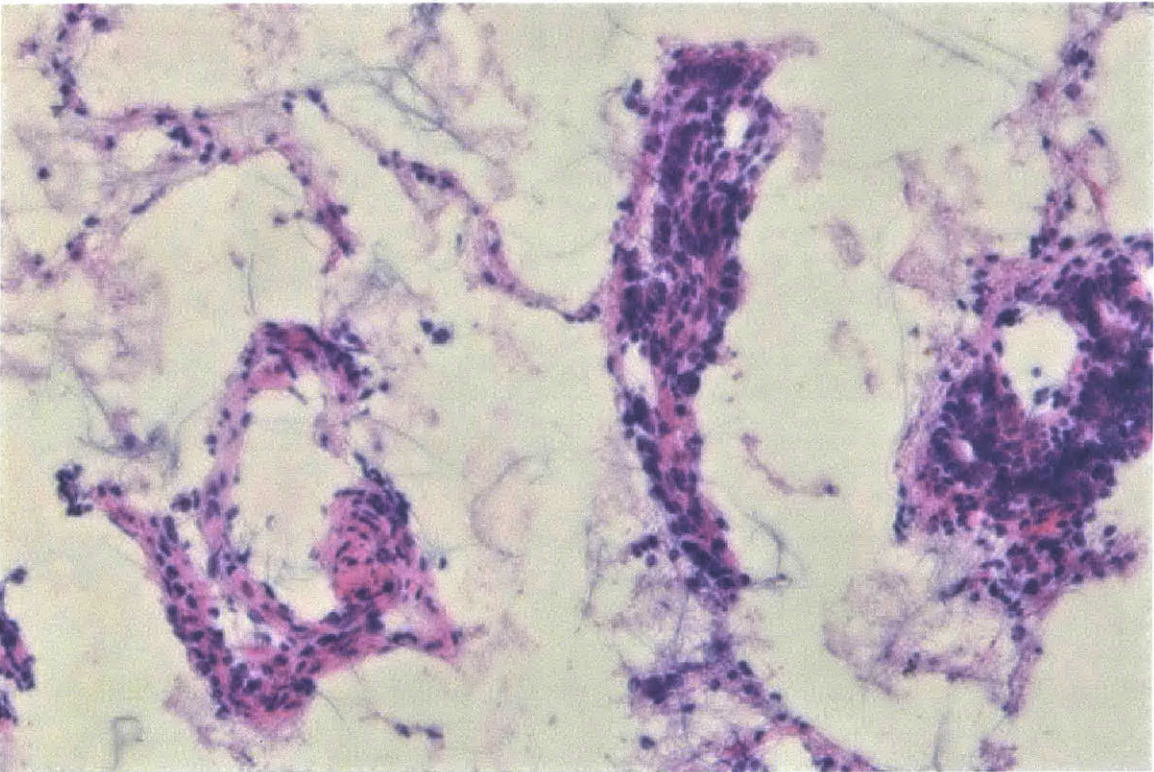


Figure 3-3: Frozen sample histology.

Cytokine concentration	Wash step	Median CV	MSE
Subject 0162	None	0.31	98365
	PBS	0.49	140102
	PBS + DTT	0.65	154076
Subject 0163	None	0.31	20115
	PBS	0.13	104671
	PBS + DTT	0.18	144091
Subject 0175	None	0.76	5527307
	PBS	0.34	2211603
	PBS + DTT	1.11	5464672
Normalized to total protein			
Subject 0162	None	0.25	425
	PBS	0.34	4259
	PBS + DTT	0.38	181421
Subject 0163	None	0.31	330
	PBS	0.52	34336
	PBS + DTT	0.28	65666
Subject 0175	None	0.77	27756
	PBS	0.19	20549
	PBS + DTT	1.05	132360
Normalized to DNA content			
Subject 0162	None	0.43	238
	PBS	0.57	2043
	PBS + DTT	0.96	28737
Subject 0163	None	0.32	56265
	PBS	0.44	54439
	PBS + DTT	1.08	4016489
Subject 0175	None	0.78	1771
	PBS	0.25	1013
	PBS + DTT	0.62	6529

Table 3.1: Error associated with lysis preparation and normalization methods.

### 3.4.3 Cytokines in endometrial biopsies of infertile women with and without endometriosis

48 cytokines were measured in the lysed endometrial biopsies from 89 subjects, 54 with endometriosis and 35 without. Patient characteristics were similar across no endometriosis, stage I-II, and stage III-IV, although the prevalence of dysmenorrhea increased with endometriosis stage (Table 3.2).

	No Endo	Stage I-II	Stage III-IV
Subjects	35	41	13
Mean Age (Years)	33.8 (27-41)	32.0 (24-39)	34.2 (30-37)
Gravidity	0.57 (0-2)	0.41 (0-2)	0.69 (0-4)
Duration of Infertility (Months)	33.3 (11-99)	29.3 (12-83)	38.2 (11-99)
Any pain	0.31	0.27	0.38
Dysmenorrhea	0.60	0.70	0.85
Dyspareunia	0.46	0.34	0.46
Biopsy total protein	9.93 (0.48-21.74)	11.87 (0-50.54)	11.67 (1.54-19.45)

Table 3.2: Subject characteristics by presence of endometriosis, shown as mean (range).

Cytokine concentrations measured from endometrial biopsies were normalized to total protein. No normalized cytokine concentrations were significantly different between patients with vs. without endometriosis when all subjects were considered, regardless of cycle phase or other patient characteristics. Principal components analysis also failed to separate subjects by either endometriosis stage or spontaneous pregnancy within 12 months of surgery (Fig. 3-4).

When patients were separated by cycle phase, GRO- $\alpha$  and SDF-1 $\alpha$  were both lower in endometriosis than control patients in endometrial biopsies taken during the luteal phase but not significantly different in the follicular phase. However, samples from endometriosis vs. control cases were not easily distinguishable based on these two cytokines alone (Fig. 3-5). Principal components analysis was thus repeated on subsets of the data from biopsies from each cycle phase; however, unsupervised analysis again failed to show any clear separation between endometriosis and control patients even in data from luteal phase only (Fig. 3-6).

### 3.4.4 Cytokines in peritoneal fluid of infertile women with and without endometriosis

The same panel of 48 cytokines was measured in peritoneal fluid samples collected from the same set of patients as the endometrial biopsies, with some small number of non-overlapping patients due to either low peritoneal fluid sample volume or lack

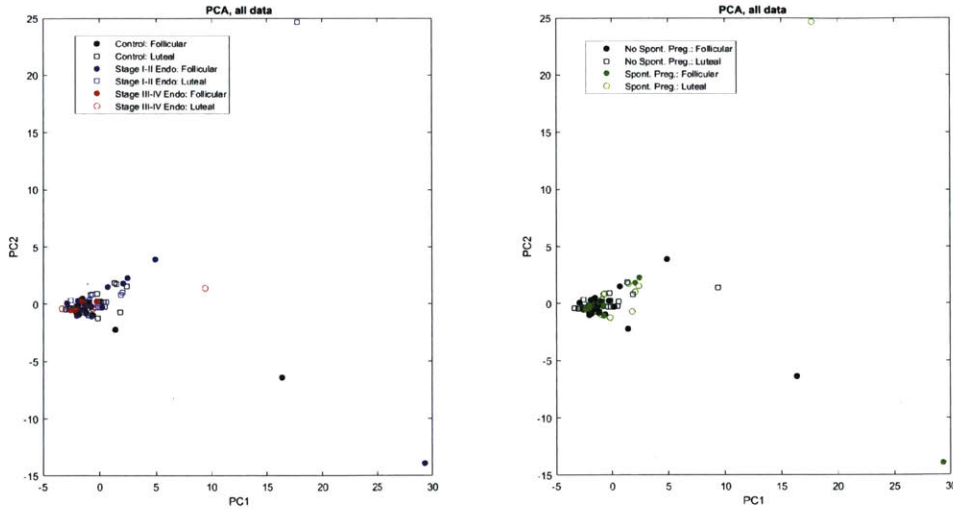


Figure 3-4: PCA on all cytokine concentrations normalized endometrial biopsy cytokines. Samples are color-coded by disease stage (A) or whether they achieved spontaneous pregnancy by 12 months of follow-up (B).

of solid tissue in biopsy samples, resulting in a total of 85 subjects with both sets of measurements. Of the 48 cytokines measured in peritoneal fluid, four cytokines (IL-8, SCGF- $\beta$ , HGF, and MCP-1) were significantly elevated in peritoneal fluid from endometriosis patients while one (IL-13) was lower. Within only luteal phase samples, IL-8, HGF, and SCGF- $\beta$  were significantly higher; in the follicular phase, IL-13 was significantly lower in endometriosis cases while IL-1RA, IP-10, and SCGF- $\beta$  were all elevated.

### 3.4.5 Comparison of endometrial biopsy and peritoneal fluid cytokines

Within the Oslo cohort of subjects, 85 subjects had sufficient peritoneal fluid volume and solid endometrial biopsy tissue for both sets of measurements to be made. Significant differences between endometriosis and control subjects either overall or within specific cycle phases did not overlap between the two sample types. We were thus interested in whether cytokines would be correlated between the endometrium and peritoneal fluid samples across patients. Although some correlations were statistically

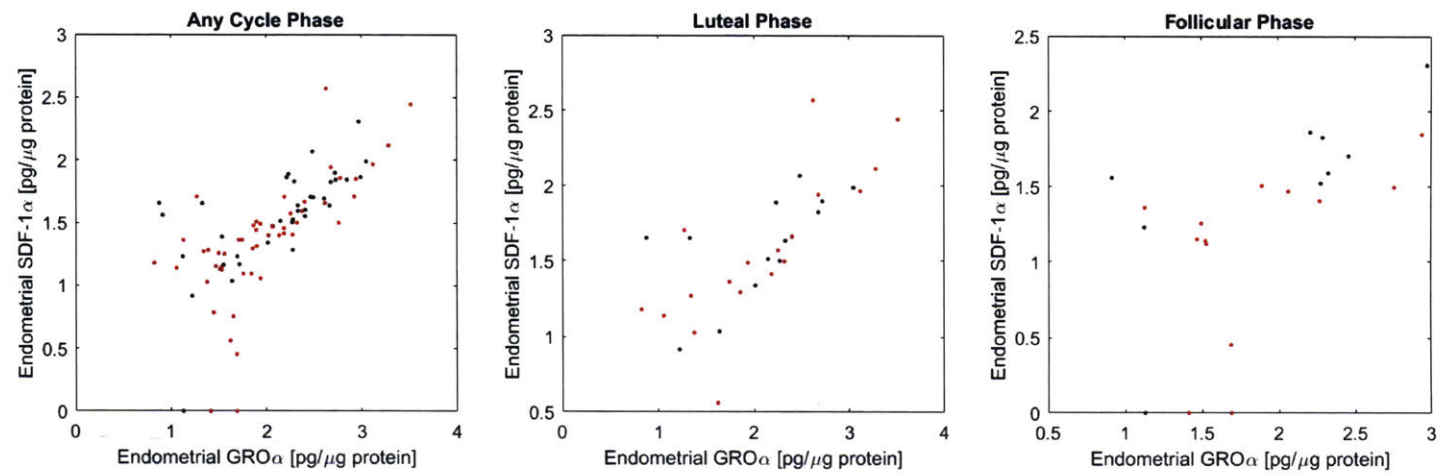


Figure 3-5: GRO $\alpha$  and SDF-1 $\alpha$  were significantly different in luteal phase but not follicular phase endometrial biopsies.

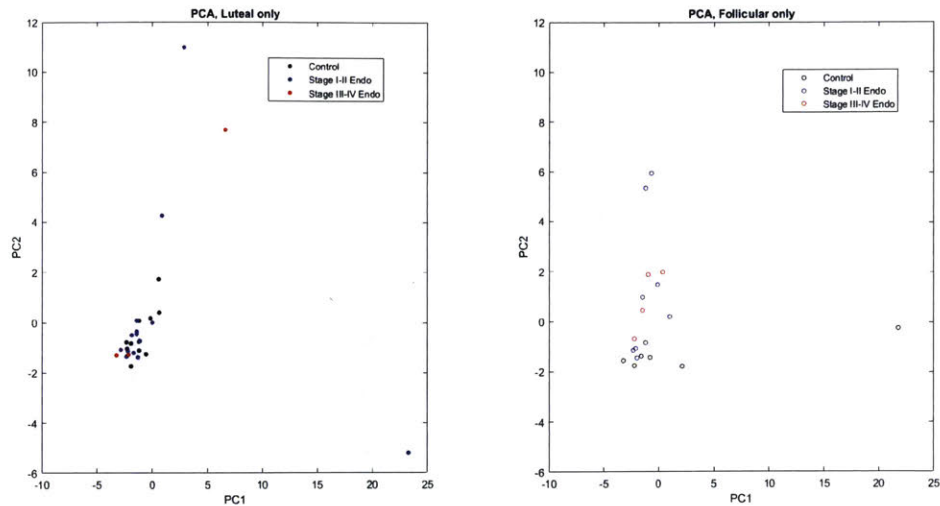


Figure 3-6: PCA on separated Luteal and Follicular phase normalized endometrial biopsy cytokines.

significant, no strong ( $|\text{Pearson } \rho| > 0.5$ ) positive or negative correlations existed between peritoneal fluid and endometrial biopsy cytokines, with the median correlation across the 45 cytokines detectable in both samples being -0.03 (Fig. 3-7).

### 3.4.6 Comparison of peritoneal fluid cytokines across patient cohorts

Several different studies within the Center for Gynepathology Research at MIT performed similar analyses on subjects recruited from multiple cohorts. Patients at Newton Wellesley Hospital were undergoing surgery primarily for pain and were generally older; patients at Oslo University Hospital were being evaluated for infertility and were generally younger adults; and adolescent patients with endometriosis and pain were recruited from Boston Children's Hospital. We aimed to compare peritoneal fluid cytokine findings across these three populations to determine how consistent our results were and to assess whether the patients' primary complaint(s) corresponded to particular differences in cytokine profiles (Fig. 3-1). In all cases, p-values reported here are not adjusted for multiple hypotheses (Table 3.3).

Few cytokines were significant across multiple cohort comparisons; only IL-8 was

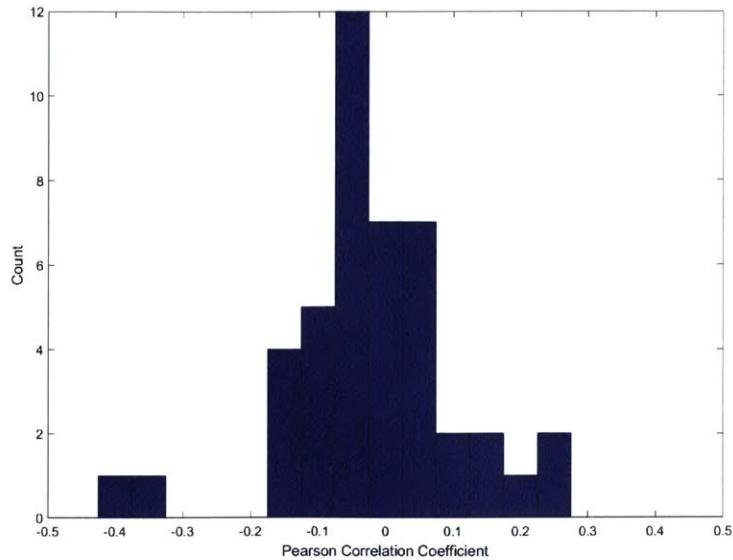


Figure 3-7: No cytokines were strongly correlated between endometrial biopsies and peritoneal fluid samples across the Oslo patient cohort.

significantly higher in endometriosis subjects from both the Oslo and Boston adult cohorts. HGF was significantly higher in endometriosis patients in the Oslo cohort but significantly lower in the adolescent endometriosis patients vs. adult controls in the Boston cohort. For most cytokines with at least one significant difference, levels were higher in endometriosis cases compared to their respective control populations. The only cytokine that was consistently lower across all three comparisons was CTACK.

### 3.4.7 Network analysis of cytokines and proteases in peritoneal fluid samples

MFIs related to cytokine, protease, and protease inhibitor (TIMP) concentrations were measured in peritoneal fluid samples from the Boston cohort of samples. A subset of this data was collected by Michael Beste and previously published in [9]. A Spearman correlation network was generated from data combined for endometriosis and control cases, for a total of 69 subjects. In the correlation network, nearly all cytokines, MMPs, and TIMPs were positively correlated with one another (Fig. 3-8). This relationship may be reflective of positive feedback among the analytes or due to



Cytokine	Oslo endo v ctrl	Boston stage III/IV endo v ctrl	Adolescent endo v adult ctrl
IL-8	higher, p=0.001	higher, p<0.001	
SCGF $\beta$	higher, p=0.001	higher, n.s.	
HGF	higher, p=0.002	higher, n.s.	lower, p=0.005
IL-13	lower, p=0.008	higher, n.s.	
MCP-1	higher, p=0.023	higher, n.s.	
MCP-3	higher, n.s.	higher, n.s.	higher, p=0.002
IL-12(p40)	higher, n.s.	lower, n.s.	higher, p<0.001
TNF- $\beta$	n.d.	equal	lower, p<0.001
$\beta$ -NGF	higher, n.s.	lower, n.s.	lower, p=0.014
CTACK	lower, n.s.	lower, n.s.	lower, p=0.004
IL-5	lower, n.s.	higher, n.s.	higher, p=0.041
IL-15	higher, n.s.	higher, n.s.	higher, p<0.001
IL-1 $\beta$	higher, n.s.	higher, p<0.001	
IL-4	higher, n.s.	higher, p<0.001	
IL-9	n.d.	higher, p=0.011	
IL-17	n.d.	higher, p=0.012	
G-CSF	higher, n.s.	higher, p<0.001	
IFN- $\gamma$	n.d.	higher, p<0.001	
RANTES	higher, n.s.	higher, p=0.003	
TNF- $\alpha$	higher, n.s.	higher, p=0.024	
IL-16	higher, n.s.	higher, p=0.029	
MIF	higher, n.s.	higher, p=0.014	

Table 3.3: Cytokine significance across three cohorts.

other confounding factors, such as fluid volume. To account for potential confounding factors, we then generated a partial correlation network using the same data (Fig. 3-9).

Most cytokines and proteases were positively correlated in the correlation network, possibly due to confounding factors such as peritoneal fluid volume. We thus proceeded to generate a partial correlation network using the same data. The partial correlation network is expected to be less sensitive to co-regulation and other non-causative relationships. Comparing between the two networks, the partial correlation network was much less dense than the regular correlation network, but the density of edges between cytokines and proteases/TIMPs was higher (Table 3.4). Of particular interest, the network showed evidence of much more complicated regulatory mechanisms, as many more negative correlations were present, suggesting more inhibitory

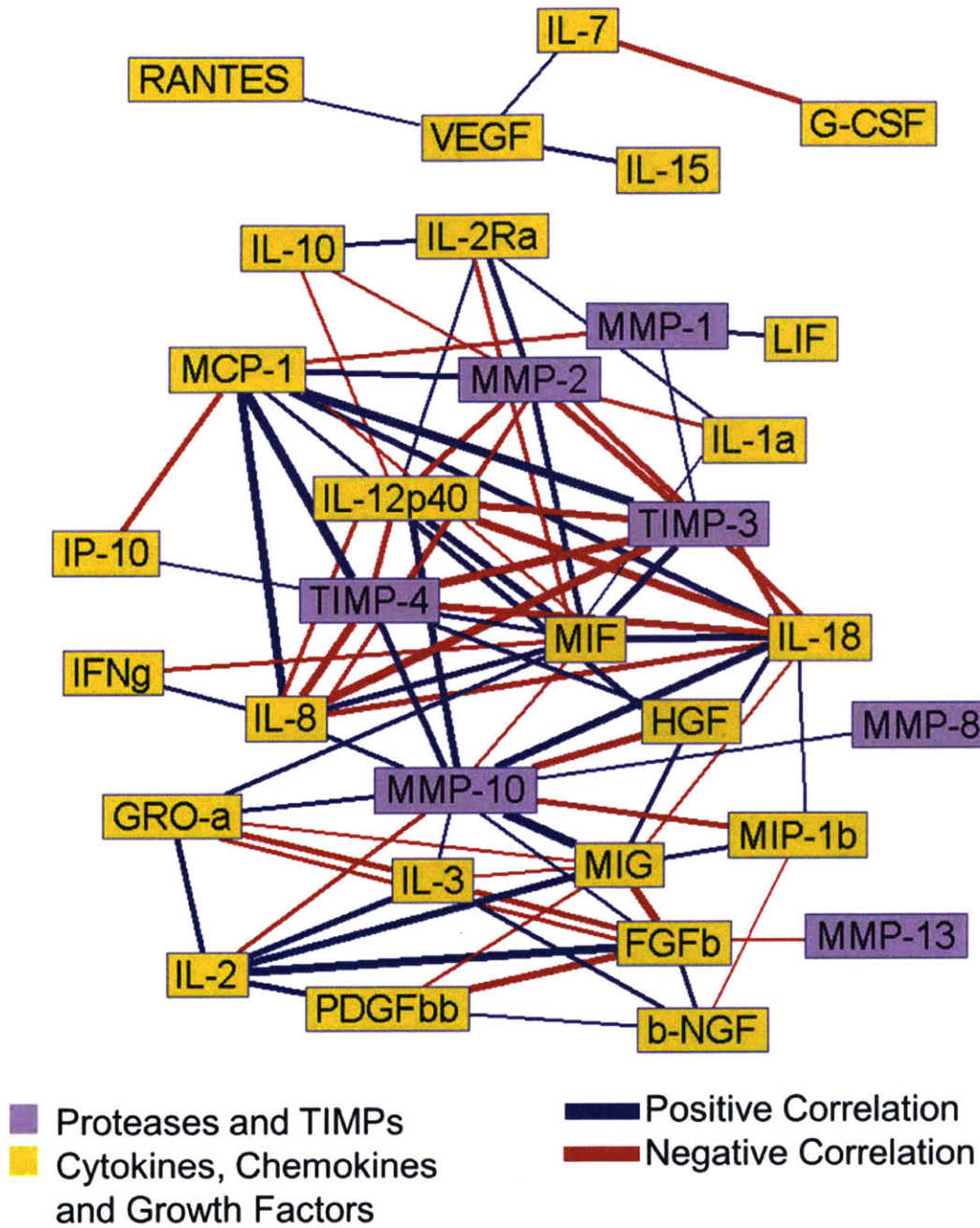


Figure 3-9: Cytokine-protease partial correlation network.

interactions. The top 10% most connected nodes in the partial correlation network were MMP-10, MIF, IL-12(p40), IL-18, MMP-2, and TIMP-4, indicating that both proteases and cytokines play a central role. The network includes partial correlations between species with known interactions, such as the inhibition of MMP-2 by TIMP-2 and TIMP-4. The network also includes partial correlations between species with no known interactions, such as between MMP-10 and IL-2, making it potentially useful as a hypothesis-generating tool.

Original Correlation Network	Edges	Pairs	Density
All 63 analytes	190	1953	9.7%
Cytokines (CK)/Growth Factors (GF)	158	1225	12.9%
CK/GF - Proteases/TIMPs	14	650	2.2%
Proteases/TIMPs	18	78	23.1%
Partial Correlation Network			
All 63 analytes	87	1953	4.5%
Cytokines (CK)/Growth Factors (GF)	47	1225	3.8%
CK/GF - Proteases/TIMPs	34	650	5.2%
Proteases/TIMPs	6	78	7.7%

Table 3.4: Density of subsets of the full and partial correlation networks.

## 3.5 Discussion and Conclusions

### 3.5.1 Use of endometrial biopsies

Here we evaluated, as far as we are aware for the first time, a panel of cytokine concentrations in lysed endometrial biopsies from a cohort of women being evaluated for infertility. As endometriosis involves an interplay between shed endometrial tissue and the peritoneal environment in which lesions develop, the investigation of inflammatory processes within the eutopic endometrium may be complementary to similar studies performed on peritoneal fluid samples [85, 9]. In this particular patient cohort, we found no strong relationships between endometrial cytokines and either endometriosis stage or fertility outcomes; however, further study on additional populations, particularly including patients with a primary complaint of pain, may

be informative.

In this work, endometrial cytokines were not significantly different across cycle phase, but GRO- $\alpha$  and SDF-1 $\alpha$  were significantly different between endometriosis and non-endometriosis subjects in the luteal phase but not in the follicular phase. Cycle phases were established by asking patients about their menstrual cycle, not by histological evaluation of the endometrial biopsies. Because we have established that at least some tissue features can be observed in FFPE and H&E-stained biopsies, and we now have FFPE biopsy samples from each patient, it is possible that examination by a pathologist could yield more accurate cycle staging for these samples.

### **3.5.2 Peritoneal fluid cytokines across cohorts**

Significance of cytokine differences between endometriosis and control cases was not generally consistent across different patient cohorts. The three cohorts here had substantial differences in terms of age and primary symptoms, and it is likely that both larger sample sizes and additional subdivision of subjects by symptoms and other patient characteristics could lead to additional insights into, for example, endometriosis-associated pain vs. endometriosis-associated infertility.

### **3.5.3 Network analysis**

Network analysis of cytokine and protease concentrations suggest that these two systems are highly interrelated in the peritoneal fluid. Unfortunately, mimicking the peritoneal fluid environment *in vitro* is nontrivial. In fact, efforts to follow up on these results by testing for causal relationships between connected nodes in the network using cell lines cultured in tissue culture plastic were largely unsuccessful. This result is actually unsurprising when considering that the cell types present in the peritoneal cavity (not only immune cells and possibly shed endometrial cells, but a large number of mesothelial cells forming the lining of the peritoneal cavity) were not adequately represented in our simple 2D culture system.

Finally, going forward, it would be informative to identify differences in cytokine/protease

networks between patients with and without endometriosis. Traditional partial correlation requires a larger number of samples than analytes, which we achieved here for all patients combined but not for disease stage-specific subsets of patients. More robust methods for partial correlation networks could improve our ability to subdivide patients into smaller categories [67]. Additionally, larger studies, or meta-analysis combining data collected across multiple sites, could allow for more in-depth characterization of patient subpopulations.

### **3.5.4 Future work: *In vitro* models for time-dependent studies**

Using primary samples collected from patients undergoing surgery, we are unable to follow disease progression or changes over time throughout the menstrual cycle. While we found some cycle-dependent associations between cytokine concentrations and endometriosis stage, it is likely that patient-to-patient variability confounded with cycle day masks real intra-patient cycle-dependent changes. In the future, *in vitro* model systems using primary cells would allow for additional types of data to be collected, including hormone response and inflammatory responses to perturbations of cytokine/protease networks.



# Chapter 4

## Benchmarking of network modeling methods

### 4.1 Acknowledgments

Work shown in this chapter was done during an internship at Novartis, supervised by Melody Morris. The author would like to thank Scott Gleim, Frédéric Sigoillot, Joseph Loureiro, and Jeremy Jenkins for scientific guidance on this project; Yuan Wang, Jaison Jacob, Nicole Renaud, and Zinger Yang for discussions about specific datasets used here; and Mike Steeves and Mikhail Serkov for technical help with cluster computing.

### 4.2 Introduction

In 2000, Schwikowski et al. demonstrated the utility of the Guilt by Association principle to assign function of yeast genes by examining the function of neighboring genes in a protein-protein interaction [155]. Since then, the scientific community has launched a massive effort to determine protein-protein interaction (PPI) networks for model organisms [169, 79, 144, 179] and humans [150, 160]. At the same time, a multitude of computational approaches have been developed for enhancing interpretation of high throughput data by enabling contextualization of genes of interest with

known molecular interactions. The promise of these algorithms is to connect genes of interest into functionally relevant networks by extending the list to include additional genes relevant to the initial list.

While many of these network contextualization algorithms have been developed in academia in the context of specific biological questions [112, 62], others are part of commercially available tools (eg. Metacore, IPA). However, despite the growing number of available algorithms, to our knowledge there has been no systematic effort to benchmark their ability to return meaningful, actionable hypotheses. In this work, we aim to characterize 18 network contextualization algorithms in terms of the fraction of novel findings in the output, degree of nodes returned, and performance for a cross validation task with the ultimate aim of applying the algorithms to contextualize and extend hits from siRNA and CRISPR phenotypic screens.

## 4.3 Methods

### 4.3.1 Network algorithms

In this work, we consider eighteen algorithms (Table 4.1) implemented as part of the Computational Biology for Drug Discovery (CBDD) collaboration between Clarivate Analytics and sixteen pharmaceutical companies. A key deliverable of CBDD is the CBDD R package which implements published algorithms in a consistent interface. Algorithms chosen were available in CBDD version 5.0 and had no major performance considerations that would limit systematic benchmarking efforts. Additionally, the aim of these algorithms was consistent with our aim: to use the network to contextualize and extend genes of interest. Of these algorithms, we divide them into three main types: node prioritization, causal reasoning, and subnet identification. Node prioritization algorithms seek to prioritize network nodes that are near input nodes, where the definition of "near" varies depending on the specific algorithm. Causal reasoning algorithms seek to prioritize network nodes that regulate input nodes based on their network connectivity. Subnetwork identification algorithms seek to identify

regions of the network that connect input nodes and include additional nodes for their connection if warranted. In the case of subnetwork identification algorithms, we wanted to be able to compare to the simplest case of network connections between nodes. Thus, we implemented two additional algorithms: StartNodeLinks, which connects input nodes, and StartNodeNeighborLinks, which includes connections between input nodes and their immediate neighbors.

	Algorithm	Algorithm Type	Output	Reference
1	Guilt by Association	Node Prioritization	Node Score	[155]
2	Neighborhood Scoring	Node Prioritization	Node Score	[132]
3	Interconnectivity	Node Prioritization	Node Score	[72]
4	Network Propagation	Node Prioritization	Node Score	[174]
5	Random Walk	Node Prioritization	Node Score	[97]
6	ToppNet HITS	Node Prioritization	Node Score	[26]
7	ToppNet KM	Node Prioritization	Node Score	[26]
8	GeneMania	Node Prioritization	Node Score	[125]
9	Hidden Nodes	Node Prioritization	Node Score	[40]
10	Overconnectivity	Node Prioritization	Node Score	[130]
11	Causal Reasoning	Causal Reasoning	Hypothesis Score	[28]
12	SigNet	Causal Reasoning	Hypothesis Score	[80]
13	Active Modules	Subnetwork ID	Network	[77]
14	Pathway Inference	Subnetwork ID	Network	[145]
15	HotNet	Subnetwork ID	Network	[173]
16	HotNet2	Subnetwork ID	Network	[110]
17	DIAMOnD	Subnetwork ID	Network	[59]
18	CASNet	Subnetwork ID	Network	[55]
19	StartNodeLinks	Subnetwork ID	Network	Custom
20	StartNodeNeighborLinks	Subnetwork ID	Network	Custom

Table 4.1: Network Algorithms

For each algorithm, parameters were chosen to moderate the behavior of the algorithms (Table 4.3.1). For example, both random walk and network propagation contain a parameter that sets the probability that the random walk will restart at the start nodes at each step; this parameter was set to 0.5 for both to allow for comparison between the two algorithms. If the value of the parameter that would result in moderate behavior was not obvious, it was set based on author recommendations.

Algorithm	Parameter	Notes
Network Propagation	alpha = 0.5 L1Threshold=0.000001	
Random Walk	r = 0.5 L1Threshold = 0.000001	
Neighborhood Scoring	alpha = 0.5	
ToppNet HITS	r = 0.5 iterations = 100 eps = 0.0001	
ToppNet KM	K = 4	
Overconnectivity	FDR = TRUE alpha = 1 background.list = "	
Hidden Nodes	fdr = TRUE alpha = 1	
GeneMANIA	network_w = 'startnodes' colNets = 'source' netCats = NULL	
Active Modules	numberOfModules = 10 iterations = 10000 activationProbability = 0.5 startTemp = 1000 dmin = 10 backgroundRuns = 100	
Pathway Inference	beta = 1 d = 2 iterations = 100 verbose = FALSE	
HotNet	iterations = 100 t = 0.1 delta = 0.01 minSize = 3 minScore = 0 scoreType = 'pvalue' sizeLimit = 10000	Limit Java heap memory
HotNet2	delta = 0.01 beta = NA iterations = 100 min.size = 3 delta.max.size = 10 min.score = 0 score.type = 'pvalue'	
DIAMOnD	n = 200 alpha = 1 method = 'default'	Default=overconnectivity

Algorithm	Parameter	Notes
Causal Reasoning	scoreThreshold = -200 correctnessThreshold = -200 enrichmentThreshold = 1.1 pollardThreshold = 1.1 trSteps = 'relaxed' unknown = 'ignore'	
SigNet	maxSteps = 2 rankBy = c("power_weight", "exp_weight", "lambda") combine = min trSteps = 'relaxed'	
General	directed = TRUE	

Table 4.2: Algorithm parameters

### 4.3.2 Data sets

We aimed to test the algorithms on a large selection of data sets of different types and confidences (Table 4.3). For high-confidence, well-characterized input sets, we used pathways from KEGG and Reactome. All sets with 20 or more nodes were included, yielding 165 sets from KEGG and 307 from Reactome. We also used curated gene-disease associations from DisGeNet [139, 138] (accessed 7 June 2016). Nodes were included in a disease set if they had at least 2 Pubmed IDs, and disease sets were run if the number of associated genes was at least 20, giving 117 disease sets. For these publicly available data sets, where fold changes and p-values are not available, nodes were assigned a  $\log_2$  fold change of 1 and p-value of 0.05 to allow input lists to be run with algorithms that require fold change or p-value.

To test the algorithms using real experimental data, 43 pooled CRISPR screens from Novartis were used as an example set of experimental data with relatively low noise. For CRISPR experiments, cells were transfected with a GFP-tagged target protein of interest and Cas9, then exposed to a pooled library of sgRNA. Cells were FACS-sorted into high- and low-GFP populations, and sgRNA count was used to calculate fold changes and RSA p-values for each targeted gene [38]. Genes were included in start lists if the RSA p-value  $< 1 \times 10^{-4}$ , and for each experiment (which

may have included multiple comparisons) the start list with length closest to 150 genes was used. Experiments were excluded from the benchmarking data if the longest start list was  $<20$  genes.

The algorithms involving causal reasoning were originally developed to identify proteins upstream of observed gene expression changes. Since this approach was not specifically relevant to the pathway and screening data described above, we also used data from the Connectivity Map [102], with more appropriate parameters for the causal reasoning algorithms.

Data Source	Data Type	# Sets	Min Size	FC	p-val	Ref
KEGG/ Reactome	Pathways	472	20	1	0.05	[87, 89, 88] [48, 35]
DisGeNET	Genetic Association	117	20	1	0.05	[139, 138]
CRISPR	Screening Results	43	20	Var	Var	Internal Data
cMAP	Differential Expression	2068	20	Var	Var	[102]

Table 4.3: Data sets used for algorithm benchmarking

### 4.3.3 Networks

Five different network sources were used for this work: two previously published undirected networks, HumanNet [109] and BarabasiNet [119]; HithubMetabase, consisting of manually curated interactions from MetaBase [18] (Clarivate Analytics) translated into Entrez IDs; HithubStringBioplex, consisting of interactions from STRING [177, 162] and BioPlex [76]; and HithubPublishable, a combination of HithubMetabase and HithubStringBioplex (Table 4.4). For networks in which edges were annotated by type of interaction and confidence, edges were included if they were high-confidence and represented either protein-protein or transcription factor-gene interactions.

### 4.3.4 Crossvalidation and target validation

Ten repeats of 10-fold crossvalidation were performed for each data set to calculate the area under the ROC curve (AUC). Each data set was divided into tenths, with one tenth left out each time; then that process was repeated ten times for a total

Network	Components	Edges	Nodes	Directed Edges (%)	TF-Gene Edges (%)	Refs
Hithub-Publishable	STRING + BIOPLEX + Metabase	597,538	18,286	22.63	7.59	[177, 162] [76, 18]
Hithub-StringBioplex	STRING + BIOPLEX	434,808	14,701	15.96	0	[177, 162] [76]
HithubMetabase	Metabase	189,675	16376	39.47	23.90	[18]
HumanNet	Human Net	476,399	16243	0	0	[109]
BarabasiNet	Barabasi Net	141,296	13,460	0	0	[119]

Table 4.4: Input network properties

of 100 lists each with 90% of the original input list. Sensitivity and specificity were found using the omitted 10% of nodes as "true" nodes to be found by the algorithms. When omitted input nodes were not included in the network used, they were excluded from the list of "true" nodes, as the use of that network prevented them from being included in the output regardless of the algorithm used.

For connectivity map data, drug target validation was used in place of crossvalidation. Sensitivity and specificity were calculated for inclusion of known drug targets in algorithm outputs.

### 4.3.5 Empirical null distributions

To determine whether nodes were highly ranked based on the network properties only (irrespective of the input list) we generated lists of randomly selected input nodes. Fold changes were chosen from a random distribution with mean 0 and standard deviation 1, with corresponding p-values. Fold change and p-value pairs were randomly assigned to all possible nodes, and the nodes with highest fold change were used as the input list. We generated 10,000 random gene lists each of lengths 50, 100, 150, 200, 300, and 500 and ran the algorithms on these input lists. We were thus able to determine, for each node, algorithm, and network, the rank above which nodes had a less than 5% chance of scoring at random. Nodes which were highly ranked with

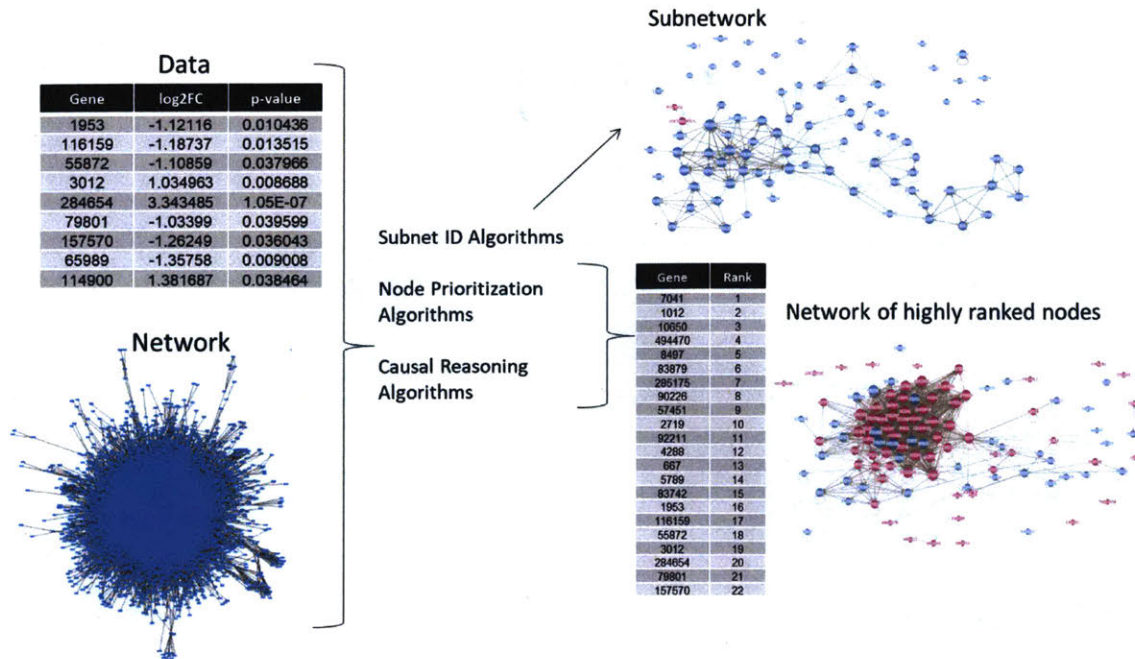


Figure 4-1: Overview of use of network algorithms.

actual input lists but had a greater than 5% chance of getting that rank or higher in the random lists were flagged as possible artifacts.

## 4.4 Results

### 4.4.1 Overview of algorithm workflow

For all algorithms considered here, inputs include a data set consisting of gene IDs, fold changes, and p-values and a network of protein-protein interactions (Fig 4-1). Algorithms are divided up into three main classes: subnetwork ID algorithms, which return highly connected subnetworks; node prioritization algorithms, which return ranked lists of genes; and causal reasoning algorithms, which return ranked lists of hypotheses corresponding to a positive or negative effect of a given gene on the observed data. In the case of node prioritization and causal reasoning algorithms, subnetworks can be constructed from the interactions among the most highly ranked genes in the output lists.

Initial characterization was performed using the genetic association datasets from

DisGeNET, as these sets were considered to contain disease-relevant gene sets but also reflected properties of real data such as the presence of false negatives, false positives, and representation of multiple biological processes. We then generalized to additional collections of datasets derived from pathway databases, hits from phenotypic CRISPR screens, and Connectivity Map gene expression response.

#### 4.4.2 Algorithms differ in ranking of start nodes

To determine which algorithms were extending the list of interesting genes beyond the input list provided, we first sought to determine the proportion of output nodes that were represented in the input. For our purposes, outputs were considered to be the top  $n$  nodes ranked by the algorithm, where  $n$  was the length of the input start list. Thus an algorithm that ranked all start nodes above all other network nodes would have a start node fraction of 1. For reference, we note that based on a typical start list size of 100 and network size of 18,286 nodes (as in HithubPublishable), an algorithm that selected output nodes entirely at random with no preference for start nodes would have a start node fraction of 0.005.

Most subnetwork ID algorithms showed a strong preference for start nodes; in the case of StartNodeLinks, ActiveModules, and the HotNet algorithms, only start nodes are scored, so these algorithms re-order start nodes but do not add any new nodes not included in the start list. Pathway Inference and CASnet also shows a strong preference for start nodes but is capable of adding some additional nodes. Of the subnetwork ID algorithms, only StartNodeNeighborLinks and DIAMOND show a preference for non-start nodes. In the case of StartNodeNeighborLinks, this is expected since by definition it extracts all neighbors of start nodes without taking into account any network properties. The fact that DIAMOND's behavior is more similar to the node prioritization algorithms is also expected, since it employs the overconnectivity node prioritization algorithm iteratively until it reaches a user-defined number of nodes (in this case 200).

Within the node prioritization algorithms, Random Walk, ToppNet HITS, and GeneMANIA showed clear preferences for start nodes. While Neighborhood Scor-

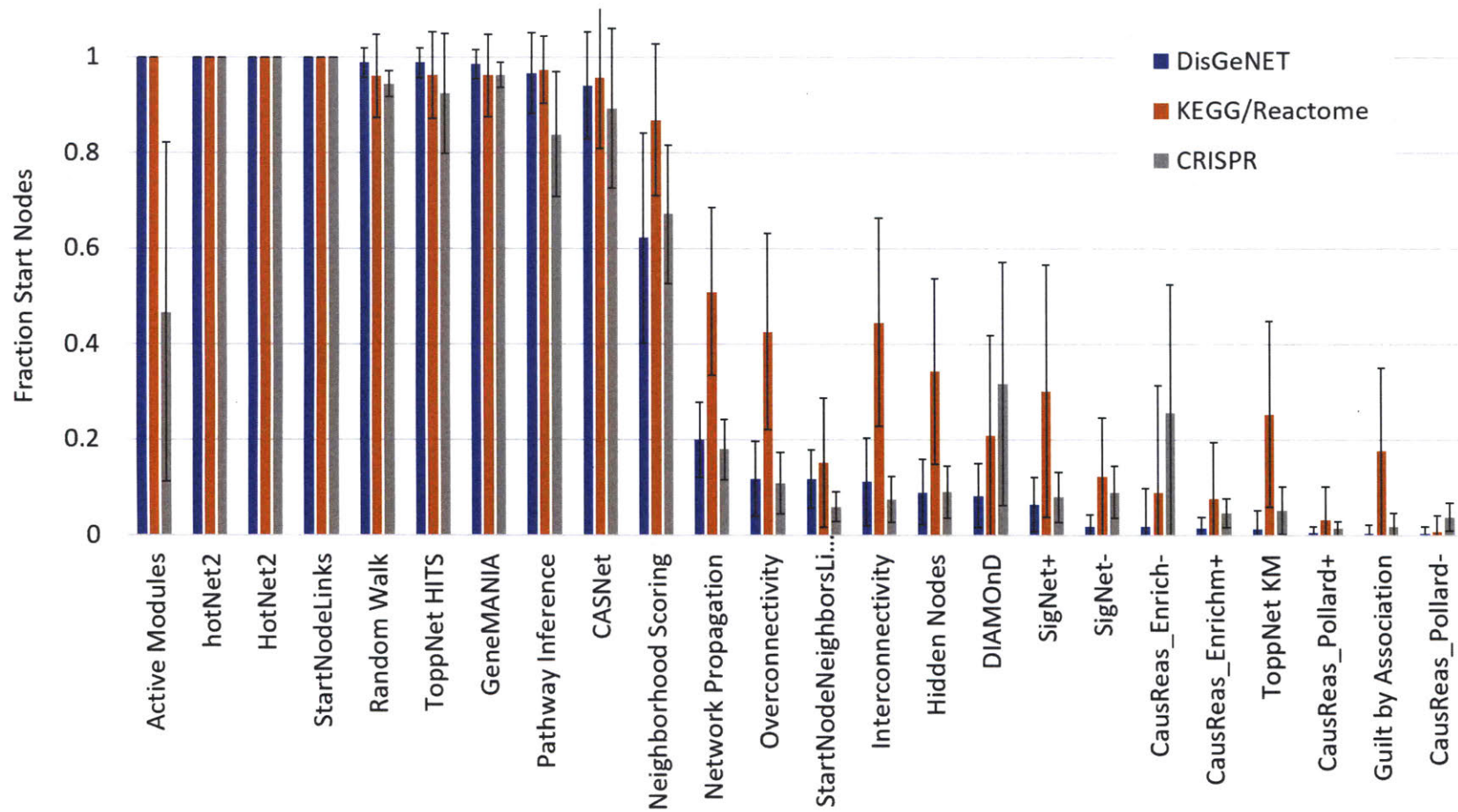


Figure 4-2: Algorithms differ in ability to add non-start nodes.

ing shows an intermediate preference, all other node prioritization algorithms have a tendency to rank non-input nodes highly. In the case of Guilt by Association, the fraction of start nodes is 0.0056, near the value expected if nodes were selected at random.

Causal reasoning algorithms are divided into different output lists based on positive and negative hypotheses and the ranking method used. As causal reasoning algorithms are intended to identify nodes that are capable of influencing the start nodes, possibly from several steps away, they generally did not have a strong preference for including the start nodes themselves in output lists.

Taken together, these results demonstrate that algorithms significantly differ in their preference for extending the input gene list to additional network nodes, and if the aim of the analysis is to bring in additional nodes, most subnetwork ID algorithms should be avoided.

### 4.4.3 Algorithms differ in preference for node degree

We also sought to understand which algorithms had a tendency to include hub nodes in the output. A common concern with interpreting the results from network algorithms is if the presence of hub nodes in results is due to actual relevance to the start nodes or simply due to the number of edges. Within lists of output nodes as defined in the previous section, some algorithms have a stronger preference for hub nodes than others.

Across all Subnetwork ID and Node Prioritization algorithms, several returned extremely high-degree outputs: StartNodeNeighborLinks, DIAMOnD, Interconnectivity, and Overconnectivity. The behavior of StartNodeNeighborLinks is not surprising, since nodes were scored based on the total number of start node-connected edges. The other three algorithms in this class, DIAMOnD, Interconnectivity, and Overconnectivity, are all enrichment-based methods.

At the other end of the spectrum, ToppNet KM and Guilt by Association returned nodes of very low degree. This is consistent with the scoring metric employed by these algorithms: both depend strongly on the fraction of a node's immediate neighbors

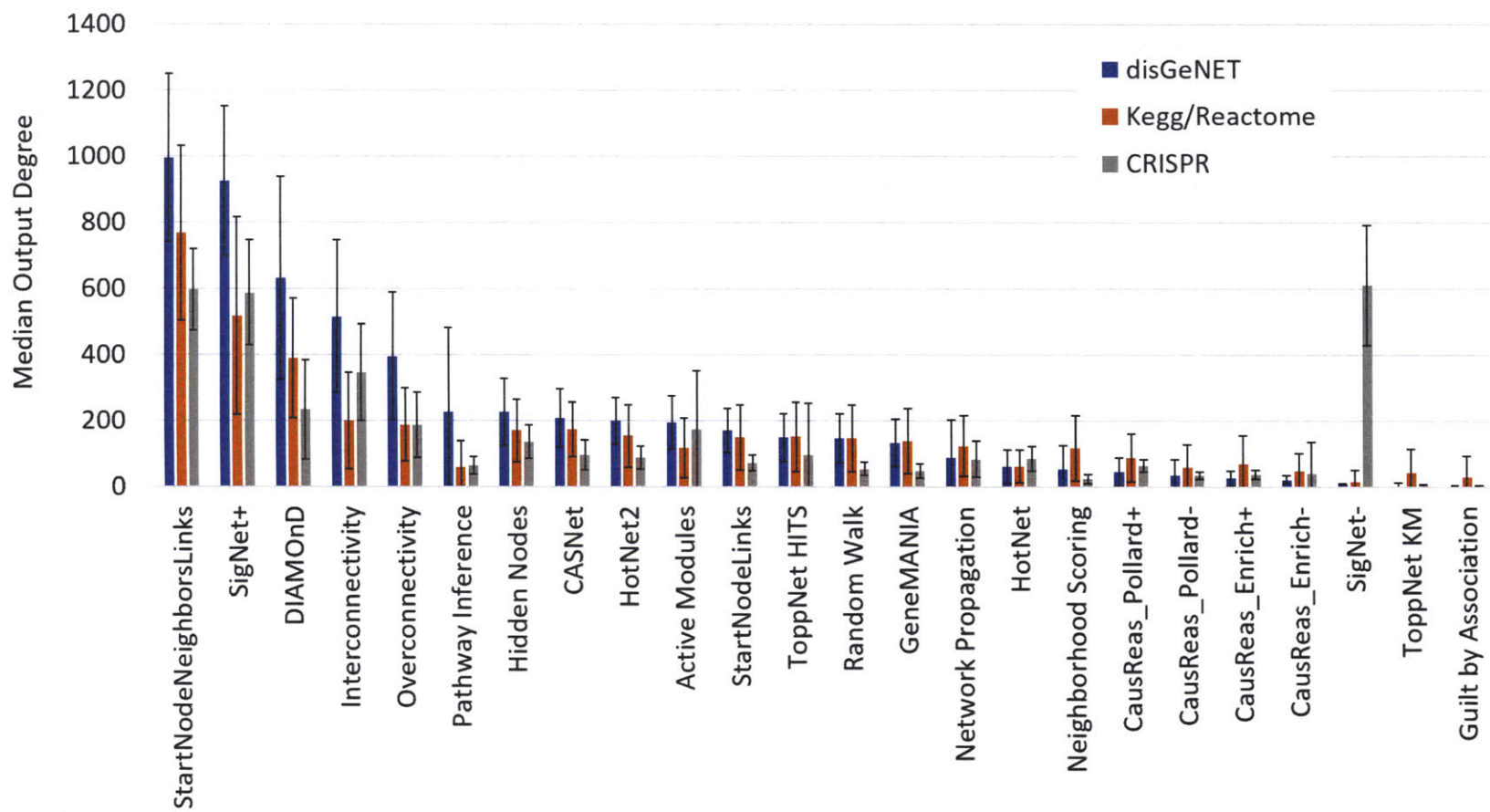


Figure 4-3: Algorithms differ in preference for high-degree nodes.

that are start nodes, meaning that these algorithms rank very highly nodes that have a degree of only one, if that one neighbor is a start node. Neighborhood Scoring uses an algorithm similar to Guilt by Association, but with a bonus for start nodes, making it intermediate in terms of node degree.

Other subnetwork ID and node prioritization algorithms had intermediate but rather variable median degree within the outputs. Several of these algorithms (eg. Pathway Inference, CASNet, HotNet, HotNet2, Active Modules, and GeneMANIA) also strongly favored start nodes, so the median degree of the output depended heavily on the degree of the start nodes. Of the remaining algorithms that showed intermediate behavior by this metric (ToppNet HITS, Hidden Nodes, Random Walk, and Network Propagation), all are walk-based.

Turning to the Causal Reasoning algorithms, we hypothesize that the results are due to the data and network processing requirements of the algorithms. For example, because we introduced a default positive fold change for the DisGeNET list, SigNet has a very high median degree for only positive hypotheses in this dataset, but both positive and negative hypotheses in the real data.

#### **4.4.4 Algorithm sensitivity and specificity found through cross-validation**

In practice, these algorithms should be most useful if they are able to identify nodes that were not found directly in experimental data. To test the ability of the algorithms to find "missing" nodes, we used 10 repeats of 10-fold cross-validation, then found the area under the ROC curve (AUC) for including the omitted nodes from the original input lists in the output (Fig. 4-4). Subnetwork ID algorithms were omitted from this analysis because most of them did not add in non-start nodes.

To summarize across individual data sets from each source, we found the fraction of data sets for which each algorithm appeared in the top 3 when ranked by AUC. While performance varied across data sources, longer-distance node prioritization algorithms generally performed the best. In data from DisGeNET, which

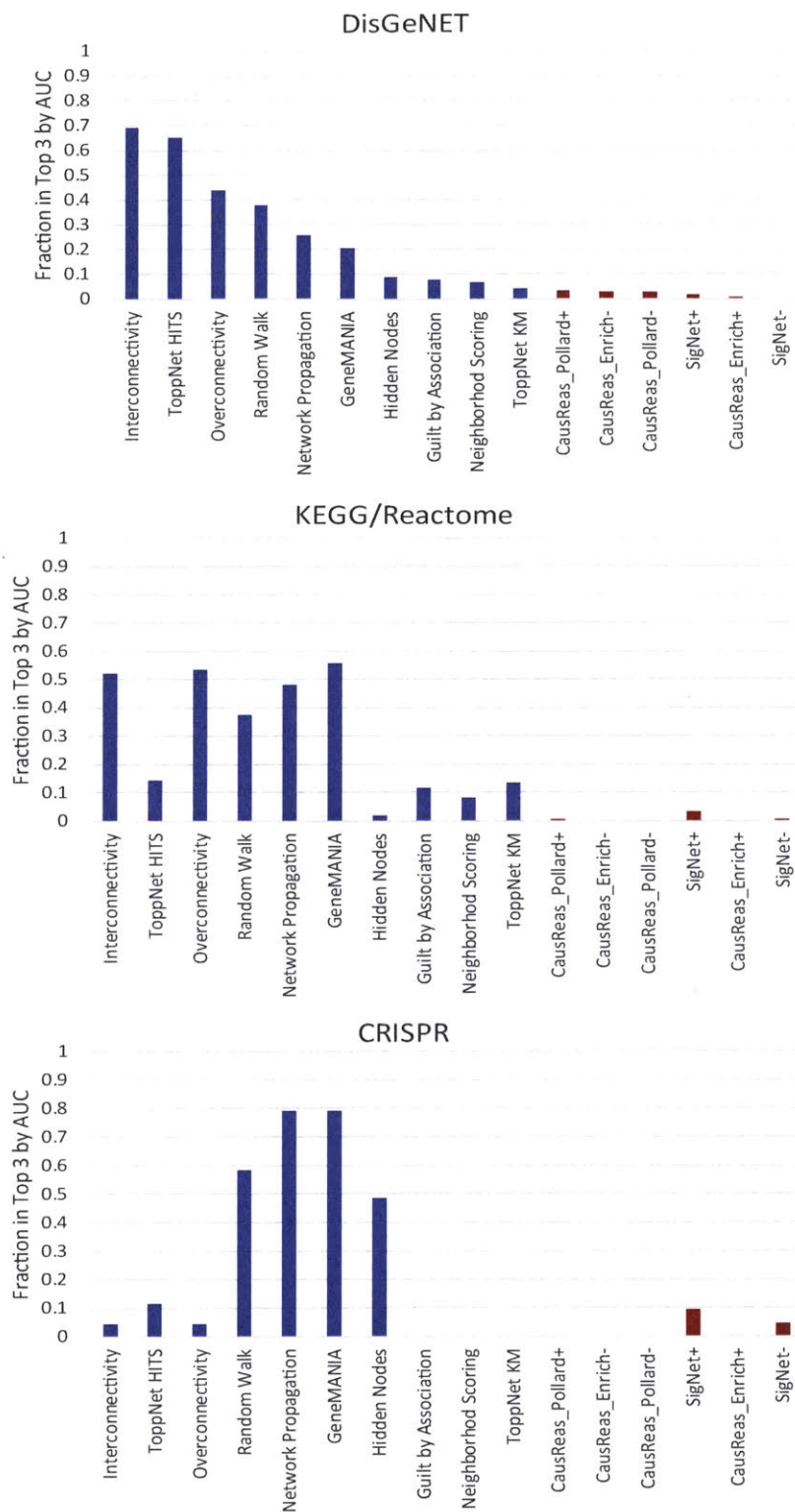


Figure 4-4: Algorithm performance was quantified by the fraction of data sets for which the algorithms ranked in the top 3 best algorithms by crossvalidation AUC.

was high confidence but non-overlapping with information included in the network, Interconnectivity, ToppNet HITS, and Overconnectivity performed the best. Short-range node prioritization algorithms (Guilt by Association, Neighborhood Scoring, and ToppNet KM) performed better in KEGG and Reactome data sets but less well in real experimental data (CRISPR). Causal reasoning algorithms were developed for a different type of task, identifying drug targets upstream of differentially expressed genes, and all causal reasoning methods were in the worse half of the algorithms by crossvalidation across all three data sources.

We also observed that, for most algorithms, data sets with very high confidence pathways such as KEGG and Reactome had much higher crossvalidation AUC than did the slightly lower-confidence DisGeNET lists, and real experimental data had much lower crossvalidation AUC.

#### **4.4.5 Use of algorithms for target identification using Connectivity Map**

Because causal reasoning algorithms were developed to identify upstream regulators of differentially expressed genes, we tested their ability to accomplish this goal using the Connectivity Map [102]. For this analysis, start nodes were differentially expressed genes after treatment with drugs with known targets and we tested the algorithms' ability to highly rank the real drug target. To our surprise, the causal reasoning algorithms did not outperform many of the node prioritization algorithms (GeneMANIA, Interconnectivity, ToppNet HITS, Random Walk, Interconnectivity, and Network Propagation) (Fig. 4-5). Of the consistently high-performing node prioritization algorithms in our previous analysis, only Overconnectivity performed worse than the causal reasoning algorithms.

#### **4.4.6 Comparison of network sources**

To determine whether network source (and associated network size and confidence) affected results, we compared areas under the ROC curves for five different networks

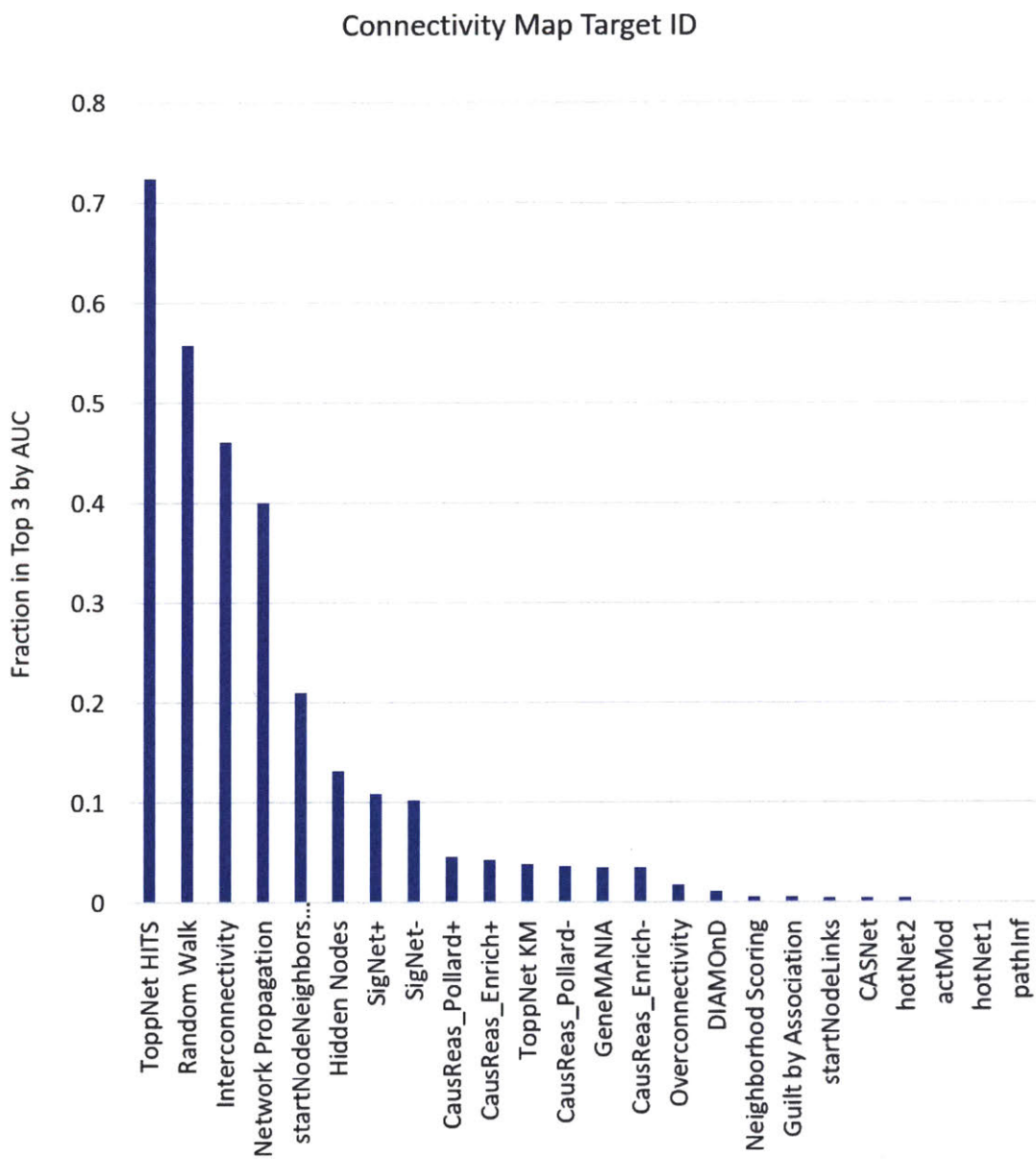


Figure 4-5: As an alternative performance metric, algorithms were ranked by the fraction of Connectivity Map datasets for which they ranked in the top 3 by target identification AUC.

(Table 4-6). Results shown up until this point were obtained using the HithubPublishable network, the largest of the five networks considered here. We also consider the freely available proportion of Hithub, HithubStringBioplex, separate from the curated content available from a vendor, HithubMetabase. Finally, we included two published networks: HumanNet and BarabasiNet. Importantly, both of these networks contained only undirected edges, so edges were assigned both directions for algorithms that required direction.

Results shown up until this point were all obtained using the HithubPublishable network, the largest of the five networks considered here. To determine whether network source (and associated network size and confidence) affected results, we compared areas under the ROC curves for five different networks (Table 4.4.6). Algorithm performance across networks was generally similar. HithubPublishable, which was the largest network, performed best in most cases with the exception of Guilt by Association, ToppNet KM, Neighborhood Scoring, and Causal Reasoning, algorithms which generally performed less well than the others.

Whether the improvement in performance seen in HithubPublishable compared to the other two Hithub networks was due to HithubStringBioplex or HithubMetabase was algorithm-dependent. Walk-based methods appeared to perform better with HithubMetabase, whereas more local methods (Guilt by Association, ToppNet KM, Neighborhood Scoring, and Overconnectivity) performed better with HithubStringBioplex. Causal reasoning and SigNet are also limited to considering information from at most two steps away, making them effectively local methods as well.

Human Net and Barabasi Net generally had worse performance than the other three networks. This may be because both of these networks are undirected. However, their performance did not seem to be particularly worse than the partially directed networks in algorithms that used edge direction.

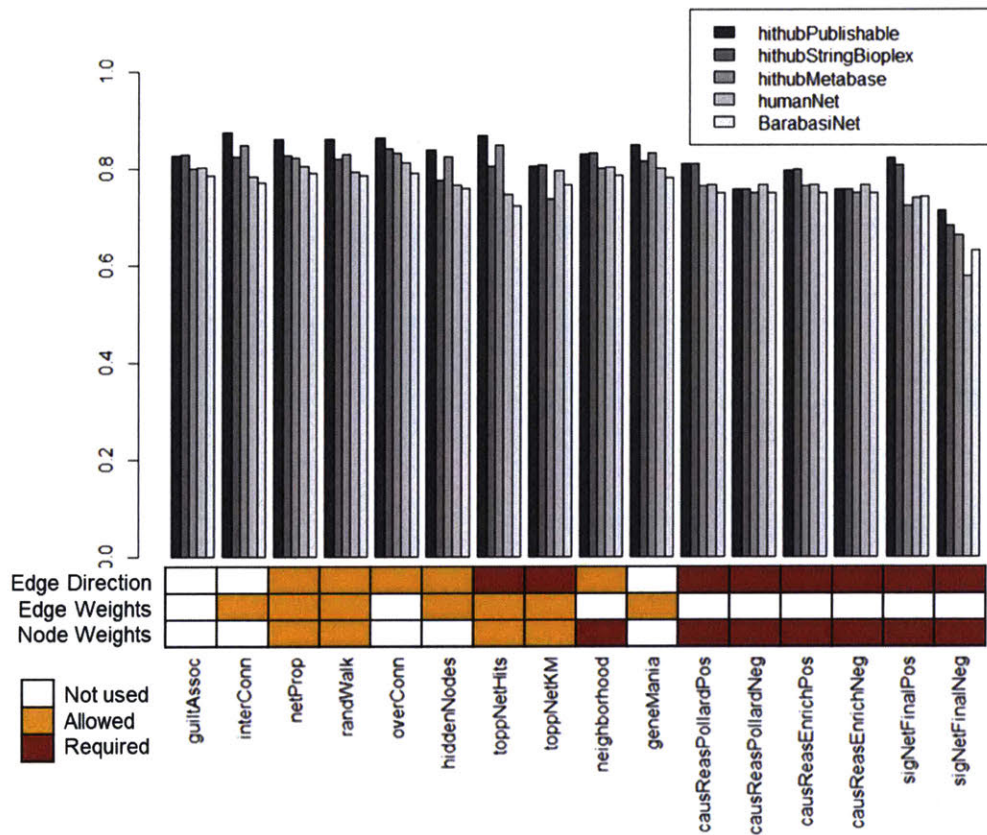


Figure 4-6: Different network sources were compared by crossvalidation AUC using DisGeNET datasets.

#### 4.4.7 Empirical significance determined using random input lists

In order to determine whether certain nodes, particularly hub nodes, are highly ranked by a given algorithm regardless of the input list, we ran 10,000 randomly selected input lists of sizes 50, 100, 150, 200, 300, and 500. For each node, the cumulative distribution of output ranks below a given threshold for each algorithm indicates the significance of that node's rank when found using real data.

Using random start node lists, cumulative distribution functions for the probability of a hub node (POLR2B) or a non-hub node (WDR4, degree 19) being ranked below a certain cutoff for an algorithm that is insensitive (Guilt by Association) or one that is sensitive to node degree (Random Walk) shows that algorithms treat nodes of varying degrees quite differently.

Empirical significance of an output node was calculated as the percent of ranks for that node in outputs generated from random input lists at or below the rank in the actual output list. For most node prioritization algorithms, no nodes were ranked in the top 100 nodes in more than 5% of randomly generated list. However, a few algorithms did tend to highly rank a few nodes even at random. These were Network Propagation (23 nodes), Hidden Nodes (37 nodes), Random Walk (36 nodes), ToppNet HITS (293 nodes), and Interconnectivity (1109 nodes).

#### 4.4.8 Algorithm choice for different tasks

The previous sections have highlighted three characteristics of the algorithms: ability to highly rank non-start nodes, tendency to highly rank hubs, and performance by cross-validation. We summarize these features (Fig. 4-8) and use these summaries as well as additional considerations highlighted to make recommendations.

If the main aim of the analysis is to prioritize and contextualize genes of interest found in the experimental results, this work indicates that ToppNet HITS, Random Walk, and GeneMANIA would accomplish the aim. Alternatively, if the analyst would like to contextualize genes of interest and also consider additional network

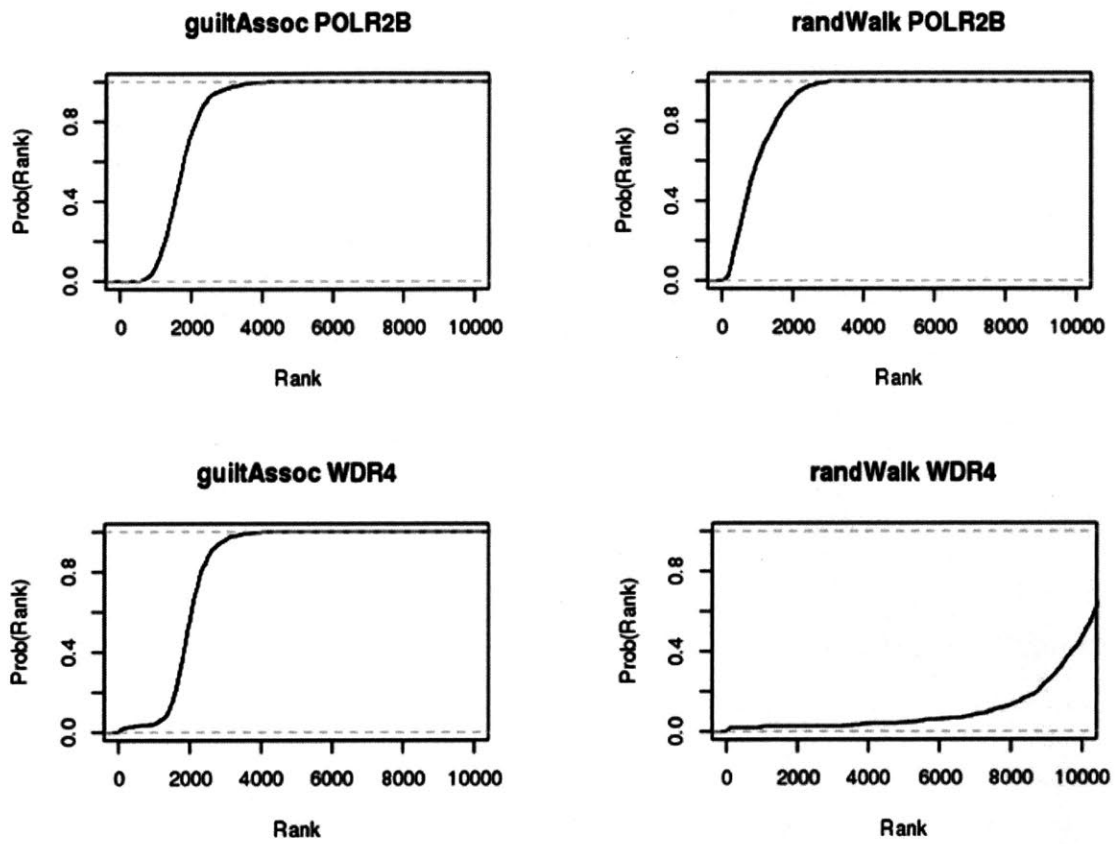


Figure 4-7: Cumulative distributions of ranks with random input lists vary by node degree and algorithm used.

AUC.Avg vs. medianDegAvg

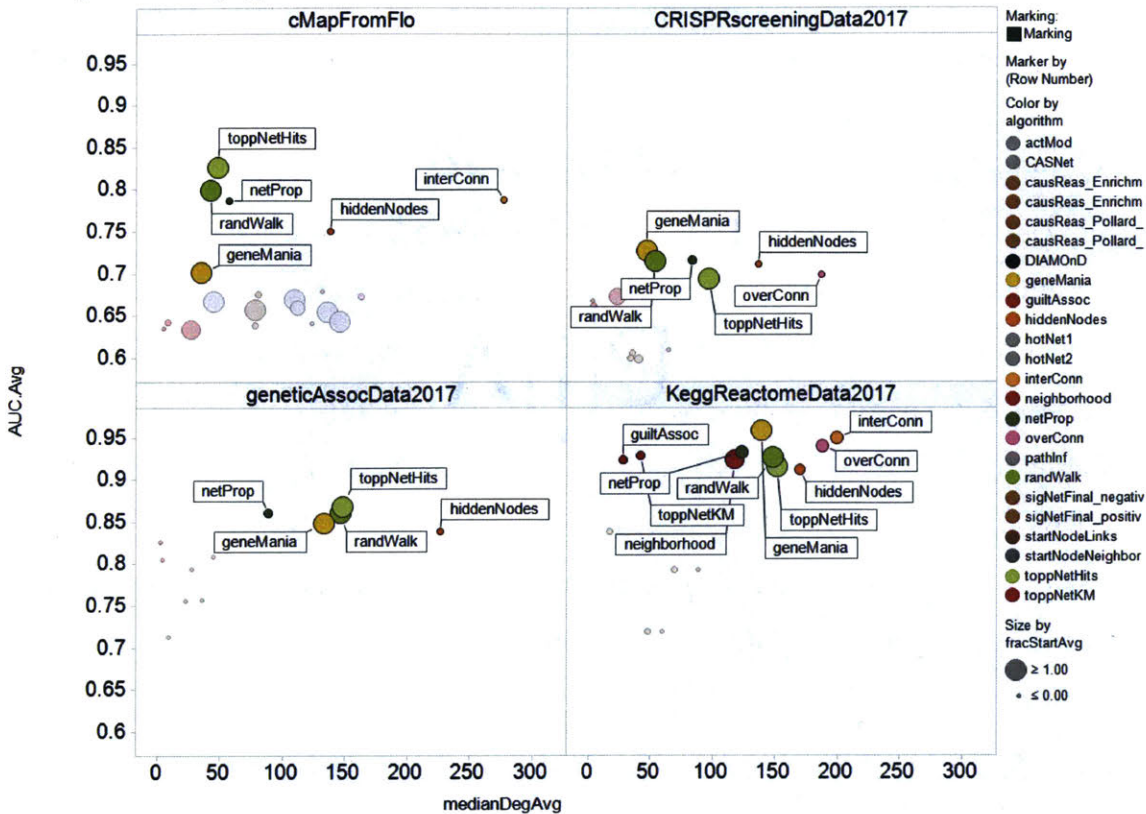


Figure 4-8: Algorithm selection can be guided by AUC, preference for high-degree nodes, and preference for start nodes.

nodes, Hidden Nodes, Network Propagation, Overconnectivity, and Interconnectivity would be more suitable. However, Interconnectivity in particular was shown to also rank a significant number of nodes highly with random input, so statistical significance of ranked nodes should be taken into account.

## 4.5 Discussion and Conclusions

### 4.5.1 Algorithm selection depends on desired outcomes.

The benchmarking results shown here suggest that certain categories of algorithms may have different applications, and the choice of algorithm(s) may depend on the specific use case. If experimental results are to be ranked for a small-scale follow-up experiment, subnetwork ID methods may actually be the preferred choice. Some node

prioritization algorithms that have a strong preference for start nodes (e.g. Random Walk, ToppNet HITS, or GeneMANIA) could also be suitable choices. Alternatively, if the purpose of using a network algorithm is to identify new nodes that may be involved in a disease process or response, Interconnectivity or Hidden Nodes could be better selections. In typical siRNA or CRISPR screening data, for example, nodes with redundant functions may be missed [136]; algorithms with a lower preference for start nodes would be more effective at identifying such missed nodes.

Surprisingly, causal reasoning algorithms performed poorly even in tests of target prediction using Connectivity Map data, which was the type of task these algorithms were developed to do. It is possible that these algorithms rely heavily on network information that is not known with sufficient accuracy, and improved network information in the future may contribute to improved performance of these algorithms.

#### **4.5.2 Effects of network size and confidence on results**

Network size and confidence were investigated here in an indirect manner by using different networks, including a relatively large but lower-confidence network (HithubStringBioplex) and a much smaller but manually-curated, high-confidence network (HithubMetabase). A more direct test of the tradeoff between network size and confidence would be to try including lower-confidence edges, for example from STRING. There would likely be a confidence threshold after which the network becomes too noisy, and larger networks cease to add useful information. Alternatively, one could directly test the effect of network quality by adding random network edges and of network quantity by removing real network edges, although this is less likely to represent how networks are identified in practice.

#### **4.5.3 Biases inherent in gold standard input lists**

In the benchmarking work done here, we used "gold standard" data sets consisting of publicly available genetic associations and pathways. In both cases, because the data did not come directly from an experiment, fold changes and p-values were not

available, so default fold changes of 1 and p-values of 0.05 were used for the genes included in the start lists, and other genes not included in the lists were treated as unmeasured. For algorithms that weight start nodes or consider whether changes in start nodes are positive or negative, these "gold standard" lists omit information that would be available in the use case of actual experimental data.

The networks used here contain information from KEGG, Reactome, or both. Thus the results of the "gold standard" start lists taken from either KEGG or Reactome rely on redundant information. For this reason, benchmarking results using DisGeNET start lists are likely more representative of real data. While Interconnectivity, Overconnectivity, and Network Propagation performed similarly well in DisGeNET and KEGG/Reactome, the relative rankings of some local (Guilt by Association and ToppNet KM) vs. more distant (Random Walk and ToppNet HITS) algorithms were reversed. Using actual experimental data from CRISPR screens, results were more similar to those found using DisGeNET, in which Random Walk and ToppNet HITS outperformed Guilt by Association and ToppNet KM.

Finally, hub nodes tend to be more frequently studied, appear more frequently in KEGG and Reactome pathways, and are actually involved in many different cell processes. In this work, we did not attempt to account for the fact that, while hubs may appear frequently within the pathways or disease-gene associations used as inputs, they may not be specific to one or a few processes and thus may contribute to high scores seen in some algorithms here out of proportion with their usefulness as specific drug targets.



# Chapter 5

## Development of a hydrogel tri-culture system to study intercellular interactions in endometrial tissue

### 5.1 Acknowledgments

Work in this chapter was done in collaboration with Christi Cook. Some figures and text appear in previously published work [34]. In addition, I would like to thank Julia Papps, Linda Stockdale, and Deborah Plana for their experimental contributions, Alex Brown and Marianna Sofman for help with hydrogel protocols, and Deborah Plana for work on implementing the mixed effects model. Confocal images shown here were taken in the Koch Institute Microscopy Core Facility, with assistance from Eliza Vasile.

### 5.2 Introduction

#### 5.2.1 Normal endometrial function

Endometrial tissue is unique in the human body in that it goes through a regular cycle of tissue destruction and regeneration. Endometrial tissue consists of a stro-

mal portion, which contains stromal fibroblasts as well as immune cells and blood vessels, surrounded by a monolayer of epithelial glands. During the menstrual cycle, endometrial tissue proliferates in response to estrogen during the first half of the cycle, then decidualizes in response to progesterone. Decidualization induces secretion of prolactin and IGFBP-1. In the absence of implantation of an embryo, progesterone withdrawal induces menstruation.

### **5.2.2 Endometriosis and adenomyosis**

Endometriosis is defined as endometrial glands and stroma outside of the uterus, and adenomyosis is similarly endometrial glands and stroma within the muscle layer of the uterus. In both cases, lesions have phenotypic differences from eutopic tissue, but eutopic tissue is also different between patients with the diseases vs. without [156, 29]. Specifically, eutopic tissue in patients with endometriosis appears to be less responsive to progesterone signaling [15, 78] and more resistant to apoptosis [42, 12] than in controls.

### **5.2.3 Immune-endometrial crosstalk**

The stromal compartment of endometrial tissue contains a large number of immune cells, particularly macrophages and natural killer (NK) cells [8]. Macrophages, in particular, are critical for both tissue breakdown during menstruation and tissue repair and angiogenesis during the proliferative phase [168], and various immune populations within the endometrium are critical in pregnancy [124]. Previous work has shown that immune cells and endometrial stromal cells communicate through secreted factors, and certain effects of this communication include elevation of genes previously shown to be upregulated in endometriosis [47].

### **5.2.4 Hydrogel models**

Poly(ethylene glycol) (PEG) hydrogel systems have been used previously to model a variety of tissue systems, including liver [129], vasculature [111], neural tissue [5], and

intestine [61]. PEG hydrogels are a fully synthetic and thus more fully controllable alternative to natural matrices such as Matrigel. Modification of PEG with cell adhesion peptides as well as protease-degradable peptides allows for tuning of gel properties to better mimic *in vivo* environments and to facilitate modification of the environment by the cells themselves [39].

## 5.3 Methods

### 5.3.1 Endometrial cell isolation

Endometrial biopsies were obtained from patients undergoing hysterectomy or endometrial biopsy at Newton Wellesley Hospital (NWH) for benign gynecological conditions, including endometriosis, adenomyosis, fibroids, and abnormal uterine bleeding. Exclusion criteria were prior endometrial ablation or uterine artery embolisation, prior endometrial cancer or current chemotherapy, post-menopause, lack of regular cycles, and known infection with HIV or hepatitis. Endometrial stromal and epithelial cells were isolated following the protocol developed by Osteen [133]. Up to three endometrial biopsies per patient were collected with a 3mm Pipelle after induction of anesthesia but before the beginning of surgery. Biopsies were expelled into DMEM/F12 medium and transported from NWH to MIT. Biopsies were then rinsed 2x in DMEM/F12 medium to remove red blood cells. Tissue was then cut into 1-2mm<sup>3</sup> pieces and enzymatically digested in 9.8 mL DMEM/F12 with 200 $\mu$ L chicken serum, 50mg collagenase IV, and 2 mg DNase for 1 hour in a 37°C water bath with periodic vortexing. After digestion, tissue was filtered through 100  $\mu$ m and 70 $\mu$ m filters.

Stromal cells passed through the filters and were further purified by differential sedimentation. Stromal cells were resuspended in 2 mL of DMEM/F12 medium with 10% FBS, then layered drop by drop over 10 mL DMEM/F12 10% FBS. Sedimentation occurred over 30 minutes at 37°C. The top 8 mL (containing stromal cells) were collected and resuspended in 2 mL DMEM/F12 10% FBS, and the sedimentation pro-

cess was repeated. The top 8 mL were again collected and filtered through a 40 $\mu$ m filter to further purify the stromal population. Stromal cells were then expanded in tissue culture plastic over 2 weeks, and red blood cells were further depleted through medium changes.

Epithelial cells were retained on the 100 $\mu$ m and 70 $\mu$ m filters after the first enzymatic digestion. A second enzymatic mix was prepared from 9.8 mL DMEM/F12, 200 $\mu$ L chicken serum, 50mg collagenase IV, 2mg DNase, 10mg hyaluronidase, and 10mg protease. Epithelial cells were backflushed from the filters and resuspended in 5mL of the second enzyme mix, and cells were incubated for 20 minutes in a 30°C water bath. Cells were then filtered through a 70 $\mu$ m filter and again backflushed with the remaining 5mL of the second enzyme mix, then incubated for 30-45 minutes in the 37°C water bath. Epithelial cells were then further purified by differential sedimentation. Cells were resuspended in 2 mL of DMEM/F12 medium with 10% FBS and layered drop by drop over 10mL DMEM/F12 10% FBS. Sedimentation occurred over 30 minutes at 37°C, after which the bottom 2 mL (containing epithelial cells) were retained and sedimentation was repeated. After the second sedimentation, the bottom 2mL were again retained.

### 5.3.2 Cell culture

Ishikawa human adenocarcinoma cells [131] (Sigma-Aldrich) and hTERT-immortalized human endometrial stromal cells (tHESCs)[100] (ATCC) were used as model endometrial epithelial and stromal cell populations. Primary endometrial stromal cells (ESCs) were also maintained in cell culture. All three cell lines were routinely cultured in phenol red-free DMEM/F12 medium with 10% dextran/charcoal-stripped FBS and 1% penicillin-streptomycin in tissue culture plastic, with medium replaced every 2 days. Following reports of possible contamination of endometrial cell lines by HeLa or other lines[99], STR profiling analysis (Genetic Resources Core Facility, Johns Hopkins School of Medicine, Institute of Genetic Medicine) was used to confirm the fidelity of the tHESCs and Ishikawa cell lines against known cell databanks.

### 5.3.3 Monocyte isolation

Peripheral blood was purchased (Research Blood Components, Boston, MA). Peripheral blood mononuclear cells were isolated using Lymphoprep (StemCell Technologies, Cambridge, MA, cat #07811) according to the manufacturer's instructions. Briefly, blood was diluted 1:1 in PBS 2% FBS. 30 mL diluted blood was layered slowly on top of 15 mL Lymphoprep in a 50 mL conical tube without mixing. Blood fractions were separated by centrifuging 20 minutes at room temperature and 800g with the brake off. The buffy coat layer was collected using a Pasteur pipette, then rinsed twice with PBS. Isolated PBMCs were frozen at  $30 \times 10^6$  per mL in 90% FBS 10% DMSO.

On the day on which gels were made, PBMCs were thawed, and monocytes were isolated by negative enrichment (StemCell Technologies, Cambridge, MA, cat #19359). PBMCs were resuspended at  $50 \times 10^6$ /mL in EasySep buffer (StemCell Technologies #20144), then incubated with monocyte isolation and human platelet removal cocktails followed by incubation with magnetic particles. EasySep buffer was added up to 2.5 mL, and cells were placed in an EasySep magnet (StemCell Technologies #18000) for 2.5 minutes, then inverted so that cells that were not bound to magnetic beads (monocytes) could be collected in a second tube. Live cells were counted using trypan blue and a hemocytometer.

### 5.3.4 Gel synthesis

Gels used here are as described in previously published work [34]. Eight-arm, 40kDa PEG macromers functionalized with vinyl sulfone (PEG-VW) were purchased from JenKem Technology (Beijing). Peptides were custom synthesized and purified to >95% by Boston Open Labs (Cambridge, MA): "MMP-CL," a dithiol crosslinking peptide containing a matrix metalloproteinase (MMP)-sensitive substrate, (Ac)GCRD-GPQGIAGQ-DRCG(Am) [135]; "PHSRN-K-RGD," a fibronectin-derived adhesion peptide, (Ac)PHSRNGGGK(Ac)GGGERCG-GGRGDSPY(Am) [20, 101]; "FN-binder," a fibronectin-binding peptide, (Ac)GCRE-TLQPVEYEMVGV(Am) [56]; and "BM-binder," a peptide with affinity for both collagen IV and laminin, (Ac)GCRE-

ISAFGLGIPFAEPPMGPRRFLPPEPKKP(Am) [83]. Peptides were reconstituted in Milli-Q water (Millipore) at 10 mM for adhesion and matrix binding peptides and 45 mM for MMP-CL.

To synthesize the hydrogels, PEG-VS was used at 5 wt%, with 1mM PHSRN-K-RGD and 0.5 mM FN-binder and BM-binder. Peptide-functionalized PEG macromers, "fPEG-VS," were synthesized by incubating peptides with PEG-VS in 1x PBS, 1M HEPES (pH 7.8) buffer for 30 minutes to create macromers with 20% of the -VS groups functionalized with peptide (2 mM final concentration). Peptide incorporation was >99% as assessed by Ellman's reaction, occurring after 30 minutes.

Stromal cells were added to the gel mix before crosslinking at a concentration of 50,000 cells/12  $\mu$ L gel. The fPEG-VS solution was crosslinked with MMP-CL, adjusted to pH 7.8 with 1 M NaOH just prior to addition, in a 0.4 thiol:VS ratio. Hydrogels were prepared on Transwell inserts (Corning cat #3470, polyester, 6.5mm diameter, 0.4 $\mu$ m pores, 0.33 cm<sup>2</sup> area) using Michael-type reaction chemistry.

Hydrogel gelation, as defined by the point at which the solution could no longer be pipetted, occurred approximately 8 minutes after crosslinker addition at pH 7.8, although it varied between 8 and 12 minutes depending on the specific hydrogel formulation. The hydrogel solution was pipetted for 2 minutes to keep stromal cells in suspension, allowed to sit in tube for 3-7 minutes (where wait time = gelation time - 5 minutes), transferred to the transwell inserts (12  $\mu$ L per insert), manually spread with a pipette tip, and then centrifuged for 4 minutes at 330 rcf so that gelation occurred in the middle of centrifugation creating a flat, meniscus-free hydrogel on top of the cell culture inserts. Plates were then incubated an additional 10 minutes at RT to allow crosslinking to proceed to completion. After gelation was complete, DMEM/F12 medium with 10% dextran-charcoal stripped FBS and 1% penicillin-streptomycin was added to the apical (top) (100  $\mu$ L) and basolateral (bottom) (600  $\mu$ L) sides of the transwell inserts to achieve hydrostatic equilibrium. Cultures were maintained in a humidified incubator at 37°C, 95% air, 5% CO<sub>2</sub>.

Endometrial epithelial cells were seeded on top of the hydrogels 24 h after initiation of stromal cultures. Ishikawa cells were harvested via trypsinization, resuspended in

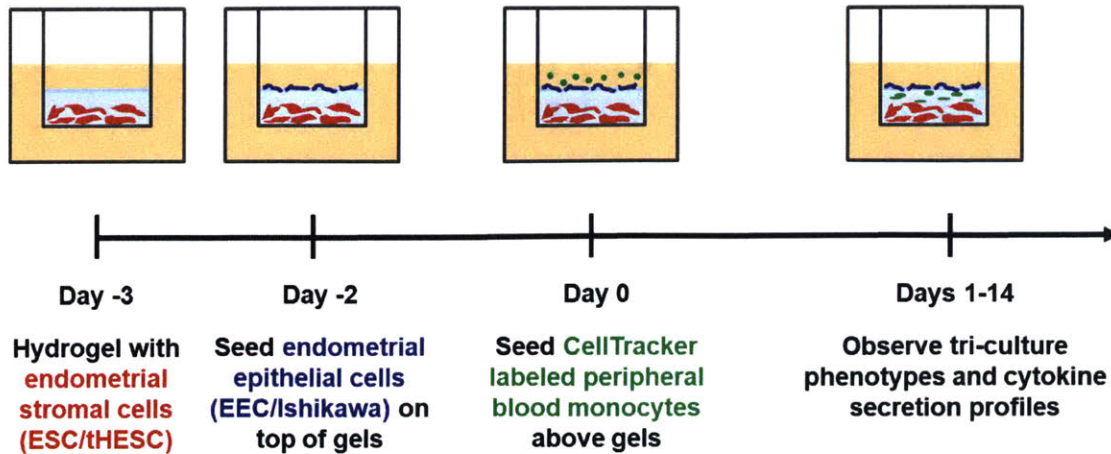


Figure 5-1: Schematic of triculture hydrogel experimental setup.

DMEM/F12/FBS, and seeded at a density of 75,000 cells per Transwell (225,000 cells per cm<sup>2</sup>). Primary epithelial cells were harvested via trypsinization and seeded at 50,000 to 75,000 cells per Transwell (150,000 to 225,000 cells per cm<sup>2</sup>). Apical medium was changed 24 h after seeding to remove non-adherent epithelial cells. On day 3 of co-culture, medium was changed to maintenance media comprising DMEM/F12 supplemented with 1% DC-FBS, 1% penicillin/ streptomycin, and 2% Cell Maintenance Supplement (Cocktail B) (LifeTechnologies CM4000) on the apical side (100  $\mu$ L) and Williams E Medium (LifeTechnologies A1217601) supplemented with 1% penicillin/streptomycin, 4% Cell Maintenance Supplement (Cocktail B) (LifeTechnologies cat #CM4000) and 100 nM hydrocortisone (Sigma cat #50-23-7) on the basolateral side (600  $\mu$ L), with changes every 2 to 3 days thereafter.

Monocytes were isolated two days after gel synthesis. When cell tracker was used to image monocytes, they were stained following isolation in a 1:1000 dilution in PBS for 30 minutes at 37°C, then rinsed in apical medium. Isolated monocytes were counted using trypan blue and added to the gels in apical medium at a concentration of  $1 \times 10^6$  cells/mL. Medium was changed after 2 days, removing monocytes that did not adhere to the gel during that time.

### 5.3.5 Imaging

At the end of the culture period, gels were fixed using 4% paraformaldehyde (Electron Microscopy Sciences) in PHEM buffer for 1 hour at room temperature, permeabilized in 0.2% TritonX-100 in PBS for 30 minutes, and blocked either overnight at 4°C or 1 hour at room temperature in 1% BSA (Sigma) in PBS. Hydrogels were incubated overnight while rocking at 4°C with CD68 or CD206 antibodies and rhodamine phalloidin (1:1000) (Life Technologies). Gels were then rinsed 3x with blocking buffer. Nuclei were stained with DAPI (1:1000) (Life Technologies) for 15 minutes at room temperature. Hydrogels were then rinsed 3 times with 1x PBS and rocked overnight at 4°C. Hydrogels were cut out of the transwell insert and mounted using Prolong Gold Antifade (Life Technologies cat #P36935) on glass coverslips.

Phase and fluorescent images were acquired using a Leica DMI 6000 microscope with Oasis Surveyor software. Confocal images were acquired using a Nikon A1R Ultrafast Spectral Scanning Confocal Microscope with Nikon NIS Elements acquisition software.

### 5.3.6 Cytokine Measurements

Concentrations of 27 cytokines, chemokines, and growth factors were measured in undiluted conditioned medium using cytokine panel I (Bio-Rad, cat #) adapted for use in a 384 well plate. Samples were run in technical duplicate. In addition, a standard curve generated by a series of 10 serial 1:3 dilutions of the manufacturer-provided standard was run in triplicate for quantification of cytokine levels in the samples. Beads were diluted 1:20 (twice the manufacturer's dilution) and added at 20 $\mu$ L per well (instead of 50 $\mu$ L). Washes were performed with PBS 0.1% tween-20 using a magnetic plate washer (BioTek 405LS), and residual liquid was removed after each wash using a hand-held magnetic bead separation block (V&P Scientific, cat #VP771HH-Q) . Samples and beads were incubated overnight at 4°C on a plate shaker instead of 30 minutes at room temperature to complete binding. Detection antibody was diluted 1:20 (twice the manufacturer's dilution) at added at 7.5 $\mu$ L per

well (instead of ). Streptavidin-PE was added at the manufacturer's recommended dilution at  $25\mu\text{L}$  per well. The assay was read using the BioPlex FLEXMAP 3D system (Bio-Rad Laboratories), and data were collected with xPONENT version 4.2 (Luminex Corporation).

For each cytokine, 5-parameter logistic curves were fit to the standards (including blanks) using the L5P function in MATLAB (MathWorks) [23]. Curve fits were used to calculate concentrations for each sample replicate. Median fluorescence intensities (MFI) for the samples below the lower asymptote or above the upper asymptote of the fit were imputed to be either the MFI of the minimum asymptote or 99% of the MFI of the maximum asymptote, respectively. Values reported in tables are the mean of 2 technical replicates for the Luminex assay and the number of gel replicates ( $n$ ) specified in figures/tables. Concentrations that fell above the highest standard but below the maximum asymptote (due to incomplete coverage of the quantifiable range by the standard curve) were judged to be unreliable; these values are given as greater than the concentration of the highest standard and excluded from statistical testing.

### 5.3.7 Principal Components Analysis

Principal components analysis was used to identify the main sources of differences in cytokine environments found in apical medium of hydrogels with different cell combinations [81]. Data input were z-scored cytokine concentrations from tHESC/Ishikawa/monocyte gels on days 6 and 12 after monocyte addition. Principal components analysis was performed using the `pca.m` function in MATLAB (The Mathworks, Natick, MA).

### 5.3.8 Mixed effects model

A mixed effects model was constructed to find the contributions of individual cell types and interactions between cell types, and to account for random effects associated with repeated trials [31]. For each cytokine, the data was fit using `fitlme` in MATLAB 2015b to the formula:

'Concentration = 1 + mono + tHESC + Ishikawa + day + mono:tHESC + mono:Ishikawa + tHESC:Ishikawa + mono:tHESC:Ishikawa + mono:day + tHESC:day + Ishikawa:day + mono:tHESC:day + mono:Ishikawa:day + tHESC:Ishikawa:day + mono:tHESC:Ishikawa:day + (1|trial) + (1|trial:mono) + (1|trial:tHESC) + (1|trial:Ishikawa) + (1|trial:day) + (1|trial:mono:tHESC) + (1|trial:mono:Ishikawa) + (1|trial:tHESC:Ishikawa) + (1|trial:mono:tHESC:Ishikawa) + (1|day:trial:mono) + (1|day:trial:tHESC) + (1|day:trial:Ishikawa) + (1|trial:day:mono:tHESC) + (1|trial:day:mono:Ishikawa) + (1|trial:day:tHESC:Ishikawa) + (1|day:trial:mono:tHESC:Ishikawa)'

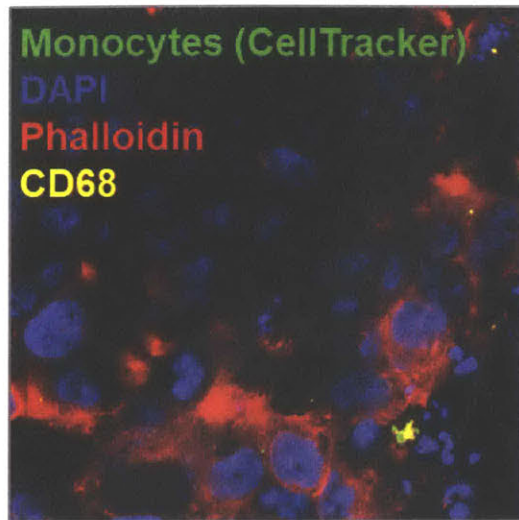
Fixed effects were presence/absence of Ishikawa cells, tHESCs, monocytes, and day of cell culture as well as combinations of those factors. Random variables were trial and all terms containing trial. For each cytokine, a model was fit using all terms, then each term was omitted and a set of models were fit to the subset of terms. The best model was then selected using the Akaike Information Criterion (AIC). From the reduced model, each term was again omitted to generate a new set of models, from which one was selected by AIC. This process was repeated until removing a term did not reduce the AIC.

## 5.4 Results

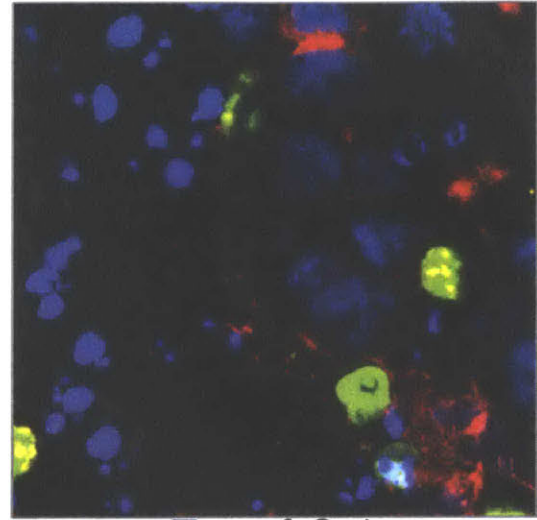
### 5.4.1 Monocytes survive, invade, and differentiate into macrophages in endometrial hydrogels.

Cell tracker-stained monocytes were added to gels with encapsulated tHESC and an Ishikawa monolayer at a concentration of 100,000/100 $\mu$ L apical medium for each gel. Gels were fixed after 7 days of triculture, and confocal microscopy showed that monocytes were present both at and below the epithelial monolayer at the top of the gel (Fig 5-2). Additionally, monocytes stained positively for CD68, indicating differentiation towards macrophages [167].

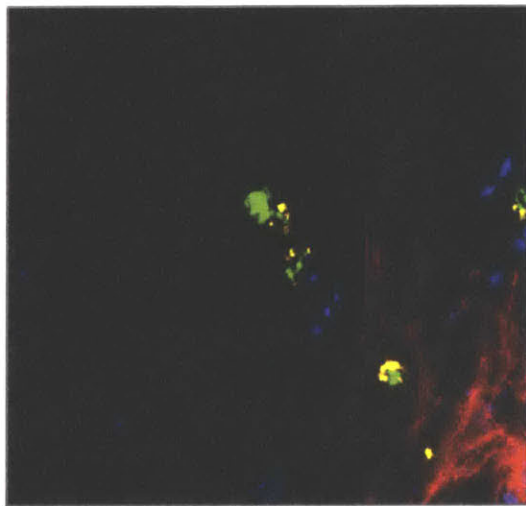
To determine whether monocytes require interactions with other cells to be able to attach or migrate into the gels, monocytes were added to gels with and without



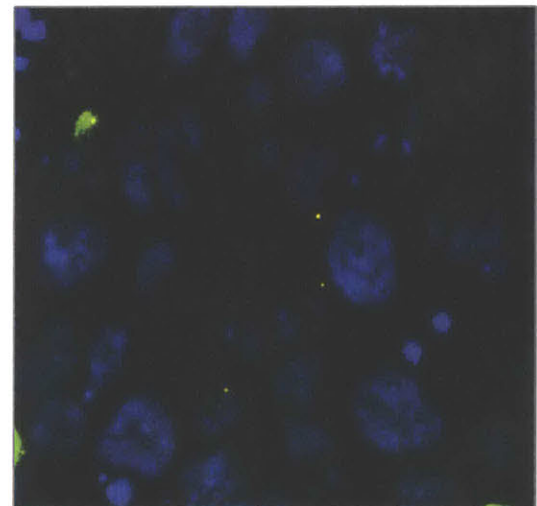
Top of Gel



Top of Gel



Interior of Gel



Interior of Gel

Figure 5-2: Monocytes survive, migrate into the gel, and differentiate in the presence of endometrial cells.

## Monocytes persist during 10 days of culture

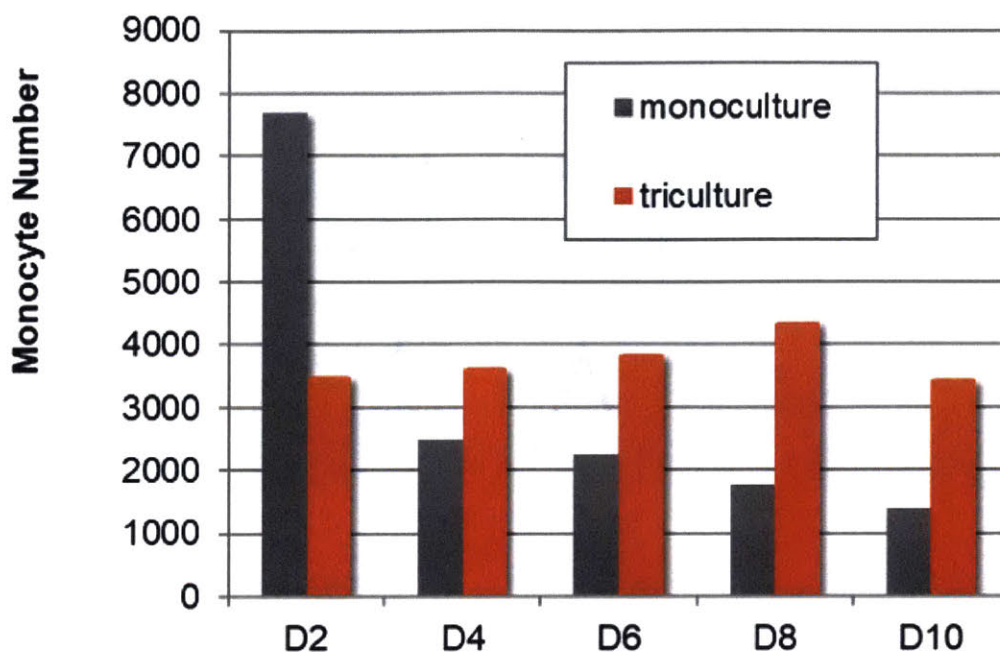


Figure 5-3: Monocytes are retained in culture over time in the presence of endometrial cells.

endometrial cells. After 10 days in culture, imaging revealed that more monocytes were retained on gels with endometrial cells than on "empty" gels, suggesting that either physical contact with or chemotactic signaling from endometrial cells induces monocyte adhesion and/or invasion into the gels. In addition, monocyte-derived cells in the triculture gels expressed CD206, a marker of alternative macrophage activation (ref), while monocytes remaining in the otherwise cell-free gels remained rounded rather than spread and did not express CD206, suggesting a lesser degree of differentiation/activation in the absence of endometrial cells.

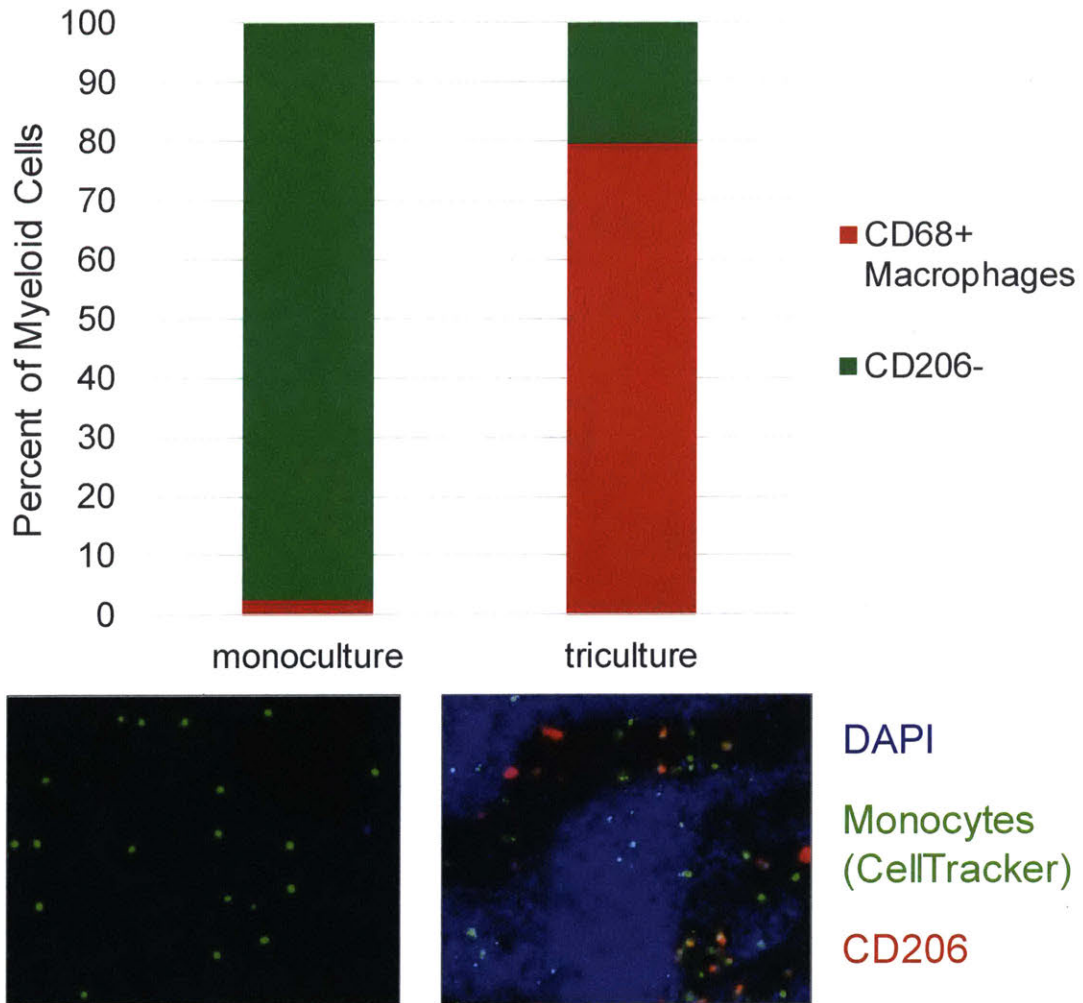


Figure 5-4: Monocytes differentiate into macrophages and express CD206 in the presence of endometrial cells.

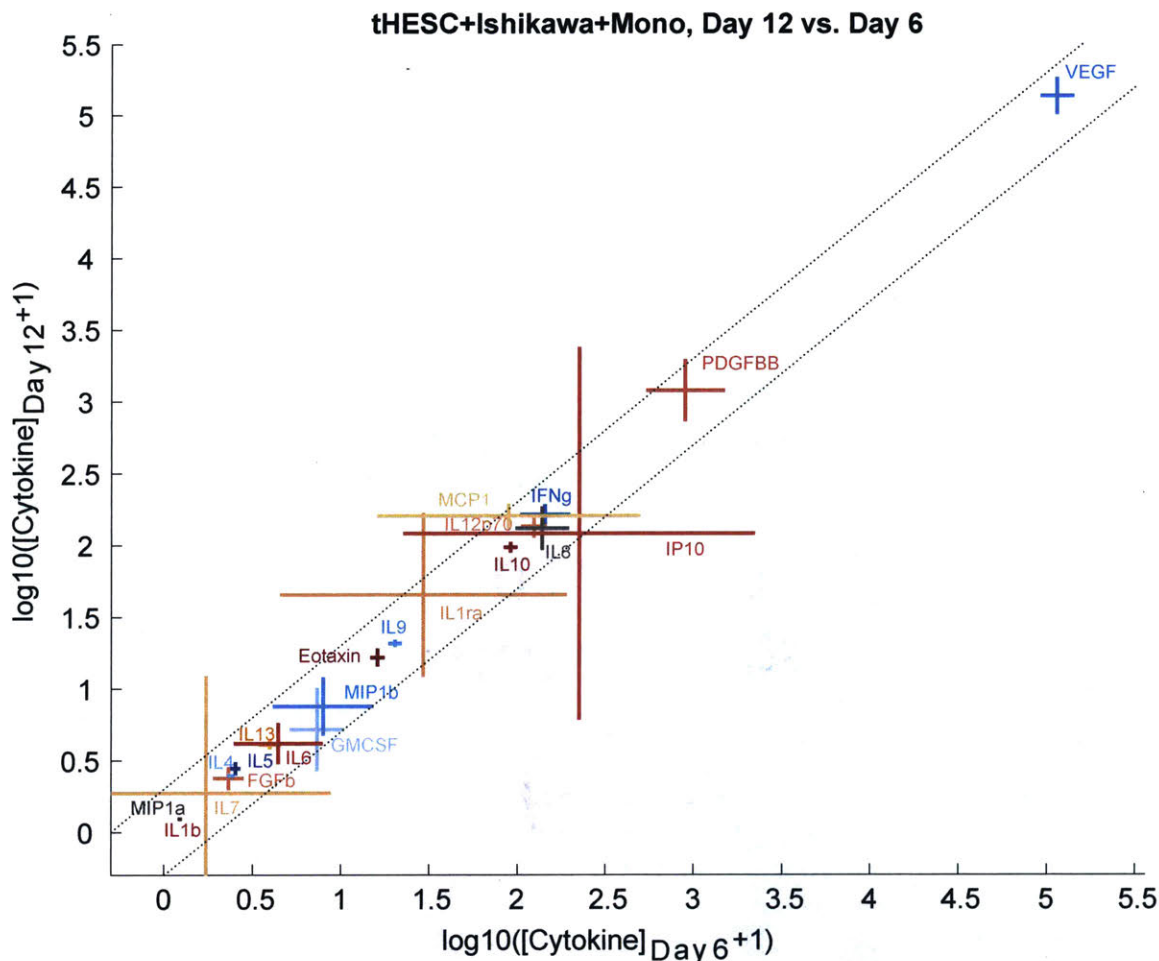


Figure 5-5: Apical cytokine concentrations are stable over time. Each cytokine is centered at the mean of three replicate gels of three monocyte donors each, with error bars representing standard deviations. A two-fold (or half-fold) change is indicated by dashed lines.

#### 5.4.2 Cytokine secretion is stable over time

Cytokine concentrations in apical medium were measured on day 6 and day 12 of coculture. In general, net cytokine production was found to be consistent over time, with less than a 2-fold change over that time period (Fig. 5-5). Additional experiments using tHESC and Ishikawa cells only also showed similar cytokine concentrations on days 4, 8, and 12 of coculture. In the absence of hormonal or inflammatory stimuli or other perturbations, cytokine secretion (in concert with any uptake of cytokines or regulatory feedback loops) seem to be stable.

### 5.4.3 Apical and basal cytokine environments differ

To further investigate properties of the endometrial triculture system, we measured cytokine levels in the basal medium as well as the apical compartment. In the absence of communication among the cell types included, two transport-based null hypotheses existed: (1) cytokines can diffuse freely across the gel, in which case apical and basal concentrations should be equal, or (2) no diffusion occurs across the gel, in which case uniform secretion would result in a 6-fold dilution of cytokines in the basal medium (600 $\mu$ L) compared to the apical medium (100 $\mu$ L). Most cytokines fell within two-fold of one of these two hypotheses, indicated by dashed and dotted lines (Fig. 5-6). Cytokines that were higher than expected in basal medium compared to apical medium included RANTES, G-CSF, IL-15, IL-17A, and IL-7.

### 5.4.4 Cytokine profiles are cell-type dependent

To understand the role of each cell type and cell-cell interactions, hydrogels were made with each individual cell type alone and in combination. For most of the 27 cytokines measured, Ishikawas were the primary secreters (Fig. 5-7).

Principal components analysis showed that the main source of variance in apical cytokine measurements was the presence or absence of Ishikawa cells (PC1, 35% variance explained), which confirmed what was observed qualitatively based on univariate cytokine measurements. Monocytes and tHESCs did not have a large effect on the overall cytokine environment, likely because the total number of monocytes remaining in the gel system by the time the measurements were made, 10,000 monocytes and 50,000 tHESCs, was small compared to the 75,000 Ishikawa cells, and because the Ishikawa cells both physically blocked diffusion of tHESC- and monocyte-secreted cytokines into the apical component and were themselves in close proximity to the apical medium.

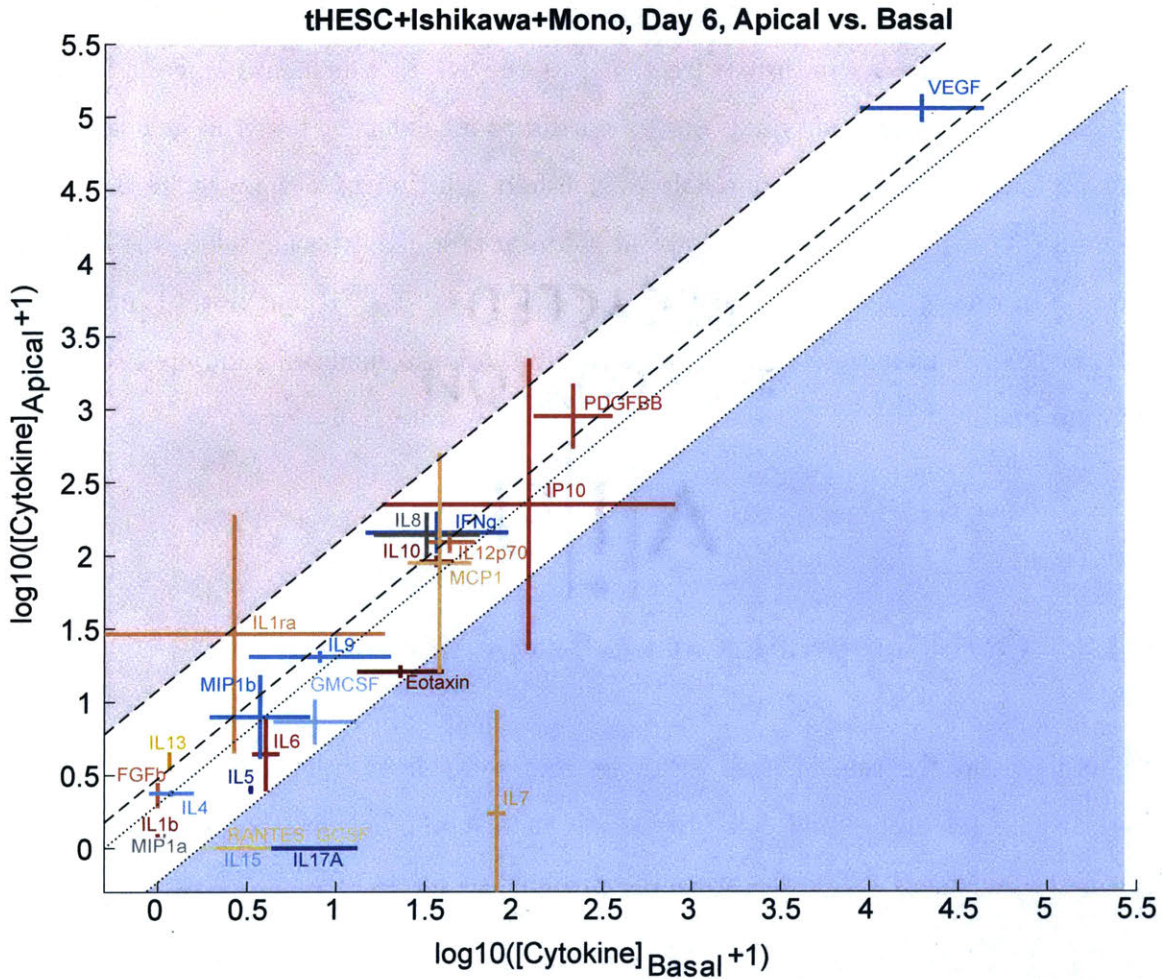


Figure 5-6: Apical and basal concentrations may be affected by diffusion, binding within the gel, dilution effects, and polarized secretion. Dotted lines represent roughly equal concentrations in apical and basal medium, corresponding to free/fast diffusion across the gel. Dashed lines represent roughly 6-fold higher concentrations in the apical medium, as would be expected from dilution effects if diffusion was negligible and production of cytokines was constant across the gel volume.

### Single cell types and triculture

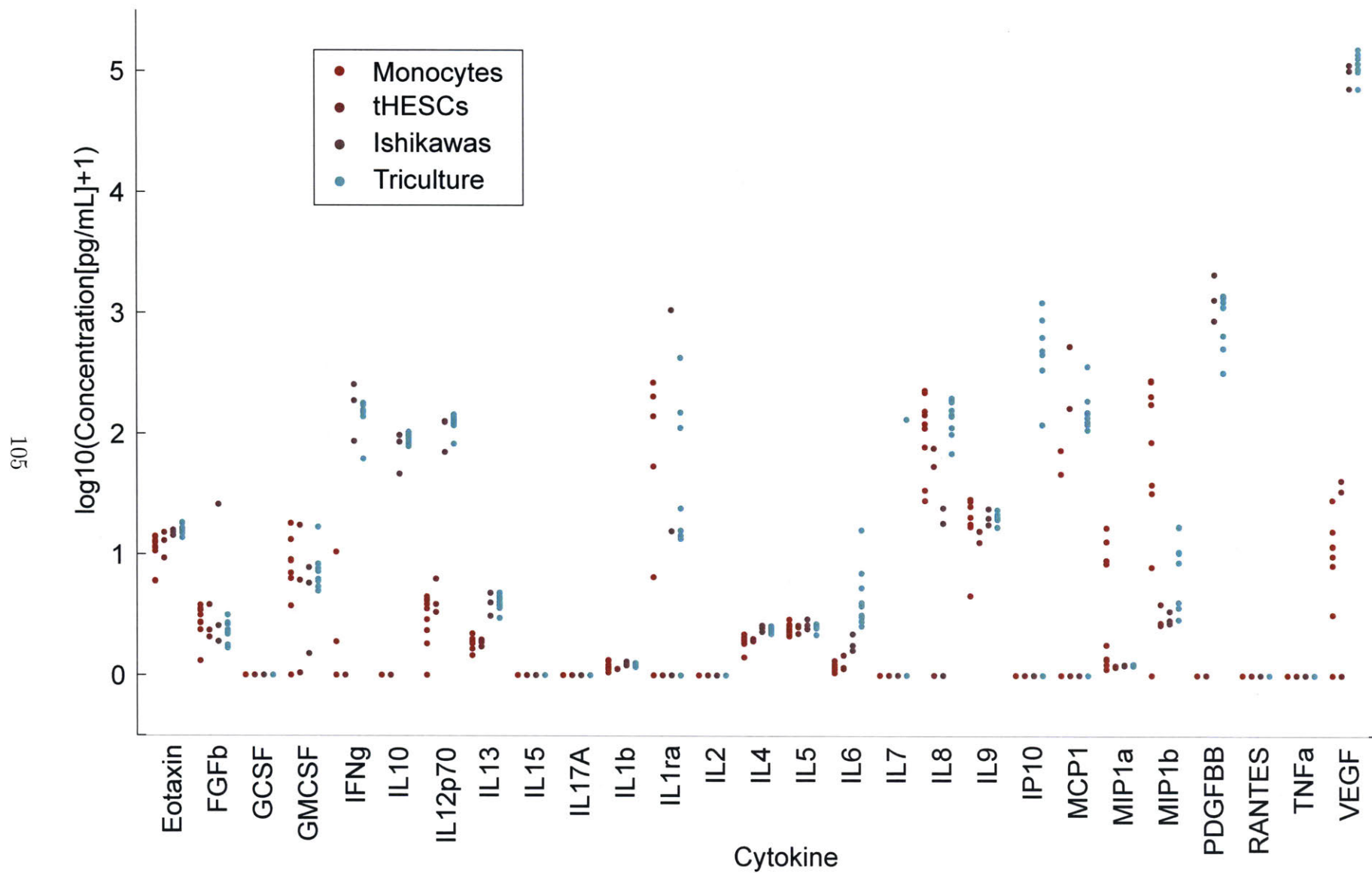


Figure 5-7: Monocytes are retained in culture over time in the presence of endometrial cells.

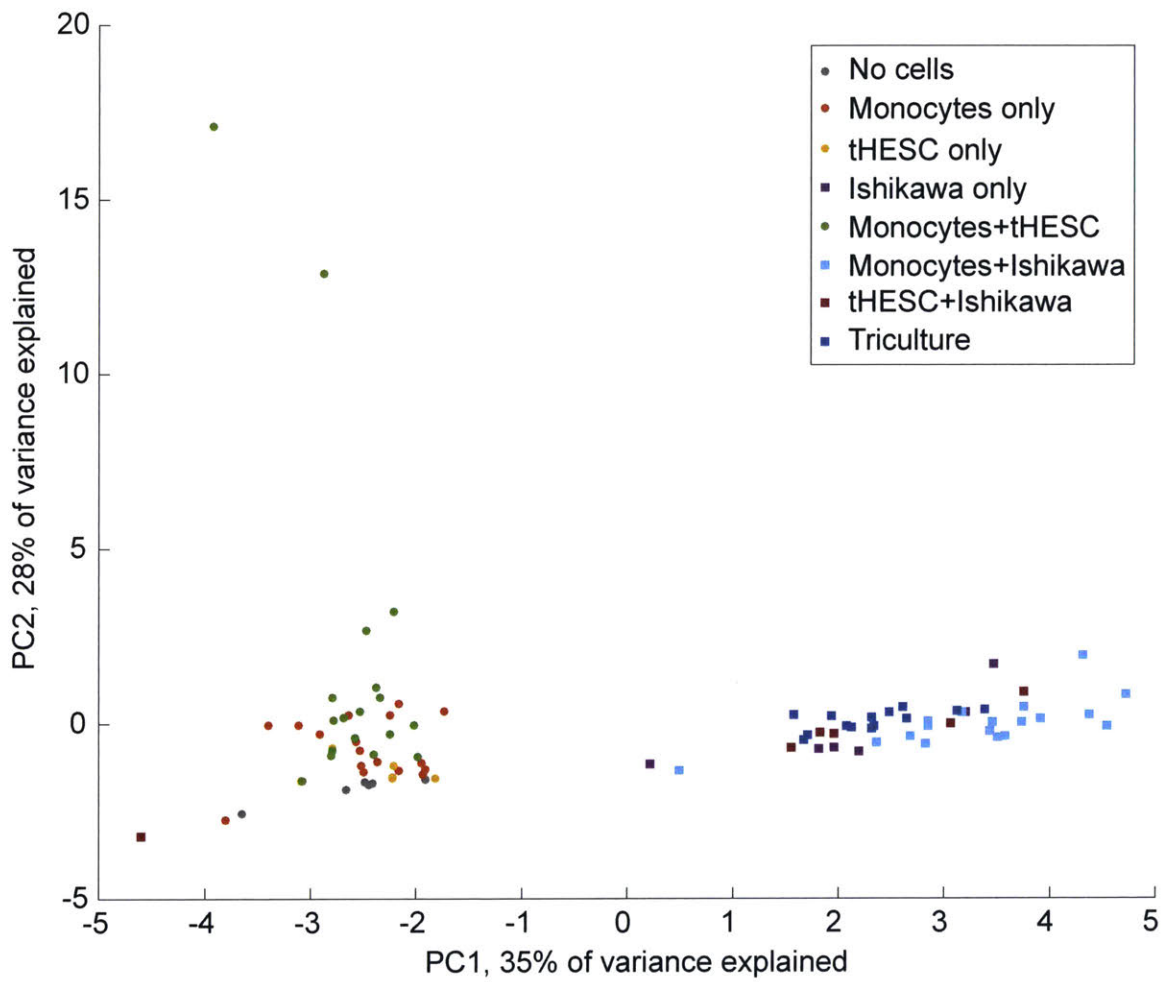


Figure 5-8: Ishikawa cells are the predominant factor in determining cytokine environment in tHESC/Ishikawa/Monocyte triculture hydrogels.

### 5.4.5 Evidence of cell-cell communication in cytokine signaling

Mixed effects modeling was employed to determine the degree to which cell-cell interactions affected the overall cytokine environments. While Ishikawa cells again had a large positive effect on secretion of many cytokines, coefficients of two-cell interactions (tHESC:Mono, Ish:Mono, and Ish:tHESC) were also important, and coefficients of three-cell interactions (Ish:tHESC:Mono) had the largest negative effects on the overall cytokine milieu, indicating that some negative feedback may occur amongst the three cell types (Fig. 5-9).

### 5.4.6 Cell lines vs. primary cells

In the experiments discussed here, primary monocytes were combined with cell lines representing endometrial stromal and epithelial cells. To determine whether cell lines were in fact appropriate models of the behavior of primary cells, we compared apical cytokine measurements from hydrogels prepared with Ishikawas and tHESCs to the apical cytokine measurements from primary cell gels (Fig. 5-10 A). Out of the 27 cytokines measured, few were similar between primary cells and cell lines (IL-1, IL-10, and IL-9). Four out of the 27 were lower in primary cells (IL-13, IL-12p70, VEGF, and PDGF-BB), all of which were secreted highly by Ishikawa cells. All other measured cytokines were either higher in the primary cell cultures or only detectable in the primary cell cultures, indicating that primary cells are capable of a much broader range of cytokine secretion than are the cell lines. Of particular interest for communication between the endometrial cells and macrophages, cytokines known to affect macrophage differentiation and activation phenotypes are qualitatively different between primary cells and cell lines, with many cytokines higher in primary cells (G-CSF, GM-CSF, IL-4, TNF-a), but others unchanged (IL-10) or lower (IL-13).

In addition, primary cells were stimulated with cAMP and MPA to induce decidualization. While previous experiments using tHESC and Ishikawa cell line co-cultures showed no significant effects of hormone stimulation on cytokine secretion, primary cells from one subject showed significant increases in IL-10 and IL-15 with decid-

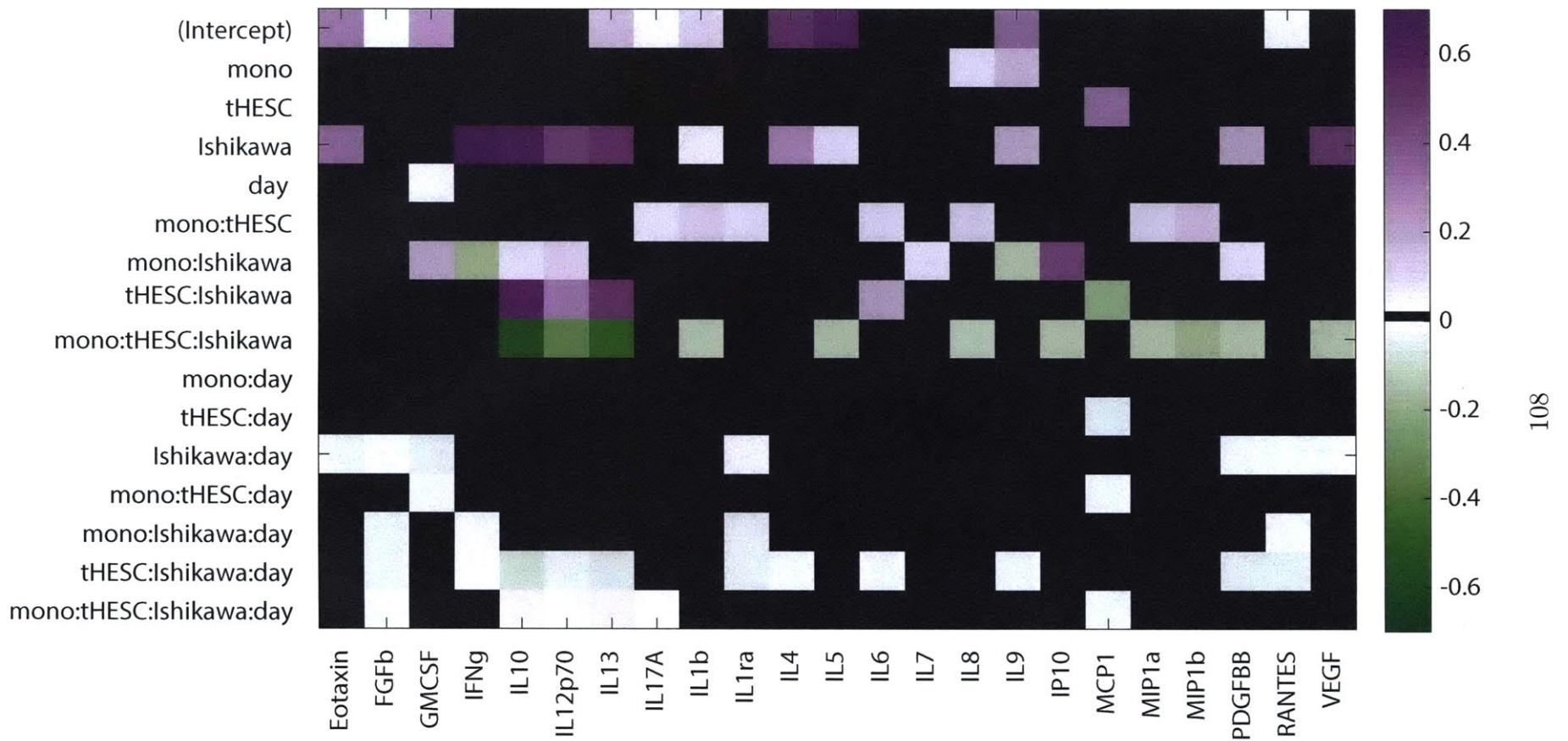


Figure 5-9: Coefficients for terms in mixed effects model indicate substantial effects of three-cell interactions.

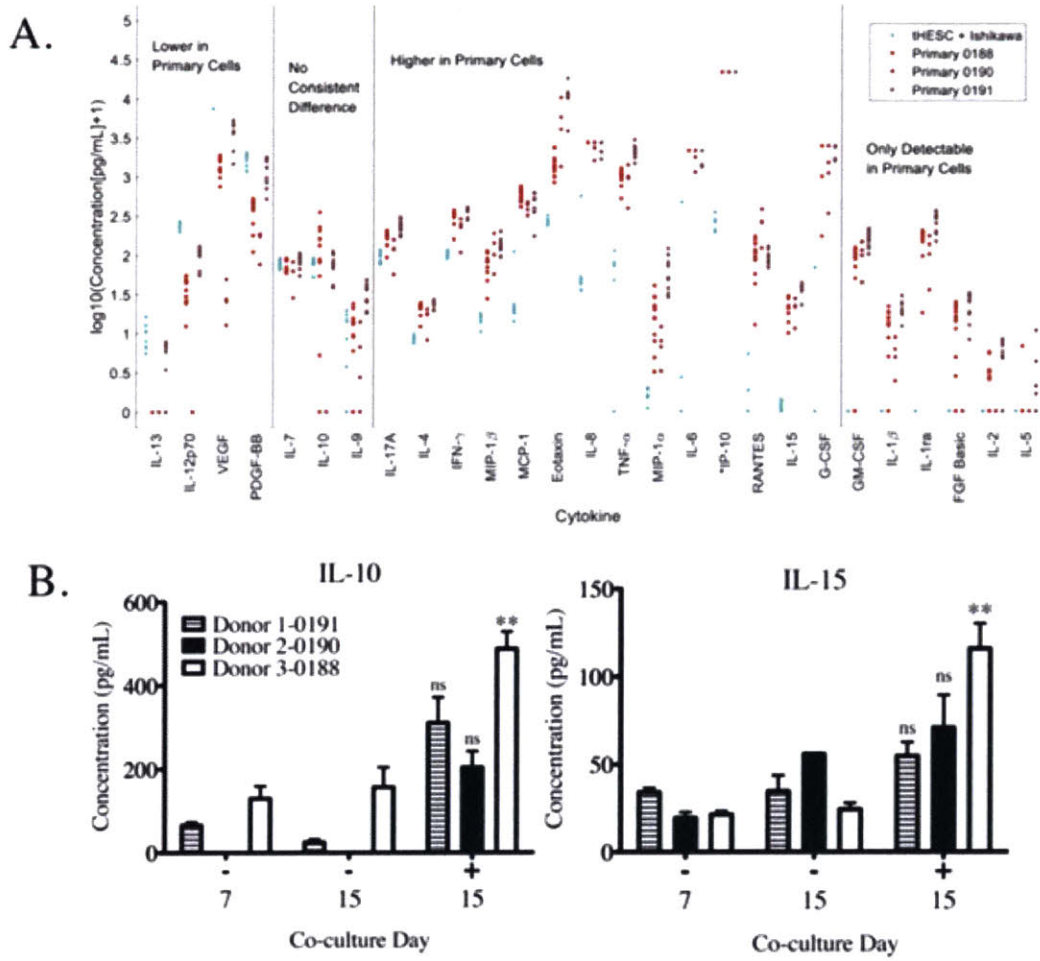


Figure 5-10: Primary cells secrete more cytokines than cell lines.

ualization, and the other two subjects had qualitatively similar effects (Fig. 5-10 B).

## **5.5 Discussion and Conclusions**

### **5.5.1 Importance of multicellular interactions in representing tissue biology**

Previous work has also suggested an important role for 3-cell interactions[148]. Interestingly, our previous work investigating two cell types in the immune system, CD4+ T cells and monocytes, showed primarily synergistic effects on cytokine secretion due to interactions between the two cell types [154]. However, in this system, multiple cytokines were observed to be lower in triculture than the sum of concentrations of that cytokine in the three monocultures.

### **5.5.2 Alternative methods for model selection**

The initial full formula for the mixed effects model used here included 32 terms, meaning that there were  $2^{32}$  (or over 4 billion) possible reduced models. Because the space was so large, not all possible models could be tested. The approach used here, removing one term at a time to give the lowest AIC, finds a local minimum but not necessarily a global minimum across all possible sets of terms. Genetic algorithms are also not guaranteed to find a global minimum, but adding terms back in at random allows for the model to "jump" from one AIC valley to another, increasing the probability that a global minimum will be found [172].

### **5.5.3 Primary endometrial cells differ from cell lines in cytokine secretion**

In the endometrial coculture system, primary ESC and EEC were much more active cytokine producers than were the tHESC and Ishikawa cell lines. While primary cells

are more difficult to handle and are obtained in limited quantities, it appears that cell lines may not be representative of primary endometrial cell behavior. In addition, eutopic endometrium has been shown to differ between healthy and endometriosis patients [156, 29], so primary cells may be useful for differentiating between healthy and disease conditions. Future work investigating cytokine communication between monocytes and endometrial cells should be done using primary cells, where sample availability allows.

#### **5.5.4 Confounding effects complicate use of transwell system for studying cell-cell communication**

In this system, the different spatial location of the three cell types makes it difficult to say with certainty which cytokine effects are due to active communication among the cell types as opposed to physical barrier or diffusion effects. Because the epithelial monolayer on top of the gel may affect levels of cytokines not only through soluble factor-mediated communication with the other cell types but also through uptake of certain cytokines or by blocking diffusion into the apical medium, it is not possible to isolate actual communication events. Similarly, cytokines secreted by the epithelial cells may be secreted in a polarized manner, and would need to diffuse through the height of the gel in order to be detected in the basal medium.

#### **5.5.5 Methods for more physiological addition of monocytes**

In the experiments discussed here, monocytes were added to the apical side of gels representing endometrial tissue, and we observed that monocytes subsequently migrated into the stromal compartment, where they would be found *in vivo*. However, *in vivo*, monocytes would migrate into the endometrial tissue by extravasating from blood vessels within the stromal compartment, not from the lumen side of the tissue. A possible extension of this system would be to have endothelial cells seeded on the bottom side of a transwell, then add the encapsulated stromal cells in hydrogel into the inside of the transwell, seed epithelial cells on top of the stromal hydrogel, and

then add monocytes into the basal compartment, possibly with some fluid movement [64, 43, 27].

# Chapter 6

## Development of an endometriosis/adenomyosis lesion model

### 6.1 Introduction

#### 6.1.1 Endometriosis

Endometriosis is a common cause of pelvic pain and infertility for which study has been limited relative to its prevalence and economic impact on society [158]. Current therapies include either hormonal medication, with often undesirable side effects, or surgery. Development of additional therapies has been hindered by lack of understanding of disease pathophysiology and the low availability of suitable models [66]. Due to the importance of cyclic hormonal changes in endometrial tissue, it is necessary to follow tissue phenotypes over time, which is not feasible for human patients[63]. Few animals other than humans undergo menstruation, limiting animal models to either non-human primates, commonly baboons [41], or other animal models such as mice in which endometriosis is induced in a more artificial manner [65, 16].

In order to better understand the physiology of endometriosis, we aimed to modify a previously developed model of eutopic endometrial tissue to better represent

endometriosis or adenomyosis lesions[34]. Lesions differ from healthy eutopic endometrial tissue in three main ways: (1) although epithelial glands do retain apical and basal polarization, entire lesions lack a clear apical and basal side, with glands mixed into the stromal compartment; (2) lesions have a more inflammatory environment; and (3) lesions have increased influx of immune cells, including macrophages [153].

### 6.1.2 Dysregulation of signaling in endometriosis

While current therapies for endometriosis consist of either hormonal medication or surgery, evidence that both intra- and inter-cellular signaling are dysregulated suggests that additional therapeutic avenues may exist. Previous work from our lab investigated inflammatory cytokine signaling in peritoneal fluid samples using unsupervised clustering through non-negative matrix factorization and found a cytokine signature (IL-8, RANTES, MIF, IL-6, MCP-1, G-CSF, MIG, HGF, IL-10, IL-16, IL-1ra, GRO $\alpha$ , and IL-1 $\beta$ ) associated with more severe endometriosis[9]. Other groups have similarly reported dysregulation of cytokine signaling in endometriosis [25, 49].

A number of intracellular signaling pathways have also been implicated in the pathogenesis of endometriosis. Following from the work that identified macrophage-secreted cytokines associated with endometriosis symptoms, Beste et al. tested a panel of kinase inhibitors and found that c-Jun inhibition most substantially decreased inflammatory cytokines [9]. Inhibition of c-Jun using bentimipimod was also shown to reduce the size (although not the number) of lesions in an induced lesion baboon model [75]. Increased phosphorylation of AKT has been observed in cultured stromal cells from endometriosis patients [92], and inhibition of AKT improved decidualization of cultured endometrial stromal cells from endometriosis patients[185]. Within the MAPK pathway, p38 was shown to decrease lesion size in mice [186], and pERK displayed less cycle variation in eutopic or ectopic endometrial cells from patients with endometriosis [126]. As endometriosis is known to involve inflammatory processes, it is likely that JAK/STAT signalling may play a role in the response to aberrant cytokine signalling in endometriosis. STAT3, specifically, has been shown to be phosphorylated

in eutopic endometrium of women with endometriosis [91].

While conflicting reports exist in the literature as to which pathways might make for the most relevant targets in endometriosis, the large number of pathways reported to be involved suggests that targeting intracellular signaling related to cytokine networks may be fruitful in the search for additional treatments for endometriosis.

### 6.1.3 Prior use of *in vitro* hydrogel models

Properties of natural tissues/matrices: Three-dimensional hydrogel culture systems have increasingly allowed for more complete representations of tissue environments *in vitro*. Specifically, hydrogels allow for the presentation of physical cues, localization of soluble factors secreted by cells, and multidirectional cell-cell interactions [114].

Several natural matrices have been used for *in vitro* 3D culture systems. Matrigel is a complex mixture of extracellular proteins produced by Engelbreth-Holm-Swarm sarcoma in mice. While it has the advantage of being a complete natural matrix, it has the disadvantages of not being chemically defined, containing unknown amounts of various growth factors, originating from a cancer cell line rather than from healthy cells, and having large variability between lots [178, 74]. Other natural matrices used *in vitro* include collagen and fibrin gels, both of which are more well-defined than Matrigel but lack many components of natural tissue matrices. Within the last 25 years, however, synthetic hydrogels including poly(ethylene glycol) (PEG) have been used for various *in vitro* applications. PEG gels are functionalized with RGD and other cell adhesion peptides as well as protease-degradable crosslinkers to allow cells to migrate and create 3D structures within the gel and peptides capable of binding cell-secreted matrix proteins [135, 142, 187].

Prior applications of functionalized PEG hydrogels include use with both stromal and epithelial cells, including for the study of fibroblast migration [11] and epithelial morphogenesis [30]. The use of cell-responsive synthetic hydrogels is intended to allow for physiological behavior of both stromal and epithelial cells as well as immune cells [115, 34].

### 6.1.4 Prior use of multicellular *in vitro* systems

As tissues generally consist of many cell types organized into a three-dimensional structure, several groups have previously attempted to model tissues using multicellular systems. Recent examples include a microfluidic triculture of endothelial cells, pericytes, and astrocytes to model transport across the blood-brain barrier [180]; mono-, co-, and tri-culture conditions to study the importance of multicellular interactions among breast cancer, stromal, and immune cells impact gene expression[148]; and a multicellular model to study drug resistance[104].

## 6.2 Methods

### 6.2.1 Endometrial cell isolation

Endometrial biopsies were obtained from patients undergoing hysterectomy or endometrial biopsy at Newton Wellesley Hospital (NWH) for benign gynecological conditions, including endometriosis, adenomyosis, fibroids, and abnormal uterine bleeding. Exclusion criteria were prior endometrial ablation or uterine artery embolisation, prior endometrial cancer or current chemotherapy, post-menopause, lack of regular cycles, and known infection with HIV or hepatitis. Endometrial stromal and epithelial cells were isolated following the protocol developed by Osteen [133]. Up to three endometrial biopsies per patient were collected with a 3mm or 4mm Pipelle after induction of anesthesia but before the beginning of surgery. Biopsies were expelled into DMEM/F12 medium and transported from NWH to MIT. Biopsies were then rinsed 2x in DMEM/F12 medium to remove red blood cells. Tissue was then cut into 1-2mm<sup>3</sup> pieces and enzymatically digested in 9.8 mL DMEM/F12 with 200 $\mu$ L chicken serum, 50mg collagenase IV, and 2 mg DNase for 1 hour in a 37°C water bath with periodic vortexing. After digestion, tissue was filtered through 100  $\mu$ m and 70 $\mu$ m filters.

Stromal cells passed through the filters and were further purified by differential sedimentation. Stromal cells were resuspended in 2 mL of DMEM/F12 medium with

10% FBS, then layered drop by drop over 10 mL DMEM/F12 10% FBS. Sedimentation occurred over 30 minutes at 37°C. The top 8 mL (containing stromal cells) were collected and resuspended in 2 mL DMEM/F12 10% FBS, and the sedimentation process was repeated. The top 8 mL were again collected and filtered through a 40 $\mu$ m filter to further purify the stromal population. Stromal cells were then expanded in tissue culture plastic over 2 weeks, and red blood cells were further depleted through medium changes. During gel synthesis, stromal cells were trypsinized and counted using trypan blue.

Epithelial cells were retained on the 100 $\mu$ m and 70 $\mu$ m filters after the first enzymatic digestion. A second enzymatic mix was prepared from 9.8 mL DMEM/F12, 200 $\mu$ L chicken serum, 50mg collagenase IV, 2mg DNase, 10mg hyaluronidase, and 10mg protease. Epithelial cells were backflushed from the filters and resuspended in 5mL of the second enzyme mix, and cells were incubated for 20 minutes in a 30°C water bath. Cells were then filtered through a 70 $\mu$ m filter and again backflushed with the remaining 5mL of the second enzyme mix, then incubated for 30-45 minutes in the 37°C water bath. Epithelial cells were then further purified by differential sedimentation. Cells were resuspended in 2 mL of DMEM/F12 medium with 10% FBS and layered drop by drop over 10mL DMEM/F12 10% FBS. Sedimentation occurred over 30 minutes at 37°C, after which the bottom 2 mL (containing epithelial cells) were retained and sedimentation was repeated. After the second sedimentation, the bottom 2mL were again retained. A 100 $\mu$ L aliquot of epithelial cells was taken for counting. Cells from this aliquot were resuspended in 100 $\mu$ L trypsin-EDTA, incubated at 37°C until cells were mostly single cells rather than glands, then counted. Epithelial cells were used on the day of biopsy collection.

### **6.2.2 Monocyte isolation**

Peripheral blood from female donors was purchased (Research Blood Components, Boston, MA). Peripheral blood mononuclear cells were isolated using Lymphoprep (StemCell Technologies, Cambridge, MA, cat #07811) according to the manufacturer's instructions. Briefly, blood was diluted 1:1 in PBS 2% FBS. 30 mL diluted

blood was layered slowly on top of 15 mL Lymphoprep in a 50 mL conical tube without mixing. Blood fractions were separated by centrifuging 20 minutes at room temperature and 800g with the brake off. The buffy coat layer was collected using a Pasteur pipette, then rinsed twice with PBS. Isolated PBMCs were frozen at  $30 \times 10^6$  per mL in 90% FBS 10% DMSO. On the day on which gels were made, PBMCs were thawed, and monocytes were isolated by negative enrichment (StemCell Technologies, Cambridge, MA, cat #19359). PBMCs were resuspended at  $50 \times 10^6$ /mL in EasySep buffer (StemCell Technologies #20144), then incubated with monocyte isolation and human platelet removal cocktails followed by incubation with magnetic particles. EasySep buffer was added up to 2.5 mL, and cells were placed in an EasySep magnet (StemCell Technologies #18000) for 2.5 minutes, then inverted so that cells that were not bound to magnetic beads (monocytes) could be collected in a second tube. Live cells were counted using trypan blue and a hemocytometer.

### 6.2.3 Triculture hydrogels

Hydrogels used here were adapted from previously published work [34, 171]. Eight-arm, 20kDa PEG macromers functionalized with norbornene (PEG-N) were purchased from JenKem Technology (Beijing). Peptides were custom synthesized and purified to >95% by Boston Open Labs (Cambridge, MA): "MMP-CL," a dithiol crosslinking peptide containing a matrix metalloproteinase (MMP)-sensitive substrate, (Ac)GCRD-LPRTG-GPQGIAGQ-DRCG(Am) [135, 171]; "PHSRN-K-RGD," a fibronectin-derived adhesion peptide, (Ac)PHSRNGGK(Ac)GGGERCG-GGRGDSPY(Am) [20, 101]; "FN-binder," a fibronectin-binding peptide, (Ac)GCRE-TLQPVYEYMGV(Am) [56]; and "BM-binder," a peptide with affinity for both collagen IV and laminin, (Ac)GCRE-ISAFLGIPFAEPPMGPRRFLPPEPKK(Am) [83]. Peptides were reconstituted in Milli-Q water (Millipore) at 10 mM for adhesion and matrix binding peptides and 15wt/wt% for MMP-CL.

PEG-N was used at 3 wt%, crosslinked with the dithiol MMP-CL at a stoichiometric ratio of 0.5 thiols per norbornene. PHSRN-K-RGD was added at a nominal concentration of 1 mM, and FN-binder and BM-binder were added at 0.5 mM. Gel mix

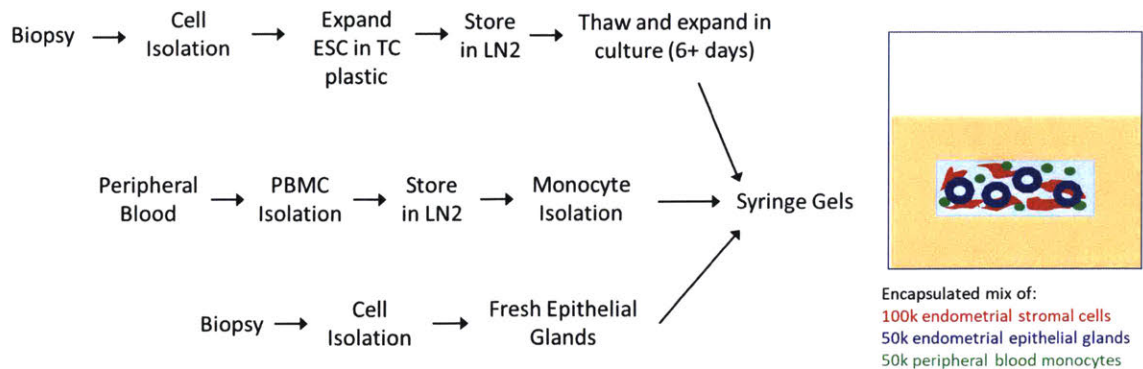


Figure 6-1: Addition of cells to syringe gels.

was prepared with 10x PBS plus milliQ water such that the overall salt concentration was equivalent to 1x PBS. Cells were added at a concentration of 100,000 ESC, 50,000 EEC, and 50,000 monocytes per 20 $\mu$ L gel. Unless otherwise indicated, IRGACURE 2959 (Ciba cat #0298913AB) was used as a photoinitiator at 0.1 wt%. Gels were prepared in 1mL syringes with the tips cut off at the 0.1mL mark, and 20 $\mu$ L gel mix were added per syringe. Crosslinking was induced by exposure to 75 mW/cm<sup>2</sup> UV for 45 seconds. Gels were then removed from the syringes and placed into DMEM/F12 medium containing 1% dextran-charcoal stripped FBS, 1% penicillin/streptomycin, 1 $\mu$ M  $\beta$ -estradiol, and 100 $\mu$ M ascorbic acid.

#### 6.2.4 Hormonal stimulation and inhibitor treatment

Triplicate gels (using cells from the same set of donors) were used for each stimulation/inhibitor condition. All gels were cultured for 2 days in base medium (DMEM/F12 supplemented with 1% dextran-charcoal stripped FBS, 1% penicillin/streptomycin, 1 $\mu$ M  $\beta$ -estradiol, and 100 $\mu$ M ascorbic acid). On day 2 of culture, gels were either moved to fresh base medium or induced to decidualize by exposure to base medium plus (conc) 8-Br-cyclic AMP (cAMP) (Sigma cat #B5386) + (conc) medroxyprogesterone acetate (MPA) (Sigma cat #M1629). A subset of gels were additionally inflamed to induce a more lesion-like phenotype by exposure to (conc) IL-1 $\beta$ . Gels were moved to fresh medium of the same type on day 4. On day 6, JNK inhibitor (Millipore Sigma, Darmstadt, Germany, cat #420128) at 100 $\mu$ M, 10 $\mu$ M, or 1 $\mu$ M or

Akt inhibitor (Millipore Sigma, cat #A6730) at  $10\mu\text{M}$ ,  $1\mu\text{M}$ , or  $0.1\mu\text{M}$  was added to treated gels, with 1% DMSO added to untreated decidualized gels as a control. Conditioned medium was frozen at  $-20^{\circ}\text{C}$  every two days, each time the gels were moved to fresh medium. Before the first assay, samples were thawed on ice and clarified by centrifugation for 15 minutes at  $2755\text{g}$  and  $4^{\circ}\text{C}$ , and the supernatant was collected in a 96-well plate for further assays.

### 6.2.5 LDH assays

Lactate dehydrogenase was measured as a relative readout of cell death. As a positive control, gels were killed by UVC-irradiation ( $254\text{ nm}$ ) using a dose of  $5\text{ J}/\text{cm}^2$  from a UVGL-58 handheld UV lamp on day 2 [188], and medium was also collected from the killed gels on days 4, 6, and 8. LDH was measured using the CytoTox 96 assay (Promega #TB163) adapted by reducing the volume to fit into a 384-well plate. Clarified conditioned medium samples were thawed on ice and diluted 1:5 in PBS, and all samples were run in technical duplicate.  $12\mu\text{L}$  of diluted sample and  $12\mu\text{L}$  of substrate mix were added to each sample well in a clear 384-well plate, and the plate was incubated 30 minutes at room temperature on a plate rotator protected from light. After the incubation,  $12\text{ uL}$  stop solution were added to each well, and absorbance was measured at  $490\text{nm}$  and  $680\text{nm}$ . LDH absorbance was taken to be the absorbance at  $490\text{nm}$  minus absorbance at  $680\text{nm}$  to correct for plate defects. Corrected absorbance was then normalized to the mean corrected absorbance from the UV-killed gels on day 4 (2 days after UV irradiation), assuming that those gels had undergone near-complete cell death.

### 6.2.6 Prolactin and IGFBP-1 ELISAs

Prolactin was measured in conditioned medium using the human prolactin DuoSet ELISA kit (R&D Systems, cat #DY682) and ELISA ancillary reagent kit (R&D Systems, cat #DY008) adapted for use in a 384 well plate. A black-walled, clear-bottom 384-well plate was coated with  $23\mu\text{L}/\text{well}$  capture antibody diluted in PBS

according to the manufacturer's instructions and incubated overnight at 4°C on a plate rotator. The plate was washed 3x with PBS 0.1% tween-20, and blocked with 46µL/well of PBS 1% BSA for 2 hours at room temperature. Samples were thawed on ice and diluted 1 to in PBS. The plate was washed 3x with PBS 0.1% tween-20, and 23µL of diluted sample were added per well. Samples were run in technical duplicate. In addition, an 8-point standard curve was generated using the manufacturer-provided standard. Samples were incubated overnight at 4°C on a plate rotator. Detection antibody was diluted in PBS 1% BSA according to the manufacturer's instructions. The plate was then washed again 3x, and 23µL diluted detection antibody were added per well. Detection antibody was incubated 2 hours at room temperature on the plate rotator. The plate was washed 3x, and 23µL diluted streptavidin-HRP were added per well and incubated 20 minutes at room temperature. A mix of 50% Substrate Reagent A and 50% Substrate Reagent B was prepared, and 23µL were added per well. Once the highest standards had turned purple, stop solution (2N H<sub>2</sub>SO<sub>4</sub>) was added at 11.5µL/well.

IGFBP-1 was measured in conditioned medium using the human IGFBP-1 DuoSet ELISA kit (R&D Systems, cat #DY871) and ELISA ancillary reagent kit (R&D Systems, cat #DY008) adapted for use in a 384 well plate. A black-walled, clear-bottom 384-well plate was coated with 23µL/well capture antibody diluted in PBS according to the manufacturer's instructions and incubated overnight at 4°C on a plate rotator. The plate was washed 3x with PBS 0.1% tween-20, and blocked with 46µL/well of PBS 5% tween-20 for 2 hours at room temperature. Samples were thawed on ice and diluted 1 to x in PBS. The plate was washed 3x with PBS 0.1% tween-20, and 23µL of diluted sample were added per well. Samples were run in technical duplicate. In addition, an 8-point standard curve was generated using the manufacturer-provided standard. Samples were incubated overnight at 4°C on a plate rotator. Detection antibody was diluted in PBS 5% tween-20 2% normal goat serum according to the manufacturer's instructions. The plate was then washed again 3x, and 23µL diluted detection antibody were added per well. Detection antibody was incubated 2 hours at room temperature on the plate rotator. The plate was washed 3x,

and  $23\mu\text{L}$  diluted streptavidin-HRP were added per well and incubated 20 minutes at room temperature. A mix of 50% Substrate Reagent A and 50% Substrate Reagent B was prepared, and  $23\mu\text{L}$  were added per well. Once the highest standards had turned purple, stop solution (2N  $\text{H}_2\text{SO}_4$ ) was added at  $11.5\mu\text{L}/\text{well}$ .

Absorbance for both ELISA plates was measured at 450nm and 540nm. Absorbance at 450nm was corrected by subtracting the absorbance at 540nm to correct for plate defects. Results were quantified by fitting 4 parameter logistic curves to the standards using the L4P function [24] in MATLAB 2015b (The Mathworks, Natick, MA).

### 6.2.7 Cytokine measurements

Concentrations of 27 cytokines, chemokines, and growth factors were measured in undiluted conditioned medium using cytokine panel I (Bio-Rad, cat #) adapted for use in a 384 well plate. Samples were run in technical duplicate. In addition, a standard curve generated by serial 1:3 dilutions of the manufacturer-provided standard was run in triplicate for quantification of cytokine levels in the samples. Beads were diluted 1:20 (twice the manufacturer's dilution) and added at  $20\mu\text{L}$  per well (instead of  $50\mu\text{L}$ ). Washes were performed with PBS 0.1% tween-20 using a magnetic plate washer (BioTek 405LS), and residual liquid was removed after each wash using a hand-held magnetic bead separation block (V&P Scientific, cat #VP771HH-Q). Samples and beads were incubated overnight at  $4^\circ\text{C}$  on a plate shaker instead of 30 minutes at room temperature to complete binding. Detection antibody was diluted 1:20 (twice the manufacturer's dilution) at added at  $7.5\mu\text{L}$  per well (instead of ). Streptavidin-PE was added at the manufacturer's recommended dilution at  $25\mu\text{L}$  per well. The assay was read using the BioPlex FLEXMAP 3D system (Bio-Rad Laboratories), and data were collected with xPONENT version 4.2 (Luminex Corporation). Median fluorescence intensities (MFI) were converted to absolute concentrations via calibration to ninepoint standard curves using the L5P function [23] in MATLAB R2015b (The Mathworks).

## 6.2.8 Network modeling

A generic protein-protein interaction network was downloaded from STRING v10[162]. Interactions were selected for high confidence and experimental evidence. To filter the network according to the cell types of interest, gene expression data from GEO was obtained for primary endometrial stromal cells (GSM423834) [120], primary endometrial epithelial cells (GSM1174412) [140], and primary peripheral blood monocytes (GSM422109) [3]. Cell-cell interactions were obtained from Ramilowski et al. [146] and also filtered by gene expression. A random walk algorithm was used to find nodes (potentially including intracellular signaling pathways and potential drug targets) closely related to hormone signalling and the cytokines affected by the IL-1 $\beta$ -induced endometriotic environment [21, 97]. Start nodes were cytokines significantly different between decidualized and decidualized + IL-1 $\beta$  stimulated gels as well as the two markers of decidualization, IGFBP-1 and prolactin, and the estrogen and progesterone receptors.

## 6.3 Results

### 6.3.1 Cell survival in primary triculture hydrogels

Several gel compositions were tested to identify a formulation that would gel consistently and withstand proteolytic degradation by the mixture of cells (primary endometrial stromal and epithelial cells and peripheral blood monocytes) over the course of 8+ days (Table 6.1. These gels are a modification of previously published work [34] (Table 6.2). Additionally, the ratio of epithelial to stromal cells was decreased from previous work [34] both to better represent lesion composition and because primary epithelial cells appear to proteolytically degrade the hydrogels more quickly than did the Ishikawa cells.

Overall cell death, as normalized to gels that were UV-treated to intentionally kill the cells, was between 6 and 69%, with highest cell death generally occurring early on in the culture period (Fig. 6-2). Decidualization and stimulation with IL-1 $\beta$  did

PEG wt%	PI wt%	SynK-RGD	BM binder	FN binder	Xlink Ratio	Gel Quality
3	0.05	1	0.5	0.5	0.5	Did not gel
3	0.1	1	0.5	0.5	0.5	Good
3	0.5	1	0.5	0.5	0.5	Good
4	0.1	1	0.5	0.5	0.5	Good
4	0.5	1	0.5	0.5	0.5	Hard to manipulate

Table 6.1: Gel formulations and overall gel quality.

Property	Endometrial Gels [34]	Lesion Gels
Gel Type	Transwell	Free-floating
Gel Volume	12 $\mu$ L	20 $\mu$ L
PEG	40 kDa PEG-VS	20 kDa PEG-N
Wt% PEG	5	3
X-link Ratio	0.4	0.5
W-link Method	pH	UV + photoinitiator
SynK-RGD (mM)	1	1
BM-binder (mM)	0.5	0.5
FN-binder (mM)	0.5	0.5

Table 6.2: Comparison of endometrial vs. lesion hydrogel systems.

not increase cell death as measured by LDH, although treatment with the highest concentration of Akt inhibitor (100  $\mu$ M) did increase LDH release substantially over the control condition (E2 only).

To determine whether cell death could be reduced by use of a different photoinitiator, we did a comparison of Irgacure and LAP (Fig. 6-3). Using the same intensity and duration of UV (which may be able to be titrated to lower levels for one or both of the photoinitiators), Irgacure-initiated gels had lower overall LDH release than did LAP-initiated gels at 2, 4, 6, and 8 days after gel synthesis. Continued gel synthesis was thus performed using Irgacure.

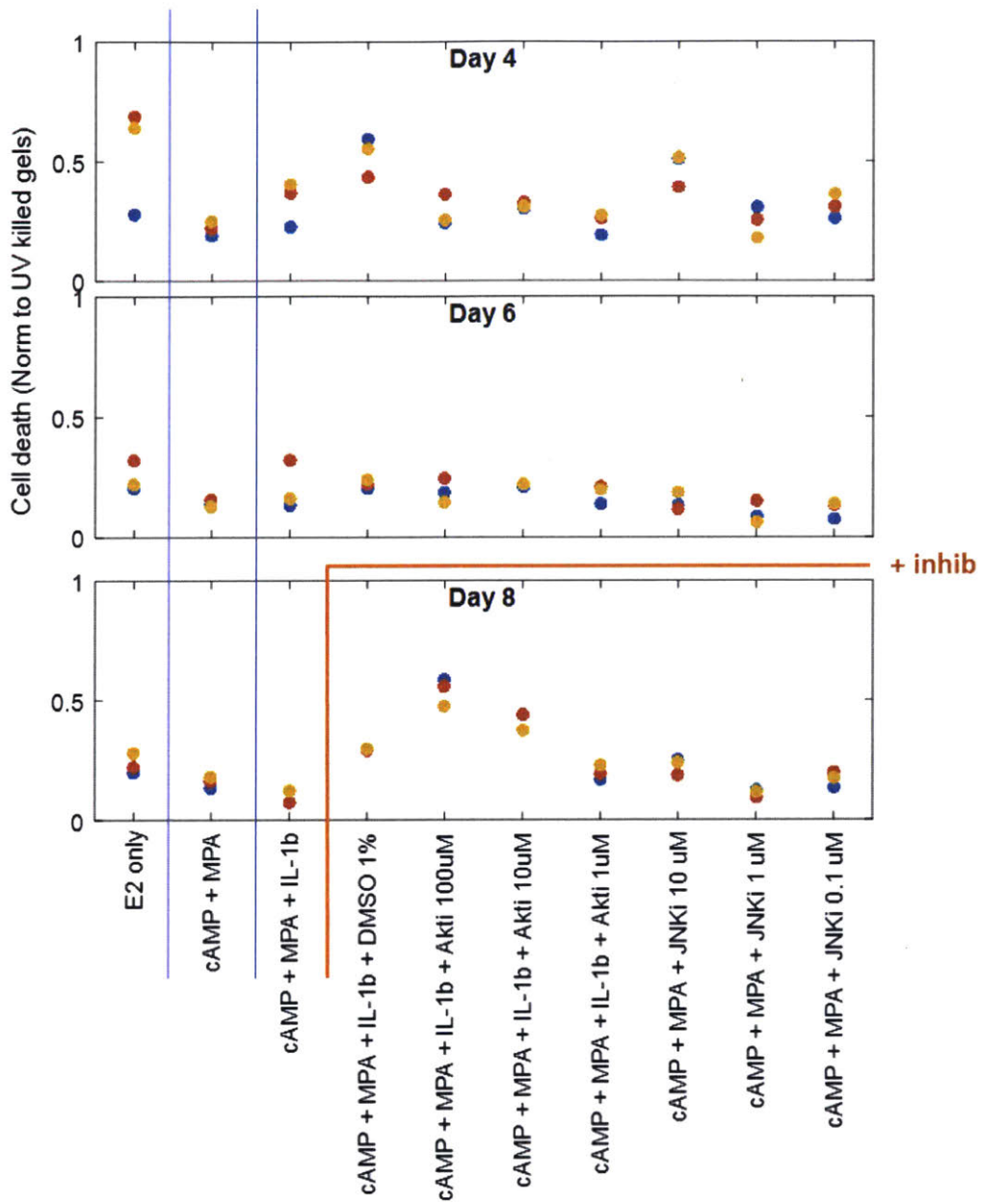


Figure 6-2: Cell death in syringe gels over time and treatment condition.

## Photoinitiator comparison: Cell death

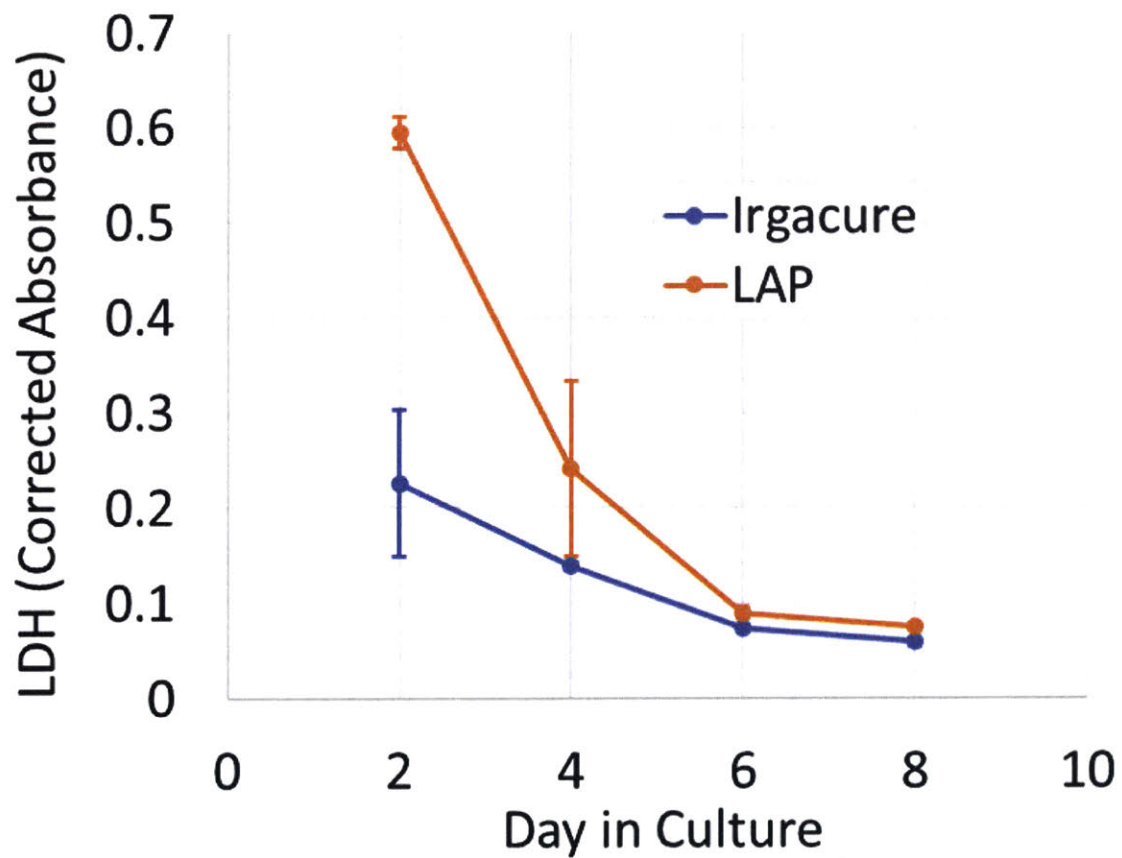


Figure 6-3: Cell death is higher in gels with LAP as the photoinitiator vs. Irgacure under the same UV conditions.

### **6.3.2 Primary triculture hydrogels respond to hormone stimulation**

To induce decidualization, gels were stimulated with cAMP + MPA every two days beginning on the second day of culture. Decidualization response as measured by either IGFBP-1 or prolactin secretion was detectable by the first medium change after stimulation, on day 4, and continued through the end of the culture period on day 8 (Fig. 6-4, first two conditions from the left).

### **6.3.3 IL-1 $\beta$ -induced inflammation decreases hormone response, and hormone responsiveness is not rescued by JNK or Akt inhibitor treatment**

IL-1 $\beta$  stimulation beginning at the same time as decidualization stimuli decreased the effect of cAMP and MPA on both IGFBP-1 and prolactin secretion (Fig. 6-4, third condition from left). Three concentrations each of JNK inhibitor and AKT inhibitor were added on day 6 (after 4 days of hormonal and IL-1 $\beta$  stimulation), but neither inhibitor had a positive effect on decidualization response as measured by either IGFBP-1 or prolactin on day 8 (after 2 days of inhibitor treatment) (Fig. 6-4, bottom plots).

### **6.3.4 Cytokine communication profiles**

Initially, we aimed to identify cytokines that were affected by decidualization, and to further find a subset of those cytokines for which the effect of decidualization was attenuated by IL-1 $\beta$ -induced inflammation. cAMP + MPA decreased medium concentrations of many cytokines, consistent with the anti-inflammatory properties of progestins (Fig. 6-5).

While hormone response was not improved by treatment of either inhibitor tested here, a few cytokines demonstrated more similar responses to cAMP + MPA stimulus in the presence of IL-1 $\beta$  plus inhibitors compared to IL-1 $\beta$  alone (Fig. 6-6). TNF $\alpha$ ,

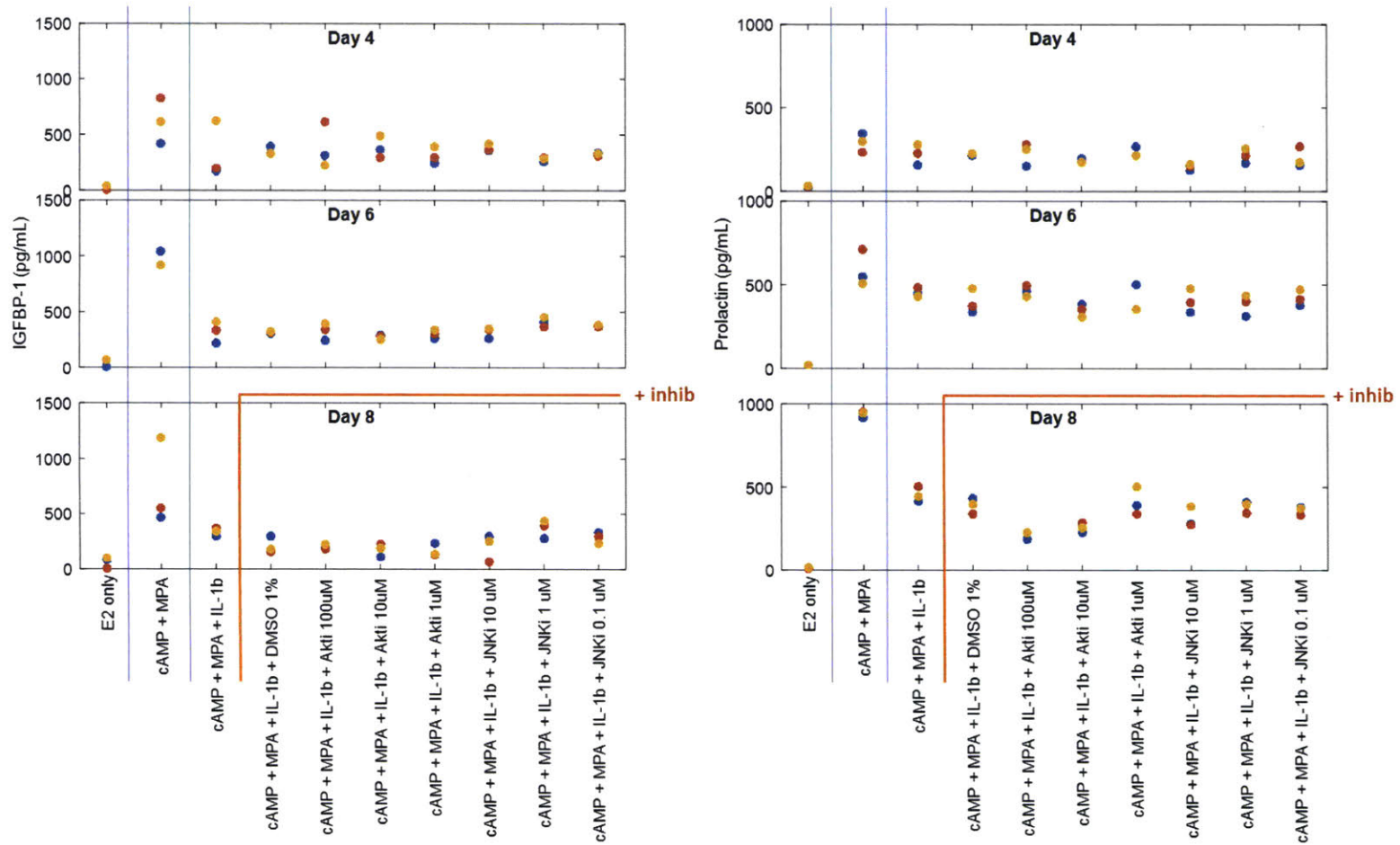


Figure 6-4: Decidualization response in triculture gels.

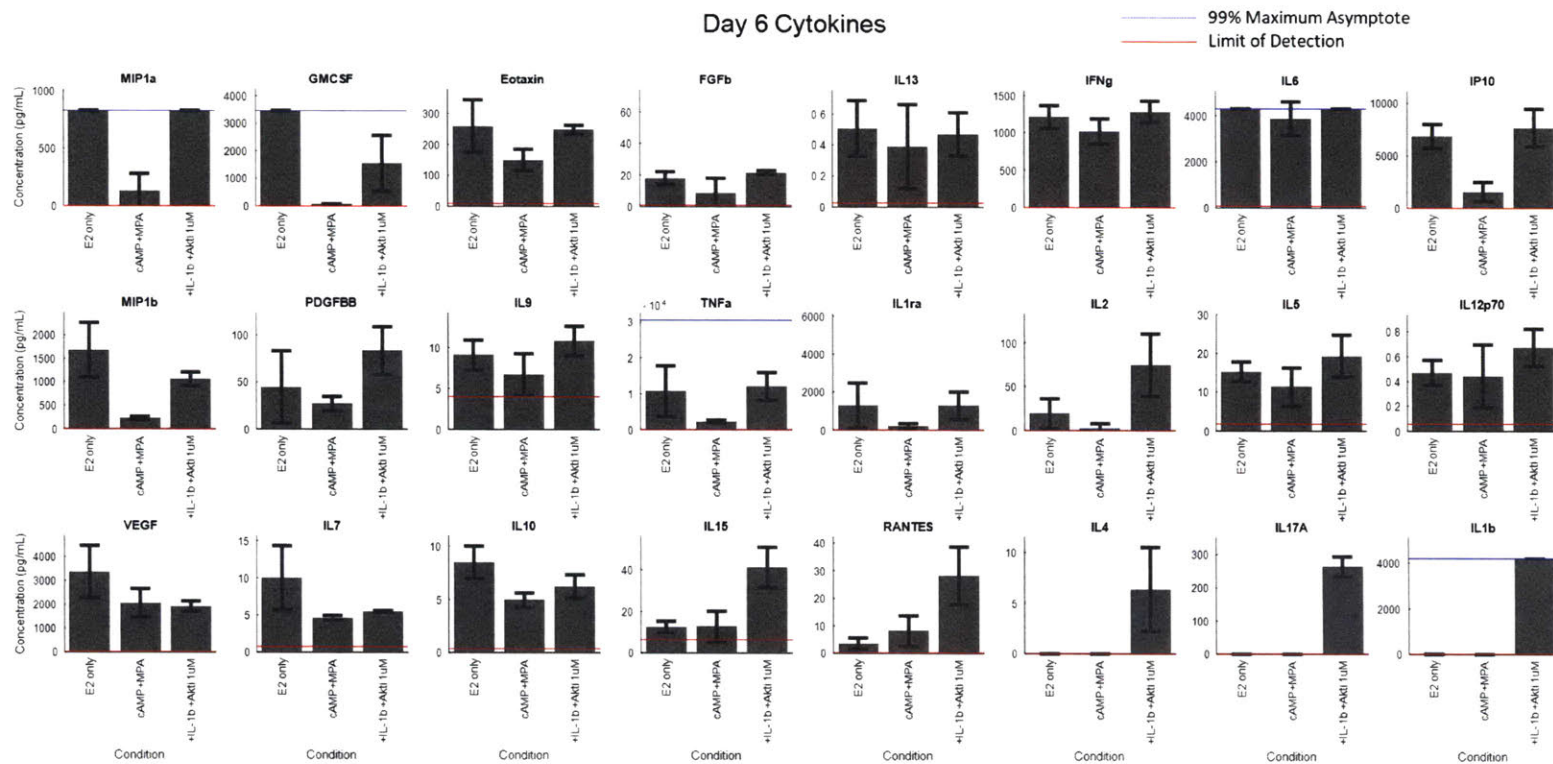


Figure 6-5: Cytokines under decidualization and IL-1 $\beta$ -induced inflammation.

IP-10, GM-CSF, and MIP-1 $\beta$  all showed decreased concentrations upon decidualization but increased levels in the presence of IL-1 $\beta$ . TNF $\alpha$  and IP-10 both responded more to AKT inhibition, whereas GM-CSF responded more to JNK inhibition and MIP-1 $\beta$  responded similarly to both.

### **6.3.5 Network model of disease**

The random walk algorithm was initiated from the cytokines affected by IL-1 $\beta$ -induced inflammation in addition to prolactin, IGFBP-1, and the estrogen and progesterone receptors. The top 100 ranked nodes were included in a network graph that relates inflammation and hormone signaling (Fig. 6-7). The network includes the start nodes used (CCL4, IL1B, IL4, IL2, IL17A, CCL3, PRL, IGFBP1, ESR1, ESR2, and PGR). Nodes added to the network include the two targets investigated here, JUN and AKT, as well as several other nodes previously reported to be involved in endometriosis: NFKB, FOS, JAKs, STATs, MAPKs, and P53. In addition, there are several nodes which interact with many nodes in the network but may not be specific to endometriosis, including UBC, UBB, and FAU.

## **6.4 Discussion and conclusions**

### **6.4.1 Cytokine response in model system recapitulates some aspects of clinical phenotypes**

In this experimental system, several cytokines were significantly affected by the cAMP+MPA stimulus after 4 days of treatment, with significant decreases in GM-CSF, IL-10, IL-1 $\beta$ , IP-10, and MIP-1 $\alpha$ . Interestingly, these differed from findings from the previous endometrial tissue model, which included primary endometrial stromal and epithelial cells but not monocytes, in which IL-10 and IL-15 were significantly increased in at least one donor due to decidualization [34]. Similar eutopic endometrial gels prepared using Ishikawas, tHESCs, and primary monocytes did not demonstrate any effect of hormone stimulus on the concentrations of the same 27

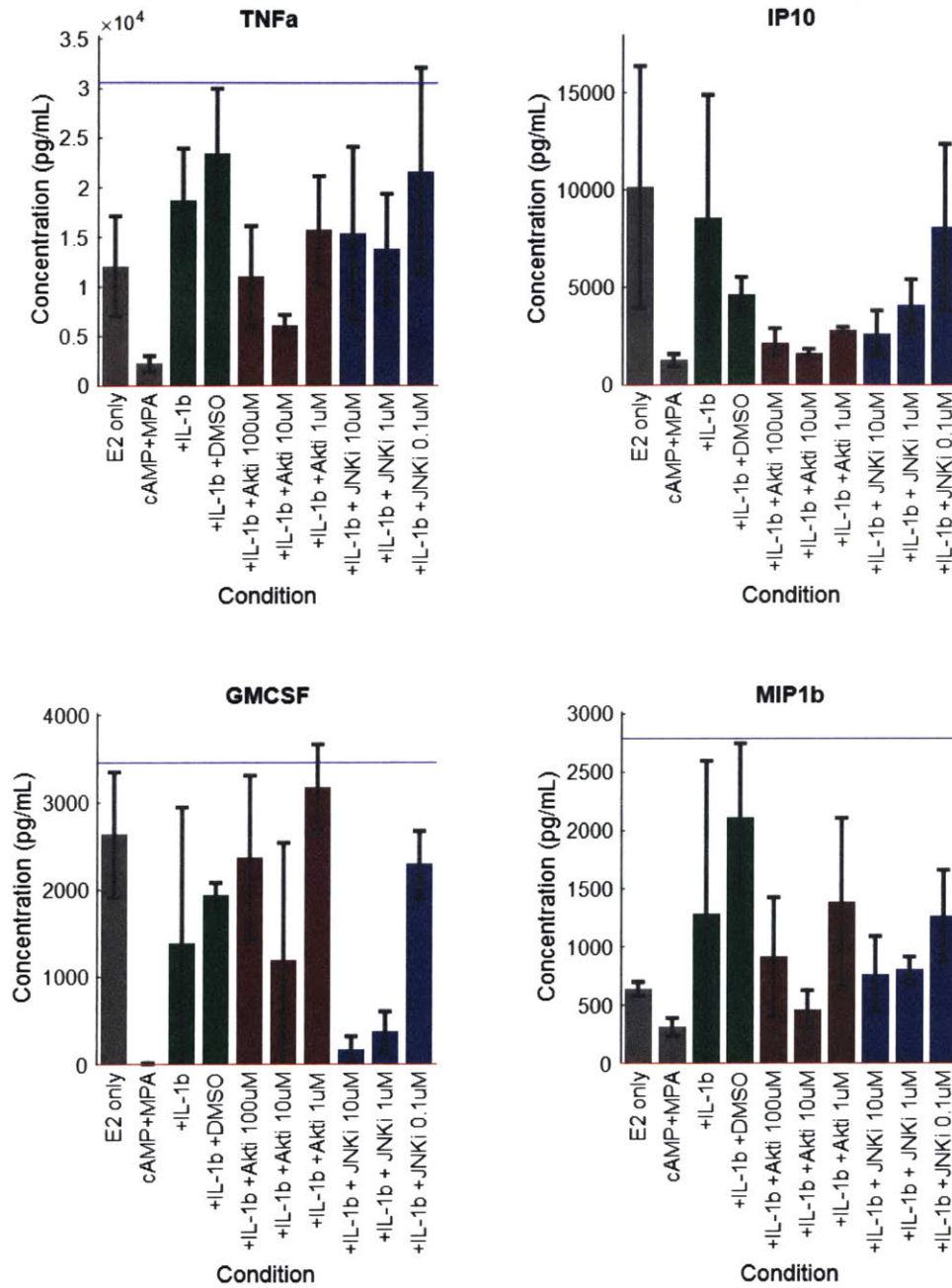


Figure 6-6: Cytokines for which AKT and/or JNK inhibitor(s) rescued decidualization response.



endometrial cells *in vitro* varies greatly across subjects. We plan to repeat the experiment shown here with additional sets of donors in order to determine how consistent the results are.

### **6.4.2 Death of primary cells in hydrogels**

The high levels of cell death observed in the gels, particularly early on in the culture period, may have an effect on both the ratio of cell types present in the gels and the behavior of remaining cells. While the stromal cells used here were in culture for a period of time before use, both primary epithelial cells and monocytes are known to have low survival in 2D culture. For monocytes, for example, it is common to observe 10% cell survival after a week of culture, even in the presence of growth factors such as GM-CSF; thus it is not surprising that large numbers of primary cells die early on in 3D culture. Further modification of the gel system, particularly the functional peptides, to improve survival of encapsulated epithelial cells and monocyte may improve the robustness of this model.

### **6.4.3 Identification of additional drug targets and/or treatment protocols**

The tests shown here of JNK and Akt inhibition did not indicate that either inhibitor was useful for improving hormone responsiveness or decreasing levels of most inflammatory cytokines. It is possible that these inhibitors require a longer treatment time to have an effect, or that diffusion or partitioning between the gel and medium necessitate additional time or higher concentrations of inhibitors for an effect to be observed. In addition, network analysis linking cytokines with hormone response suggest possible additional targets, including JAKs and STATs, NF $\kappa$ B, and MAPKs. It is not clear whether some or all of these inhibitors are harmful during pregnancy[32]. Previous work has also suggested that combination therapies may be a more effective strategy, for example by targeting both ERK and AKT pathways[117].

Finally, we have investigated only inhibitors of intracellular signaling pathways,

but antibodies against inflammatory cytokines or their corresponding receptors may be another approach. Based on immunostaining of intact gels (not shown), it may take an extended period of time (>24 hours) for large molecules such as antibodies to diffuse into the gels, necessitating a longer treatment time. Ongoing efforts to increase porosity of the gels may improve transport of large molecules.

#### **6.4.4 Use of model system to study cell-cell communication**

Earlier work in this thesis investigated the effects of cell-cell communication in a simplified system involving CD4<sup>+</sup> T cells and monocytes [154]. More recent work investigated cell-cell interactions in a eutopic endometrium model consisting of monocytes, endometrial stromal cells, and endometrial epithelial cells. In both cases, we could gain insight into intercellular communication by studying cytokines produced by individual cell types as well as pairs or higher order combinations of cell types. All three cell types included here as well as interactions between these cell types have been shown to play a role in the function of the eutopic endometrium, particularly in menstruation and regrowth of the endometrial layer during the menstrual cycle, and all three cell types have also shown aberrant behavior in endometriosis [13, 107]. Because no single cell type can be isolated as the driving cause of the disease, communication among the three cell types is clearly important for disease progression. In addition, the lesion syringe model system has fewer confounding factors (e.g. apical and basal medium compartments, epithelial monolayer barrier to diffusion, etc.), making it a more convenient system with which to study cell-cell communication.

#### **6.4.5 Phenotype and activity of myeloid cells in lesion model**

As endometriosis lesions are known to have a large population of immune cells, it would be of particular interest to investigate the effects of myeloid populations on the overall lesion model behavior. Previous studies involving the eutopic endometrial tissue model suggested that monocytes may differentiate and express markers of alternative activation when exposed to endometrial stromal and epithelial cells. As

peritoneal macrophages in endometriosis patients have been shown to have a more alternatively activated phenotype [4], it would be of interest to see whether monocytes 1 differentiate into macrophages in the gels and 2 display markers of alternative activation. Thus far, efforts to stain fixed  $20\mu\text{L}$  gels have had mixed results, but more recent work in the lab has shown that gels can be cryosectioned and stained, potentially allowing for a more thorough investigation of monocyte/macrophage phenotype. Myeloid cells have also been shown to affect the matrix environment [93], which is another potential avenue for future work, particularly if macrophage phenotype could be shown to influence tissue properties to induce a more or less fibrotic state.

#### **6.4.6 Use of lesion model for personalized medicine applications**

Endometriosis is a heterogeneous disease, with at least 3 different broad types of lesions: peritoneal endometriosis, ovarian cysts or endometriomas, and rectovaginal nodules [17, 123]. Patients also present with a diverse set of symptoms of varying severity [175, 52], and only subsets of patients respond favorably to current hormonal therapies. As such, it is likely that patients will respond differently to any additional therapies that are developed. The lesion model presented here could potentially be used to test an individual's cells for drug response using two different approaches.

The simpler approach would be to simply dissect and then enzymatically digest an entire endometrial biopsy, containing a mix of endometrial stromal and epithelial cells, a variety of immune cells, and red blood cells. In this manner, all cell types would be derived from an individual patient, although precise numbers or proportions of each cell type would not be controlled. In addition, lesions are known to have large amounts of heme [94], which has not been included in the lesion model system presented in this chapter.

An alternative approach would be to expand epithelial cells following a protocol currently in development in the Griffith Lab (personal communication, Christi Cook

and Julia Papps, 2017). Stromal cells from the same biopsy could be expanded as they are for the current system. A separate blood sample could be taken from the same patient either before or after surgery, with PBMCs isolated and frozen. Expansion of the epithelial cells could possibly allow for testing of more drugs, concentrations, or treatment times than we have been able to achieve from un-expanded epithelial cells currently.

#### **6.4.7 Intercellular network models**

The network modeling approach used here may be useful for identifying novel potential drug targets, as it successfully identified several intracellular signaling pathways implicated in endometriosis in previously published literature, but several caveats remain. First, gene expression is not necessarily representative of protein level or protein activity. For most genes, when that gene is considered across different cells, gene expression and protein level are generally correlated [113]. However, expression levels across different genes do not correlate well with protein levels, and protein activity changes on a much shorter time scale than transcription and translation. Mass spectrometry data would provide a more directly relevant measure of which proteins are present in the cell types of interest, and has previously been used to infer intercellular networks within the immune system [149]. Additionally, the particular data sets used here had different numbers of expressed genes. Many fewer genes were detected in the epithelial cells, possibly because a different array was used, which led to fewer epithelial proteins being included in the network. A second drawback to the use of network algorithms as used here is that certain nodes, particularly hub nodes, tend to be ranked highly regardless of the input. Confidence in the relevance of the highly ranked nodes found here to endometriosis and the experimental model used depends on further tests using input lists selected randomly from the cytokines measured. Nodes that are highly ranked when using randomly selected input lists can then be excluded from the network and/or from further experimental follow-up.

# Chapter 7

## Conclusions and Future Work

### 7.1 Summary of findings and impact on field

#### 7.1.1 Multicellular Interactions

Previous work has shown that interactions among cell types influence systems-level behavior of tissues. Work in this thesis has shown additional evidence for the importance of cell-cell interactions in a two-cell system (CD4+ T cells and monocytes) and two related three-cell systems (endometrial stromal and epithelial cells and monocytes/macrophages).

Early work in this thesis adopted a very simplified model of CD4+ T cells and monocytes in suspension, cultured for 24 hours in different fractional mixtures. In this system, cytokine secretion was generally synergistic; most cytokines were increased as a result of interactions between the two cell types. This finding makes rational sense as both cell types are involved in mounting an immune response, and signals from the innate immune system in particular are critical for stimulating the adaptive immune system to respond.

Subsequent work involving stromal, epithelial, and myeloid cells in the endometrium and endometriotic lesion model systems further demonstrated the importance of studying multicellular systems. Including even three-cell interactions improved the mixed-effects model for over half of the cytokines (14/23) in the system, suggesting

that higher-order interactions rather than just pairs of interacting cells are worth further study.

Finally, while multicellular interactions were not explicitly studied in the variety of patient samples analyzed in Chapter 3 of this thesis, it is likely that certain differences between *in vivo* and *in vitro* measurements were due to the absence of some cell types in the *in vitro* systems. Culture of peritoneal fluid cells or even coculture of representative cell lines did not replicate the cytokine environment observed in the peritoneal fluid itself. It is likely that interactions between the cell types investigated here and additional cell types (mesothelial cells, NK cells, endothelial cells, etc.) contribute substantially to cytokine regulation *in vivo*.

### 7.1.2 *In Vitro* Model Systems

The most basic type of *in vitro* assay consists of a simple 2D culture of a single cell line, either from a cancer or genetically modified to survive outside of the body. Over time, *in vitro* assays have advanced to use 3D hydrogel scaffolds [114], primary non-cancerous cells [134], and co-cultures of multiple cell types [170] so as to better represent complex tissues or organoids [53] and even replicate some functions of multi-organ systems [44].

In this work, we used two different 3D PEG hydrogel models that incorporated primary cells and allowed the cells to modify their environment, the first an endometrial tissue model published in Cook et al. [34], and the second a modification of that system to better represent endometriotic lesions. Our earlier work with clinical samples suggested that the ability to follow cells from an individual patient over time, particularly through a hormonal cycle, would be of value, as patient-to-patient variability confounded our ability to detect cycle-dependent changes. While monocytes and epithelial cells do not survive well in 2D culture, these 3D systems allowed us to culture stromal and epithelial cells and monocytes over time and test their response to hormones and inflammatory cues. In addition, monocytes are exposed to 3D cues and tissue matrix as they extravasate, migrate into their destination tissues, and differentiate into macrophages; exposure to 3D cues should thus improve the physi-

ological relevance of the environment to monocyte/macrophage behavior. (mention particular integrin engagement)

### 7.1.3 Patient Stratification in Endometriosis

Work shown in this thesis and elsewhere [9, 34] has suggested that (1) endometriosis patients have a wide variety of symptoms and (2) relevant samples from cohorts of endometriosis and control samples have widely different behaviors *in vitro*. Due to the high patient-to-patient variability, it is possible that enrolling larger numbers of patients and stratifying by symptoms or inflammatory signatures could greatly improve our ability to identify potential novel therapeutic approaches. It is unclear, for example, if endometriomas have the same disease pathobiology as does deep infiltrating endometriosis, or why some patients experience high levels of pain despite having mild disease according to ASRM criteria. In fact, the World Endometriosis Research Foundation (WERF) has established protocols to standardize collection of samples and data across many practices around the world, so that much larger patient populations can be studied going forward [176, 143, 51].

## 7.2 Future work

### 7.2.1 Characterization of Endometriotic Lesion Model

The endometriotic lesion model used here was modified from a previous model of endometrial tissue developed by Christi Cook [34]. As such, peptide concentrations and other aspects of gel formulation were not thoroughly investigated for this particular system but were taken from that model. It is possible that encapsulated primary cells may have different phenotypes depending on the concentrations of various peptides in the gel. Additionally, matrix deposition was not measured in this system.

Cell death in the lesion model was relatively high. EDU staining could elucidate whether cell death as measured by LDH was due to one cell type more so than the others. It is likely that epithelial cells and monocytes are largely responsible for the

cell death, as these cells are more fragile in tissue culture. Slight modifications of the PEG gel, crosslinking protocol, or medium composition could possibly improve survival of these cell types.

### **7.2.2 Macrophage differentiation and activation in lesion model**

Monocytes were previously shown to differentiate into alternatively activated macrophages in the presence of endometrial cell lines in the endometrial tissue model, but lesion gels were never successfully stained for macrophage markers. As macrophage phenotype is thought to play a role in proliferation and invasiveness of endometriotic lesions, testing whether monocytes encapsulated in the gels differentiate and whether phenotype is affected by the inflammatory milieu induced by IL-1 $\beta$  stimulation would provide an assessment of the use of the model for studying immune-endometriosis interactions.

As an alternative, macrophages can be differentiated from monocytes in 2D and induced to adopt classical or alternative activation phenotypes before addition to the gels. This process was not attempted here because of logistical difficulties in timing macrophage differentiation, stromal cell expansion, and availability of sufficient epithelial cells from fresh endometrial biopsies on the day of surgery. However, the switch in biopsy collection protocol from 3mm to 4mm Pipelle biopsies greatly improved the reliability of epithelial cell isolation, and tuning of macrophage phenotype would provide an additional dimension along which to alter the model to be more representative of lesion biology.

### **7.2.3 Intercellular communication in lesion model**

Similarly, cytokine secretion by each individual cell type and combinations of cell types was studied in the endometrium model. Very few monocytes/macrophages remained in the gel by the end of the culture period, however, so the myeloid contribution to the overall cytokine environment in that system was very small. In the lesion model, where cells are all encapsulated in the gel, monocyte persistence is expected to be much higher, possibly allowing the myeloid component to contribute

more to the cytokine milieu.

#### **7.2.4 In-gel measurement of cytokines**

Hydrogels used in this work were designed to be compatible with sortase degradation [171]. Measurement of cytokines within the gel itself would provide a more accurate view of what the cells encapsulated in the gel are actually exposed to. Considering that cells within the gel are actively secreting and consuming cytokines as well as matrix that may selectively bind certain cytokines, it is likely that the gel cytokine environment differs substantially from the supernatant cytokines measured here [33]. It would be valuable to first compare whether in-gel cytokine measurements are in fact very different from supernatant measurements and, if so, repeat the analyses from Chapter 6 using the in-gel cytokine concentrations.

#### **7.2.5 Experimental methods for multicellular interactions**

In some cases, such as the induction of IP-10 secretion by monocytes stimulated by  $\text{IFN}\gamma$  produced by activated CD4+ T cells observed in Chapter 2, cellular sources of observed cytokines can be inferred from prior knowledge and then tested experimentally. However, to definitively identify the cellular sources of proteins secreted as a consequence of intercellular communication, such cytokines need to be experimentally linked to the cell type of origin.

One option for linking cell types to secreted proteins is to use heavy and light medium to label cells before mixing them. This technique could be used for up to three cell types (using heavy, light, and neutral medium), albeit only for short time points in culture. Given the current culture system of  $20\mu\text{L}$  gels, conditioned medium from multiple gels would need to be combined to achieve enough protein for mass spectrometry. Alternatively, we have tested some larger transwell gels with the same gel height but larger radius, and it is possible that larger syringe gels could be similarly synthesized.

An alternative method for linking cytokine production to certain cell types is by

staining for intracellular cytokines. Cytokine secretion could be blocked using monensin or brefeldin A, after which gels could be stained and imaged or sortase dissolved followed by staining of cells for flow cytometry. In either case, cytokine staining would be limited to a small number of cytokines at once, and blocking cytokine secretion is known to be imperfect.

# Bibliography

- [1] Alexander R. Abbas, Kristen Wolslegel, Dhaya Seshasayee, Zora Modrusan, and Hilary F. Clark. Deconvolution of blood microarray data identifies cellular activation patterns in systemic lupus erythematosus. *PloS One*, 4(7):e6098, Jan 2009.
- [2] A.R. Abbas, D. Baldwin, Y. Ma, W. Ouyang, A. Gurney, F. Martin, S. Fong, M. van Lookeren Campagne, P. Godowski, P.M. Williams, A.C. Chan, and H.F. Clark. Immune response in silico (IRIS): immune-specific genes identified from a compendium of microarray expression data. *Genes and immunity*, 6(4):319–31, Jun 2005.
- [3] Petronela Ancuta, Kuang-yu Liu, Vikas Misra, Vanessa Sue Wacleche, Annie Gosselin, Xiaobo Zhou, and Dana Gabuzda. Transcriptional profiling reveals developmental relationship and distinct biological functions of CD16+ and CD16-monocyte subsets. *BMC Genomics*, 19:1–19, 2009.
- [4] Monica Bacci, Annalisa Capobianco, Antonella Monno, Lucia Cottone, Francesca Di Puppo, Barbara Camisa, Margherita Mariani, Chiara Brignole, Mirco Ponzoni, Stefano Ferrari, Paola Panina-Bordignon, Angelo A. Manfredi, and Patrizia Rovere-Querini. Macrophages are alternatively activated in patients with endometriosis and required for growth and vascularization of lesions in a mouse model of disease. *The American Journal of Pathology*, 175(2):547–56, 2009.
- [5] Christopher Barry, Matthew T. Schmitz, Nicholas E. Propson, Zhonggang Hou, Jue Zhang, Bao K. Nguyen, Jennifer M. Bolin, Peng Jiang, Brian E. McIntosh, Mitchell D. Probasco, Scott Swanson, Ron Stewart, James A. Thomson, Michael P. Schwartz, and William L. Murphy. Uniform neural tissue models produced on synthetic hydrogels using standard culture techniques. *Experimental Biology and Medicine*, 242(17):1679–1689, 2017.
- [6] Brenda L. Bartlett and Stephen K. Tyring. Ustekinumab for chronic plaque psoriasis. *The Lancet*, 371(9625):1639 – 1640, 2008.
- [7] Izhar Ben-Shlomo, Rami Rauch, Orna Avsian-Kretchmer, and Aaron J. W. Hsueh. Matching receptome genes with their ligands for surveying paracrine/autocrine signaling systems. *Molecular Endocrinology*, 21(8):2009–2014, 2007.

- [8] Marina Berbic, Lauren Schulke, Robert Markham, Natsuko Tokushige, Peter Russell, and Ian S Fraser. Macrophage expression in endometrium of women with and without endometriosis. *Human reproduction (Oxford, England)*, 24(2):325–32, feb 2009.
- [9] M. T. Beste, N. Pfaffle-Doyle, E. A. Prentice, S. N. Morris, D. A. Lauffenburger, K. B. Isaacson, and L. G. Griffith. Molecular network analysis of endometriosis reveals a role for c-Jun-regulated macrophage activation. *Science Translational Medicine*, 6(222):222ra16–222ra16, 2014.
- [10] Christopher R. Bolen, Mohamed Uduman, and Steven H. Kleinstejn. Cell subset prediction for blood genomic studies. *BMC Bioinformatics*, 12(1):258, Jun 2011.
- [11] Katrin Bott, Zee Upton, Karsten Schrobback, Martin Ehrbar, Jeffrey A. Hubbell, Matthias P. Lutolf, and Simone C. Rizzi. The effect of matrix characteristics on fibroblast proliferation in 3D gels. *Biomaterials*, 31(32):8454 – 8464, 2010.
- [12] Donald P. Braun, Jianchi Ding, Fehr Shaheen, James C. Willey, Nasir Rana, and W. Paul Dmowski. Quantitative expression of apoptosis-regulating genes in endometrium from women with and without endometriosis. *Fertility and Sterility*, 87(2):263–268, 2007.
- [13] K.L. Bruner, W.H. Rodgers, L.I. Gold, M. Korc, J.T. Hargrove, L.M. Matrisian, and K.G. Osteen. Transforming growth factor beta mediates the progesterone suppression of an epithelial metalloproteinase by adjacent stroma in the human endometrium. *Proceedings of the National Academy of Sciences*, 92(16):7362–7366, 1995.
- [14] Kaylon L. Bruner-Tran, Alessandra C. Carvalho-Macedo, Antoni J. Duleba, Marta A. Crispens, and Kevin G. Osteen. Experimental endometriosis in immunocompromised mice after adoptive transfer of human leukocytes. *Fertility and sterility*, 93(8):2519–24, May 2010.
- [15] Kaylon L. Bruner-Tran, Esther Eisenberg, Grant R. Yeaman, Ted A. Anderson, Judith McBean, and Kevin G. Osteen. Steroid and cytokine regulation of matrix metalloproteinase expression in endometriosis and the establishment of experimental endometriosis in nude mice. *The Journal of Clinical Endocrinology & Metabolism*, 87(10):4782–4791, 2002.
- [16] Kaylon L. Bruner-Tran, Deborah Webster-Clair, and Kevin G. Osteen. Experimental endometriosis. *Annals of the New York Academy of Sciences*, 955(1):328–339, 2002.
- [17] Serdar E. Bulun. Endometriosis. *New England Journal of Medicine*, 360(3):268–279, 2009.

- [18] Svetlana Bureeva, Svetlana Zvereva, Valentin Romanov, and Tatiana Serebryiskaya. *Manual Annotation of Protein Interactions*, pages 75–95. Humana Press, Totowa, NJ, 2009.
- [19] Richard O. Burney and Linda C. Giudice. Pathogenesis and pathophysiology of endometriosis. *Fertility and Sterility*, 98(3):511–519, 2012.
- [20] Elena Cambria, Kasper Renggli, Caroline C. Ahrens, Christi D. Cook, Carsten Kroll, Andrew T. Krueger, Barbara Imperiali, and Linda G. Griffith. Covalent modification of synthetic hydrogels with bioactive proteins via sortase-mediated ligation. *Biomacromolecules*, 16(8):2316–2326, 2015.
- [21] Tolga Can, Orhan Çamoğlu, and Ambuj K. Singh. Analysis of protein-protein interaction networks using random walks. *Proceedings of the 5th International Workshop on Bioinformatics - BIOKDD '05*, page 61, 2005.
- [22] Annalisa Capobianco and Patrizia Rovere-Querini. Endometriosis, a disease of the macrophage. *Frontiers in immunology*, 4(January):9, Jan 2013.
- [23] Guiseppe Cardillo. Five parameters logistic regression - there and back again, 2012.
- [24] Guiseppe Cardillo. Four parameters logistic regression - there and back again, 2012.
- [25] Ashwini L. Chand, Andrew S. Murray, Rebecca L. Jones, Natalie J. Hannan, Lois A. Salamonsen, and Luk Rombauts. Laser capture microdissection and cDNA array analysis of endometrium identify ccl16 and ccl21 as epithelial-derived inflammatory mediators associated with endometriosis. *Reproductive Biology and Endocrinology*, 5(1):18, May 2007.
- [26] Jing Chen, Bruce J. Aronow, and Anil G. Jegga. Disease candidate gene identification and prioritization using protein interaction networks. *BMC Bioinformatics*, 10(1):73, Feb 2009.
- [27] Wen L.K. Chen, Collin Edington, Emily Suter, Jiajie Yu, Jeremy J. Velazquez, Jason G. Velazquez, Michael Shockley, Emma M. Large, Raman Venkataramanan, David J. Hughes, Cynthia L. Stokes, David L. Trumper, Rebecca L. Carrier, Murat Cirit, Linda G. Griffith, and Douglas A. Lauffenburger. Integrated gut/liver microphysiological systems elucidates inflammatory inter-tissue crosstalk. *Biotechnology and Bioengineering*, 114(11):2648–2659, 2017.
- [28] Leonid Chindelevitch, Daniel Ziemek, Ahmed Enayetallah, Ranjit Randhawa, Ben Sidders, Christoph Brockel, and Enoch S. Huang. Causal reasoning on biological networks: interpreting transcriptional changes. *Bioinformatics*, 28(8):1114–1121, 2012.

- [29] Hye Won Chung, Yan Wen, Sun Hee Chun, Camran Nezhat, Bock Hi Woo, and Mary Lake Polan. Matrix metalloproteinase-9 and tissue inhibitor of metalloproteinase-3 mRNA expression in ectopic and eutopic endometrium in women with endometriosis: A rationale for endometriotic invasiveness. *Fertility and Sterility*, 75(1):152–159, 2001.
- [30] I.-Ming Chung, Nduka O. Enemchukwu, Sirajud D. Khaja, Niren Murthy, Athanasios Mantalaris, and Andrés J. García. Bioadhesive hydrogel microenvironments to modulate epithelial morphogenesis. *Biomaterials*, 29(17):2637 – 2645, 2008.
- [31] David C. Clarke, Melody K. Morris, and Douglas A. Lauffenburger. Normalization and statistical analysis of multiplexed bead-based immunoassay data using mixed-effects modeling. *Molecular & Cellular Proteomics*, 12(1):245–262, 2013.
- [32] Megan E. B. Clowse, Steven R. Feldman, John D. Isaacs, Alexandra B. Kimball, Vibeke Strand, Richard B. Warren, Daniel Xibillé, Yan Chen, Donald Frazier, Jamie Geier, James Proulx, and Amy Marren. Pregnancy outcomes in the tofacitinib safety databases for rheumatoid arthritis and psoriasis. *Drug Safety*, 39(8):755–762, Aug 2016.
- [33] Christi D. Cook. *Illuminating Epithelial-Stromal Communication Using Engineered Synthetic Matrix Microenvironments*. PhD thesis, Massachusetts Institute of Technology, 2017.
- [34] Christi D. Cook, Abby S. Hill, Margaret Guo, Linda Stockdale, Julia P. Papps, Keith B. Isaacson, Douglas A. Lauffenburger, and Linda G. Griffith. Local remodeling of synthetic extracellular matrix microenvironments by co-cultured endometrial epithelial and stromal cells enables long-term dynamic physiological function. *Integrative Biology*, 9:271–289, 2017.
- [35] David Croft, Antonio Fabregat Mundo, Robin Haw, Marija Milacic, Joel Weiser, Guanming Wu, Michael Caudy, Phani Garapati, Marc Gillespie, Maulik R. Kamdar, Bijay Jassal, Steven Jupe, Lisa Matthews, Bruce May, Stanislav Palatnik, Karen Rothfels, Veronica Shamovsky, Heeyeon Song, Mark Williams, Ewan Birney, Henning Hermjakob, Lincoln Stein, and Peter D’Eustachio. The reactome pathway knowledgebase. *Nucleic Acids Research*, 42(D1):D472–D477, 2014.
- [36] Rahil Dahlén, Maria K Magnusson, Antal Bajor, Anders Lason, Kjell-Arne Ung, Hans Strid, and Lena Öhman. Global mucosal and serum cytokine profile in patients with ulcerative colitis undergoing anti-TNF therapy. *Scandinavian Journal of Gastroenterology*, 50(9):1118–1126, 2015.
- [37] V. A. Danis, M. Millington, V. J. Hyland, and D. Grennan. Cytokine production by normal human monocytes: inter-subject variation and relationship to an IL-1 receptor antagonist (IL-1Ra) gene polymorphism. *Clinical & Experimental Immunology*, 99(2):303–310, 1995.

- [38] Rowena DeJesus, Francesca Moretti, Gregory McAllister, Zuncai Wang, Phil Bergman, Shanming Liu, Elizabeth Frias, John Alford, John S Reece-Hoyes, Alicia Lindeman, Jennifer Kelliher, Carsten Russ, Judith Knehr, Walter Carbone, Martin Beibel, Guglielmo Roma, Aylwin Ng, John A Tallarico, Jeffery A Porter, Ramnik J Xavier, Craig Mickanin, Leon O Murphy, Gregory R Hoffman, and Beat Nyfeler. Functional CRISPR screening identifies the ufmylation pathway as a regulator of sqstm1/p62. *eLife*, 5:e17290, Jun 2016.
- [39] Ross Devolder and Hyun Joon Kong. Hydrogels for in vivo-like three-dimensional cellular studies. *Wiley Interdisciplinary Reviews: Systems Biology and Medicine*, 4(4):351–365, 2012.
- [40] Zoltán Dezső, Yuri Nikolsky, Tatiana Nikolskaya, Jeremy Miller, David Cherba, Craig Webb, and Andrej Bugrim. Identifying disease-specific genes based on their topological significance in protein networks. *BMC Systems Biology*, 3(1):36, Mar 2009.
- [41] Thomas M. D’Hooghe. Clinical relevance of the baboon as a model for the study of endometriosis. *Fertility and Sterility*, 68(4):613 – 625, 1997.
- [42] W.P. Dmowski, J. Ding, N. Rana, B.B. Fernandez, and Braun D.P. Apoptosis in endometrial glandular and stromal cells in women with and without endometriosis. *Human reproduction (Oxford, England)*, 16(9):1802–8, Sep 2001.
- [43] Karel Domansky, Walker Inman, James Serdy, Ajit Dash, Matthew H. M. Lim, and Linda G. Griffith. Perfused multiwell plate for 3D liver tissue engineering. *Lab Chip*, 10:51–58, 2010.
- [44] Collin D. Edington, Wen Li, Kelly Chen, Emily Geishecker, Timothy Kassis, and Luis R. Soenksen. Interconnected Microphysiological Systems for Quantitative Biology and Pharmacology Studies. *Scientific Reports*, 8(1):1–18, 2018.
- [45] M.J. Elliott, R.N. Maini, M. Feldmann, J.R. Kalden, C. Antoni, J.S. Smolen, B. Leeb, F.C. Breedveld, J.D. Macfarlane, J.A. Bijl, and J.N. Woody. Randomised double-blind comparison of chimeric monoclonal antibody to tumour necrosis factor  $\alpha$  (cA2) versus placebo in rheumatoid arthritis. *The Lancet*, 344(8930):1105 – 1110, 1994. Originally published as Volume 2, Issue 8930.
- [46] Jemma Evans and Lois A. Salamonsen. Decidualized human endometrial stromal cells are sensors of hormone withdrawal in the menstrual inflammatory cascade1. *Biology of Reproduction*, 90(1):14, 1–12, 2014.
- [47] Kathleen M. Eyster, Keith A. Hansen, Emily Winterton, Olga Klinkova, Donis Drappeau, and Connie J. Mark-Kappeler. Reciprocal communication between endometrial stromal cells and macrophages. *Reproductive Sciences*, 17(9):809–822, 2010.

- [48] Antonio Fabregat, Steven Jupe, Lisa Matthews, Konstantinos Sidiropoulos, Marc Gillespie, Phani Garapati, Robin Haw, Bijay Jassal, Florian Korninger, Bruce May, Marija Milacic, Corina Duenas Roca, Karen Rothfels, Cristoffer Sevilla, Veronica Shamovsky, Solomon Shorser, Thawfeek Varusai, Guilherme Viteri, Joel Weiser, Guanming Wu, Lincoln Stein, Henning Hermjakob, and Peter D'Eustachio. The reactome pathway knowledgebase. *Nucleic Acids Research*, 46(D1):D649–D655, 2018.
- [49] Yan-Yan Fan, Hong-Yu Chen, Wei Chen, Yi-Nan Liu, Yan Fu, and Li-Na Wang. Expression of inflammatory cytokines in serum and peritoneal fluid from patients with different stages of endometriosis. *Gynecological Endocrinology*, 0(0):1–6, 2018.
- [50] Amelie Fassbender, Lut Overbergh, Eefje Verdrengh, Cleophas M. Kyama, Alexandra Vodolazakaia, Attila Bokor, Christel Meuleman, Karen Peeraer, Carla Tomassetti, Etienne Waelkens, Chantal Mathieu, and Thomas D’Hooghe. How can macroscopically normal peritoneum contribute to the pathogenesis of endometriosis? *Fertility and Sterility*, 96(3):697 – 699, 2011.
- [51] Amelie Fassbender, Nilufer Rahmioglu, Allison F. Vitonis, Paola Vigan, Linda C. Giudice, Thomas M. D’Hooghe, Lone Hummelshoj, G. David Adamson, and Christian M. Becker for the WERF EPHeC Working Group. World Endometriosis Research Foundation Endometriosis Phenome and Biobanking Harmonisation Project: I. Surgical phenotype data collection in endometriosis research. *Fertility and Sterility*, 102(5):1244–1253, 2014.
- [52] Arnaud Fauconnier, Charles Chapron, Jean Bernard Dubuisson, Marco Vieira, Bertrand Dousset, and Gérard Bréart. Relation between pain symptoms and the anatomic location of deep infiltrating endometriosis. *Fertility and Sterility*, 78(4):719–726, 2002.
- [53] Katherine Ellen Foley. Organoids: A better in vitro model. *Nature Methods*, 14(6):559–562, 2017.
- [54] Ziv Frankenstein, Uri Alon, and Irun R Cohen. The immune-body cytokine network defines a social architecture of cell interactions. *Biology direct*, 1:32, Jan 2006.
- [55] Raj K. Gaire, Lorey Smith, Patrick Humbert, James Bailey, Peter J. Stuckey, and Izhak Haviv. Discovery and analysis of consistent active sub-networks in cancers. *BMC Bioinformatics*, 14(2):S7, Jan 2013.
- [56] Xiaoyan Gao and Michael J. Groves. Fibronectin-binding peptides. i. isolation and characterization of two unique fibronectin-binding peptides from gelatin. *European Journal of Pharmaceutics and Biopharmaceutics*, 45(3):275 – 284, 1998.

- [57] Georg Gasteiger and Alexander Y. Rudensky. Interactions between innate and adaptive lymphocytes. *Nature Reviews Immunology*, 14(9):631–639, 2014.
- [58] Mark C. Genovese, Roy Fleischmann, Alan J. Kivitz, Maria Rell-Bakalarska, Renata Martincova, Stefano Fiore, Patricia Rohane, Hubert van Hoogstraten, Anju Garg, Chunpeng Fan, Janet van Adelsberg, Steven P. Weinstein, Neil M. H. Graham, Neil Stahl, George D. Yancopoulos, Tom W. J. Huizinga, and Désirée van der Heijde. Sarilumab Plus Methotrexate in Patients With Active Rheumatoid Arthritis and Inadequate Response to Methotrexate: Results of a Phase III Study. *Arthritis & Rheumatology*, 67(6):1424–1437, 2015.
- [59] Susan Dina Ghiassian, Jörg Menche, and Albert-László Barabási. A DIseAse MODule Detection (DIAMOnD) algorithm derived from a systematic analysis of connectivity patterns of disease proteins in the human interactome. *PLOS Computational Biology*, 11(4):1–21, 04 2015.
- [60] Linda C Giudice and Lee C Kao. Endometriosis. *Lancet*, 364(9447):1789–99, 2004.
- [61] Nikolce Gjorevski and Matthias P. Lutolf. Synthesis and characterization of well-defined hydrogel matrices and their application to intestinal stem cell and organoid culture. *Nature Protocols*, 12(11):2263–2274, 2017.
- [62] Heike Goehler, Maciej Lalowski, Ulrich Stelzl, Stephanie Waelter, Martin Stroedicke, Uwe Worm, Anja Droege, Katrin S. Lindenberg, Maria Knoblich, Christian Haenig, Martin Herbst, Jaana Suopanki, Eberhard Scherzinger, Claudia Abraham, Bianca Bauer, Renate Hasenbank, Anja Fritzsche, Andreas H. Ludewig, Konrad Buessow, Sarah H. Coleman, Claire-Anne Gutekunst, Bernhard G. Landwehrmeyer, Hans Lehrach, and Erich E. Wanker. A protein interaction network links git1, an enhancer of huntingtin aggregation, to huntington’s disease. *Molecular Cell*, 15(6):853 – 865, 2004.
- [63] Erin Greaves, Hilary O.D. Critchley, Andrew W. Horne, and Philippa T.K. Saunders. Relevant human tissue resources and laboratory models for use in endometriosis research. *Acta Obstetricia et Gynecologica Scandinavica*, 96(6):644–658, 2017.
- [64] Linda G. Griffith and Melody A. Swartz. Capturing complex 3D tissue physiology in vitro. *Nature Reviews Molecular Cell Biology*, 7(3):211–224, 2006.
- [65] Ruth Grümmer. Animal models in endometriosis research. *Human Reproduction Update*, 12(5):641–649, 2006.
- [66] Sun Wei Guo and David L. Olive. Two unsuccessful clinical trials on endometriosis and a few lessons learned. *Gynecologic and Obstetric Investigation*, 64(1):24–35, 2007.

- [67] Min Jin Ha and Wei Sun. Partial correlation matrix estimation using ridge penalty followed by thresholding and re-estimation. *Biometrics*, 70(3):762–770, 2014.
- [68] T. Harada, A. Kaponis, T. Iwabe, F. Taniguchi, G. Makrydimas, N. So, M. Paschopoulos, E. Paraskevaidis, and N. Terakawa. Apoptosis in human endometrium and endometriosis. *Human Reproduction Update*, 10(1):29–38, Jan 2004.
- [69] B. Hodgkinson, P.W.A. Meyer, E. Musenge, M. Ally, R. Anderson, and M. Tikly. Exaggerated circulating Th-1 cytokine response in early rheumatoid arthritis patients with nodules. *Cytokine*, 60(2):561–4, Nov 2012.
- [70] D. Hornung, F. Bentzien, D. Wallwiener, L. Kiesel, and R.N. Taylor. Chemokine bioactivity of RANTES in endometriotic and normal endometrial stromal cells and peritoneal fluid. *Molecular human reproduction*, 7(2):163–8, Feb 2001.
- [71] D. Hornung, I.P. Ryan, V.A. Chao, J.L. Vigne, E.D. Schriock, and R.N. Taylor. Immunolocalization and regulation of the chemokine RANTES in human endometrial and endometriosis tissues and cells. *The Journal of clinical endocrinology and metabolism*, 82(5):1621–8, May 1997.
- [72] Chia-Lang Hsu, Yen-Hua Huang, Chien-Ting Hsu, and Ueng-Cheng Yang. Prioritizing disease candidate genes by a gene interconnectedness-based approach. *BMC Genomics*, 12(3):S25, Nov 2011.
- [73] Wolfgang Hueber, Dhavalkumar D. Patel, Thaddeus Dryja, Andrew M. Wright, Irina Koroleva, Gerard Bruin, Christian Antoni, Zoe Draelos, Michael H. Gold, Patrick Durez, Paul P. Tak, Juan J. Gomez-Reino, C. Stephen Foster, Rosa Y. Kim, C. Michael Samson, Naomi S. Falk, David S. Chu, David Callanan, Quan Dong Nguyen, Kristine Rose, Asifa Haider, and Franco Di Padova. Effects of AIN457, a fully human antibody to interleukin-17A, on psoriasis, rheumatoid arthritis, and uveitis. *Science Translational Medicine*, 2(52):1–11, 2010.
- [74] Chris S. Hughes, Lynne M. Postovit, and Gilles A. Lajoie. Matrigel: a complex protein mixture required for optimal growth of cell culture. *Proteomics*, 10(9):1886–1890, 2010.
- [75] Mostafa Hussein, Daniel C. Chai, Cleophas M. Kyama, Jason M. Mwenda, Stephen S. Palmer, Jean-Pierre Gotteland, and Thomas M. D’Hooghe. c-Jun NH2-terminal kinase inhibitor bentamapimod reduces induced endometriosis in baboons: an assessor-blind placebo-controlled randomized study. *Fertility and Sterility*, 105(3):815 – 824.e5, 2016.
- [76] Edward L. Huttlin, Lily Ting, Raphael J. Bruckner, Fana Gebreab, Melanie P. Gygi, John Szpyt, Stanley Tam, Gabriela Zarraga, Greg Colby, Kurt Baltier, Rui Dong, Virginia Guarani, Laura Pontano Vaites, Alban Ordureau, Ramin

- Rad, Brian K. Erickson, Martin Wühr, Joel Chick, Bo Zhai, Deepak Kolipakkam, Julian Mintseris, Robert A. Obar, Tim Harris, Spyros Artavanis-Tsakonas, Mathew E. Sowa, Pietro De Camilli, Joao A. Paulo, J. Wade Harper, and Steven P. Gygi. The BioPlex Network: A Systematic Exploration of the Human Interactome. *Cell*, 162(2):425–440, 2015.
- [77] Trey Ideker, Owen Ozier, Benno Schwikowski, and F Andrew. Discovering regulatory and signalling circuits in molecular interaction networks. *Bioinformatics*, 18:233–240, 2002.
- [78] Toshio M. Igarashi, Kaylon L. Bruner-Tran, Grant R. Yeaman, Bruce A. Lessey, Dean P. Edwards, Esther Eisenberg, and Kevin G. Osteen. Reduced expression of progesterone receptor-B in the endometrium of women with endometriosis and in cocultures of endometrial cells exposed to 2,3,7,8-tetrachlorodibenzo-p-dioxin. *Fertility and Sterility*, 84(1):67–74, 2005.
- [79] Takashi Ito, Tomoko Chiba, Ritsuko Ozawa, Mikio Yoshida, Masahira Hattori, and Yoshiyuki Sakaki. A comprehensive two-hybrid analysis to explore the yeast protein interactome. *Proceedings of the National Academy of Sciences*, 98(8):4569–4574, 2001.
- [80] Savina Jaeger, Junxia Min, Florian Nigsch, Miguel Camargo, Janna Hutz, Allen Cornett, Stephen Cleaver, Alan Buckler, and Jeremy L. Jenkins. Causal network models for predicting compound targets and driving pathways in cancer. *Journal of Biomolecular Screening*, 19(5):791–802, 2014.
- [81] Kevin A. Janes and Michael B. Yaffe. Data-driven modelling of signal-transduction networks. *Nature reviews. Molecular cell biology*, 7(11):820–8, Nov 2006.
- [82] Jani R. Jensen, Craig A. Witz, Robert S. Schenken, and Rajeshwar R. Tekmal. A potential role for colony-stimulating factor 1 in the genesis of the early endometriotic lesion. *Fertility and Sterility*, 93(1):251–256, 2010.
- [83] Glynis Johnson and Samuel W Moore. Identification of a structural site on acetylcholinesterase that promotes neurite outgrowth and binds laminin-1 and collagen iv. *Biochemical and Biophysical Research Communications*, 319(2):448 – 455, 2004.
- [84] Claus Jørgensen, Andrew Sherman, Ginny I. Chen, Adrian Pasculescu, Alexei Poliakov, Marilyn Hsiung, Brett Larsen, David G. Wilkinson, Rune Linding, and Tony Pawson. Cell-specific information processing in segregating populations of eph receptor ephrin-expressing cells. *Science*, 326(5959):1502–1509, 2009.
- [85] Hilde Jørgensen, Abby S. Hill, Michael T. Beste, Manu P. Kumar, Evan Chiswick, Peter Fedorcsak, Keith B. Ksaacson, Douglas A. Lauffenburger, Linda G. Griffith, and Erik Qvigstad. Peritoneal fluid cytokines related

- to endometriosis in patients evaluated for infertility. *Fertility and Sterility*, 107(5):1191–1199, 2017.
- [86] Emmanuel Kalu, Nazira Sumar, Theodoros Giannopoulos, Pinika Patel, Carolyn Croucher, Elizabeth Sherriff, and Amolak Bansal. Cytokine profiles in serum and peritoneal fluid from infertile women with and without endometriosis. *Journal of Obstetrics and Gynaecology Research*, 33(4):490–495, 2007.
- [87] Minoru Kanehisa, Miho Furumichi, Mao Tanabe, Yoko Sato, and Kanae Morishima. KEGG: new perspectives on genomes, pathways, diseases and drugs. *Nucleic Acids Research*, 45(D1):D353–D361, 2017.
- [88] Minoru Kanehisa and Susumu Goto. KEGG: Kyoto encyclopedia of genes and genomes. *Nucleic Acids Research*, 28(1):27–30, 2000.
- [89] Minoru Kanehisa, Yoko Sato, Masayuki Kawashima, Miho Furumichi, and Mao Tanabe. KEGG as a reference resource for gene and protein annotation. *Nucleic Acids Research*, 44(D1):D457–D462, 2016.
- [90] T. Kantola, K. Klintrup, J. P. Väyrynen, J. Vornanen, R. Bloigu, T. Karhu, K. H. Herzig, J. Näpänkangas, J. Mäkelä, T. J. Karttunen, A. Tuomisto, and M. J. Mäkinen. Stage-dependent alterations of the serum cytokine pattern in colorectal carcinoma. *British Journal of Cancer*, 107(10):1729–1736, 2012.
- [91] Byung Gak Kim, Jung-Yoon Yoo, Tae Hoon Kim, Jung-Ho Shin, John F. Langenheim, Susan D. Ferguson, Asgerally T. Fazleabas, Steven L. Young, Bruce A. Lessey, and Jae-Wook Jeong. Aberrant activation of signal transducer and activator of transcription-3 (STAT3) signaling in endometriosis. *Human Reproduction*, 30(5):1069–1078, 2015.
- [92] Tae Hoon Kim, Yanni Yu, Lily Luo, John P. Lydon, Jae-Wook Jeong, and J. Julie Kim. Activated akt pathway promotes establishment of endometriosis. *Endocrinology*, 155(5):1921–1930, 2014.
- [93] N. Kitamura, S. Nishinarita, T. Takizawa, Y. Tomita, and T. Horie. Cultured human monocytes secrete fibronectin in response to activation by proinflammatory cytokines. *Clinical and Experimental Immunology*, 120(1):66–70, 2000.
- [94] Hiroshi Kobayashi, Yoshihiko Yamada, Seiji Kanayama, Naoto Furukawa, Take-toshi Noguchi, Shoji Haruta, Shozo Yoshida, Mariko Sakata, Toshiyuki Sado, and Hidekazu Oi. The role of iron in the pathogenesis of endometriosis. *Gynecological Endocrinology*, 25(1):39–52, 2009.
- [95] Yoshiro Kobayashi. Mechanism underlying silent cleanup of apoptotic cells. *Microbiology and Immunology*, 55(2):71–75, 2011.
- [96] Katrin Franzika Koenig, Isabel Groeschl, Satu Sinikka Pesickova, Vladimir Tesar, Ute Eisenberger, and Marten Trendelenburg. Serum cytokine profile in patients with active lupus nephritis. *Cytokine*, 60(2):410 – 416, 2012.

- [97] Sebastian Köhler, Sebastian Bauer, Denise Horn, and Peter N. Robinson. Walking the interactome for prioritization of candidate disease genes. *The American Journal of Human Genetics*, 82(4):949 – 958, 2008.
- [98] Teuvo Kohonen. The self-organizing map. *Neurocomputing*, 21(1):1 – 6, 1998.
- [99] Christopher Korch, Monique A. Spillman, Twila A. Jackson, Britta M. Jacobsen, Susan K. Murphy, Bruce A. Lessey, V. Craig Jordan, and Andrew P. Bradford. Dna profiling analysis of endometrial and ovarian cell lines reveals misidentification, redundancy and contamination. *Gynecologic Oncology*, 127(1):241 – 248, 2012.
- [100] Graciela Krikun, Gil Mor, Ayesha Alvero, Seth Guller, Frederick Schatz, Eva Sapi, Mizanur Rahman, Rebeca Caze, Mazin Qumsiyeh, and Charles J. Lockwood. A novel immortalized human endometrial stromal cell line with normal progestational response. *Endocrinology*, 145(5):2291–2296, 2004.
- [101] William Kuhlman, Ikuo Taniguchi, Linda G. Griffith, and Anne M. Mayes. Interplay between PEO tether length and ligand spacing governs cell spreading on RGD-modified PMMA-g-PEO comb copolymers. *Biomacromolecules*, 8(10):3206–3213, 2007.
- [102] Justin Lamb, Emily D. Crawford, David Peck, Joshua W. Modell, Irene C. Blat, Matthew J. Wrobel, Jim Lerner, Jean-Philippe Brunet, Aravind Subramanian, Kenneth N. Ross, Michael Reich, Haley Hieronymus, Guo Wei, Scott A. Armstrong, Stephen J. Haggarty, Paul A. Clemons, Ru Wei, Steven A. Carr, Eric S. Lander, and Todd R. Golub. The connectivity map: Using gene-expression signatures to connect small molecules, genes, and disease. *Science*, 313(5795):1929–1935, 2006.
- [103] Justin Lamb, Sridhar Ramaswamy, Heide L Ford, Bernardo Contreras, Robert V Martinez, Frances S Kittrell, Cynthia A Zahnow, Nick Patterson, Todd R Golub, and Mark E Ewen. A Mechanism of Cyclin D1 Action Encoded in the Patterns of Gene Expression in Human Cancer. *Cell*, 114:323–334, 2003.
- [104] Surya P. Lamichhane, Neha Arya, Esther Kohler, Shengnan Xiang, Jon Christensen, and V. Prasad Shastri. Recapitulating epithelial tumor microenvironment in vitro using three dimensional tri-culture of human epithelial, endothelial, and mesenchymal cells. *BMC Cancer*, 16(1):581, Aug 2016.
- [105] Julia Lasserre, Ho-Ryun Chung, and Martin Vingron. Finding associations among histone modifications using sparse partial correlation networks. *PLOS Computational Biology*, 9(9):1–12, 09 2013.
- [106] Ken S. Lau, Virna Cortez-Retamozo, Sarah R. Philips, Mikael J. Pittet, Douglas A. Lauffenburger, and Kevin M. Haigis. Multi-Scale In Vivo Systems Analysis Reveals the Influence of Immune Cells on TNF-alpha-Induced Apoptosis in the Intestinal Epithelium. *PLOS Biology*, 10(9):1–14, 09 2012.

- [107] Dan I. Lebovic, Victor A. Chao, and Robert N. Taylor. Peritoneal macrophages induce rantes (regulated on activation, normal t cell expressed and secreted) chemokine gene transcription in endometrial stromal cells. *The Journal of Clinical Endocrinology & Metabolism*, 89(3):1397–1401, 2004.
- [108] Maciej Lech, Regina Gröbmayer, Marc Weidenbusch, and Hans Joachim Anders. Tissues use resident dendritic cells and macrophages to maintain homeostasis and to regain homeostasis upon tissue injury: The immunoregulatory role of changing tissue environments. *Mediators of Inflammation*, 2012.
- [109] Insuk Lee, U. Martin Blom, Peggy I. Wang, Jung Eun Shim, and Edward M. Marcotte. Prioritizing candidate disease genes by network-based boosting of genome-wide association data. *Genome Research*, 21(7):1109–1121, 2011.
- [110] Mark D.M. Leiserson, Fabio Vandin, Hsin Ta Wu, Jason R. Dobson, Jonathan V. Eldridge, Jacob L. Thomas, Alexandra Papoutsaki, Younhun Kim, Beifang Niu, Michael McLellan, Michael S. Lawrence, Abel Gonzalez-Perez, David Tamborero, Yuwei Cheng, Gregory A. Ryslik, Nuria Lopez-Bigas, Gad Getz, Li Ding, and Benjamin J. Raphael. Pan-cancer network analysis identifies combinations of rare somatic mutations across pathways and protein complexes. *Nature Genetics*, 47(2):106–114, 2015.
- [111] Julia E. Leslie-Barbick, Jennifer E. Saik, Daniel J. Gould, Mary E. Dickinson, and Jennifer L. West. The promotion of microvasculature formation in poly(ethylene glycol) diacrylate hydrogels by an immobilized vegf-mimetic peptide. *Biomaterials*, 32(25):5782 – 5789, 2011.
- [112] Janghoo Lim, Tong Hao, Chad Shaw, Akash J. Patel, Gábor Szabó, Jean-François Rual, C. Joseph Fisk, Ning Li, Alex Smolyar, David E. Hill, Albert-László Barabási, Marc Vidal, and Huda Y. Zoghbi. A protein-protein interaction network for human inherited ataxias and disorders of purkinje cell degeneration. *Cell*, 125(4):801 – 814, 2006.
- [113] Emma Lundberg, Linn Fagerberg, Daniel Klevebring, Ivan Matic, Tamar Geiger, Juergen Cox, Cajsja Älgenäs, Joakim Lundberg, Matthias Mann, and Mathias Uhlen. Defining the transcriptome and proteome in three functionally different human cell lines. *Molecular Systems Biology*, 6(1), 2010.
- [114] M.P. Lutolf and J.A. Hubbell. Synthetic biomaterials as instructive extracellular microenvironments for morphogenesis in tissue engineering. *Nature biotechnology*, 23(1):47–55, 2005.
- [115] M.P. Lutolf, H.G. Schmoekel, A.T. Metters, F.E. Weber, G.B. Fields, and J.A. Hubbell. Synthetic matrix metalloproteinase-sensitive hydrogels for the conduction of tissue regeneration : Engineering cell-invasion characteristics. *Proceedings of the National Academy of Sciences*, 2003.

- [116] Alberto Mantovani, Subhra K Biswas, Maria Rosaria Galdiero, Antonio Sica, and Massimo Locati. Macrophage plasticity and polarization in tissue repair and remodelling. *The Journal of Pathology*, 229(2):176–185, 2013.
- [117] Sachiko Matsuzaki and Claude Darcha. Co-operation between the akt and erk signaling pathways may support growth of deep endometriosis in a fibrotic microenvironment in vitro. *Human Reproduction*, 30(7):1606–1616, 2015.
- [118] Philip J Mease, Désirée van der Heijde, Christopher T Ritchlin, Masato Okada, Raquel S Cuchacovich, Catherine L Shuler, Chen-Yen Lin, Daniel K Braun, Chin H Lee, and Dafna D Gladman. Ixekizumab, an interleukin-17a specific monoclonal antibody, for the treatment of biologic-naive patients with active psoriatic arthritis: results from the 24-week randomised, double-blind, placebo-controlled and active (adalimumab)-controlled period of . . . . *Annals of the Rheumatic Diseases*, 76(1):79–87, 2017.
- [119] Jörg Menche, Amitabh Sharma, Maksim Kitsak, Susan Dina Ghiassian, Marc Vidal, Joseph Loscalzo, and Albert-László Barabási. Uncovering disease-disease relationships through the incomplete interactome. *Science*, 347(6224), 2015.
- [120] Anatoly Mikhailik, James Mazella, Sharon Liang, and Linda Tseng. Notch ligand-dependent gene expression in human endometrial stromal cells. *Biochemical and Biophysical Research Communications*, 388(3):479 – 482, 2009.
- [121] Miles A. Miller, Aaron S. Meyer, Michael T. Beste, Zainab Lasisi, Sonika Reddy, Karen W. Jeng, Chia-Hung Chen, Jongyoon Han, Keith Isaacson, Linda G. Griffith, and Douglas A. Lauffenburger. Adam-10 and -17 regulate endometriotic cell migration via concerted ligand and receptor shedding feedback on kinase signaling. *Proceedings of the National Academy of Sciences*, 110(22):E2074–E2083, 2013.
- [122] Seyed Reza Mirhafez, Ahmadreza Zarifian, Mahmoud Ebrahimi, Ramin Fakhre Ale Ali, Amir Avan, Mohammad Tajfard, Mohsen Mohebbati, Saeid Es-lami, Amir Ali Rahsepar, Hamid Reza Rahimi, Hassan Mehrad-Majd, Gordon A. Ferns, and Majid Ghayour-Mobarhan. Relationship between serum cytokine and growth factor concentrations and coronary artery disease. *Clinical Biochemistry*, 48(9):575 – 580, 2015.
- [123] Grant W. Montgomery and Linda C. Giudice. New lessons about endometriosis -somatic mutations and disease heterogeneity. *New England Journal of Medicine*, 376(19):1881–1882, 2017.
- [124] Gil Mor, Ingrid Cardenas, Vikki Abrahams, and Seth Guller. Inflammation and pregnancy: the role of the immune system at the implantation site. *Annals of the New York Academy of Sciences*, 1221:80–7, mar 2011.

- [125] Sara Mostafavi, Debajyoti Ray, David Warde-Farley, Chris Grouios, and Quaid Morris. Genemania: a real-time multiple association network integration algorithm for predicting gene function. *Genome Biology*, 9(1):S4, Jun 2008.
- [126] William Murk, Cem S Atabekoglu, Hakan Cakmak, Aylin Heper, Arzu Ensari, Umit A Kayisli, and Aydin Arici. Extracellularly Signal-Regulated Kinase Activity in the Human Endometrium : Possible Roles in the Pathogenesis of Endometriosis. *Journal of Clinical Endocrinology & Metabolism*, pages 3532–3540, 2008.
- [127] Anitha S Nair, Hareesh B Nair, D Ph, Richard S Lucidi, Alyson J Kirchner, S Schenken, Rajeshwar Rao Tekmal, and Craig A Witz. Modeling the early endometriotic lesion : mesothelium-endometrial cell co-culture increases endometrial invasion and alters mesothelial and endometrial gene transcription. *Fertility and Sterility*, 90(October), 2008.
- [128] Parameswaran Nair, Sally Wenzel, Klaus F. Rabe, Arnaud Bourdin, Njira L. Lugogo, Piotr Kuna, Peter Barker, Stephanie Sproule, Sandhia Ponnarambil, and Mitchell Goldman. Oral Glucocorticoid-Sparing Effect of Benralizumab in Severe Asthma. *New England Journal of Medicine*, 376(25):2448–2458, 2017.
- [129] Jaclyn A. Shepard Neiman, Ritu Raman, Vincent Chan, Mary G. Rhoads, Micha Sam B. Raredon, Jeremy J. Velazquez, Rachel L. Dyer, Rashid Bashir, Paula T. Hammond, and Linda G. Griffith. Photopatterning of hydrogel scaffolds coupled to filter materials using stereolithography for perfused 3d culture of hepatocytes. *Biotechnology and Bioengineering*, 112(4):777–787, 2015.
- [130] Yuri Nikolsky, Evgeny Sviridov, Jun Yao, Damir Dosymbekov, Vadim Ustyan-sky, Valery Kaznacheev, Zoltan Dezso, Laura Mulvey, Laura E. Macconail, Wendy Winckler, Tatiana Serebryiskaya, Tatiana Nikolskaya, and Kornelia Polyak. Genome-wide functional synergy between amplified and mutated genes in human breast cancer. *Cancer Research*, 68(22):9532–9540, 2008.
- [131] M Nishida, K Kasahara, M Kaneko, H Iwasaki, and K Hayashi. [establishment of a new human endometrial adenocarcinoma cell line, ishikawa cells, containing estrogen and progesterone receptors]. *Nihon Sanka Fujinka Gakkai zasshi*, 37(7):1103–1111, July 1985.
- [132] Daniela Nitsch, Joana P. Gonçalves, Fabian Ojeda, Bart de Moor, and Yves Moreau. Candidate gene prioritization by network analysis of differential expression using machine learning approaches. *BMC Bioinformatics*, 11(1):460, Sep 2010.
- [133] Kevin G. Osteen, George A. Hill, Joel T. Hargrove, and Fred Gorstein. Development of a method to isolate and culture highly purified populations of stromal and epithelial cells from human endometrial biopsy specimens. *Fertility and Sterility*, 52(6):965–72, Dec 1989.

- [134] Cuiping Pan, Chanchal Kumar, Sebastian Bohl, Ursula Klingmueller, and Matthias Mann. Comparative Proteomic Phenotyping of Cell Lines and Primary Cells to Assess Preservation of Cell Type-specific Functions. *Molecular & Cellular Proteomics*, 8(3):443–450, 2009.
- [135] J. Patterson and Jeffrey A. Hubbell. Enhanced proteolytic degradation of molecularly engineered peg hydrogels in response to mmp-1 and mmp-2. *Biomaterials*, 31(30):7836 – 7845, 2010.
- [136] Jingyu Peng, Yuexin Zhou, Shiyu Zhu, and Wensheng Wei. High-throughput screens in mammalian cells using the CRISPR-cas9 system. *FEBS Journal*, 282(11):2089–2096, 2015.
- [137] Mariana M. Pereira, Taciana P. Sant’Ana Santos, Roque Aras, Ricardo D. Couto, Maria Luiza B. Sousa Atta, and Ajax M. Atta. Serum levels of cytokines and chemokines associated with cardiovascular disease in brazilian patients treated with statins for dyslipidemia. *International Immunopharmacology*, 18(1):66 – 70, 2014.
- [138] Janet Piñero, Àlex Bravo, Núria Queralt-Rosinach, Alba Gutiérrez-Sacristán, Jordi Deu-Pons, Emilio Centeno, Javier GarcíÀña-GarcíÀña, Ferran Sanz, and Laura I. Furlong. Disgenet: a comprehensive platform integrating information on human disease-associated genes and variants. *Nucleic Acids Research*, 45(D1):D833–D839, 2017.
- [139] Janet Piñero, Núria Queralt-Rosinach, Àlex Bravo, Jordi Deu-Pons, Anna Bauer-Mehren, Martin Baron, Ferran Sanz, and Laura I. Furlong. Disgenet: a discovery platform for the dynamical exploration of human diseases and their genes. *Database*, 2015:bav028, 2015.
- [140] T. T. Piltonen, J. Chen, D. W. Erikson, T. L. B. Spitzer, F. Barragan, J. T. Rabban, H. Huddleston, J. C. Irwin, and L. C. Giudice. Mesenchymal stem/progenitors and other endometrial cell types from women with polycystic ovary syndrome (pcos) display inflammatory and oncogenic potential. *The Journal of Clinical Endocrinology & Metabolism*, 98(9):3765–3775, 2013.
- [141] Wenlian Qiao, Gerald Quon, Elizabeth Csaszar, Mei Yu, Quaid Morris, and Peter W. Zandstra. PERT: a method for expression deconvolution of human blood samples from varied microenvironmental and developmental conditions. *PLoS Computational Biology*, 8(12):e1002838, Jan 2012.
- [142] G. P. Raeber, M. P. Lutolf, and J. A. Hubbell. Molecularly engineered PEG hydrogels: A novel model system for proteolytically mediated cell migration. *Biophysical Journal*, 89(2):1374–1388, 2005.
- [143] Nilufer Rahmioglu, Amelie Fassbender, Allison F. Vitonis, Shelley S. Tworoger, Lone Hummelshoj, Thomas M. D’Hooghe, G. David Adamson, Linda C. Giudice, Christian M. Becker, Krina T. Zondervan, and Stacey A. Missmer. World

- Endometriosis Research Foundation Endometriosis Phenome and Biobanking Harmonization Project: III. Fluid biospecimen collection, processing, and storage in endometriosis research. *Fertility and Sterility*, 102(5):1233–1243, 2014.
- [144] J C Rain, L Selig, H De Reuse, V Battaglia, C Reverdy, S Simon, G Lenzen, F Petel, J Wojcik, V Schächter, Y Chemama, a Labigne, and P Legrain. The protein-protein interaction map of *Helicobacter pylori*. *Nature*, 409(6817):211–215, 2001.
- [145] Dilip Rajagopalan and Pankaj Agarwal. Inferring pathways from gene lists using a literature-derived network of biological relationships. *Bioinformatics*, 21(6):788–793, 2005.
- [146] Jordan A. Ramilowski, Tatyana Goldberg, Jayson Harshbarger, Edda Kloppman, Marina Lizio, Venkata P. Satagopam, Masayoshi Itoh, Hideya Kawaji, Piero Carninci, Burkhard Rost, and Alistair R. R. Forrest. A draft network of ligand-receptor-mediated multicellular signalling in human. *Nature Communications*, 6:7866, 2015.
- [147] Manjula Reddy, Cuc Davis, Jackson Wong, Paul Marsters, Charles Pendley, and Uma Prabhakar. Modulation of CLA, IL-12R, CD40L, and IL-2R $\alpha$  expression and inhibition of IL-12- and IL-23-induced cytokine secretion by CNTO 1275. *Cellular Immunology*, 247(1):1 – 11, 2007.
- [148] Mary C. Regier, Lindsey J. Maccoux, Emma M. Weinberger, Keil J. Regehr, Scott M. Berry, David J. Beebe, and Elaine T. Alarid. Transitions from mono- to co- to tri-culture uniquely affect gene expression in breast cancer, stromal, and immune compartments. *Biomedical Microdevices*, 18(4), 2016.
- [149] Jan C. Rieckmann, Roger Geiger, Daniel Hornburg, Tobias Wolf, Ksenya Kveler, David Jarrossay, Federica Sallusto, Shai S. Shen-Orr, Antonio Lanzavecchia, Matthias Mann, and Felix Meissner. Social network architecture of human immune cells unveiled by quantitative proteomics. *Nature Immunology*, (August 2016):1–14, 2017.
- [150] Jean-François Rual, Kavitha Venkatesan, Tong Hao, Tomoko Hirozane-Kishikawa, Amélie Dricot, Ning Li, Gabriel F. Berriz, Francis D. Gibbons, Matija Dreze, Nono Ayivi-Guedehoussou, Niels Klitgord, Christophe Simon, Mike Boxem, Stuart Milstein, Jennifer Rosenberg, Debra S. Goldberg, Lan V. Zhang, Sharyl L. Wong, Giovanni Franklin, Siming Li, Joanna S. Albala, Janghoo Lim, Carlene Fraughton, Estelle Llamosas, Sebiha Cevik, Camille Bex, Philippe Lamesch, Robert S. Sikorski, Jean Vandenhaute, Huda Y. Zoghbi, Alex Smolyar, Stephanie Bosak, Reynaldo Sequerra, Lynn Doucette-Stamm, Michael E. Cusick, David E. Hill, Frederick P. Roth, and Marc Vidal. Towards a proteome-scale map of the human protein-protein interaction network. *Nature*, 437(7062):1173–1178, 2005.

- [151] Lois A. Salamonsen and L. J. Lathbury. Endometrial leukocytes and menstruation. *Human reproduction update*, 6(1):16–27, 2000.
- [152] John A. Sampson. Peritoneal endometriosis due to the menstrual dissemination of endometrial tissue into the peritoneal cavity. *American Journal of Obstetrics and Gynecology*, 14(4):422, 1927.
- [153] Claudia Scheerer, Petia Bauer, Vito Chiantera, Jalid Sehoul, Andreas Kaufmann, and Sylvia Mechsner. Characterization of endometriosis-associated immune cell infiltrates (emaici). *Archives of Gynecology and Obstetrics*, 294(3):657–664, Sep 2016.
- [154] Sarah B. Schrier, Abby S. Hill, Deborah Plana, and Douglas A. Lauffenburger. Synergistic Communication between CD4+ T Cells and Monocytes Impacts the Cytokine Environment. *Scientific Reports*, 6(June):1–11, 2016.
- [155] B Schwikowski, P Uetz, and S Fields. A network of protein-protein interactions in yeast. *Nature biotechnology*, 18(12):1257–1261, 2000.
- [156] Kathy L. Sharpe-Timms. Endometrial anomalies in women with endometriosis. *Annals of the New York Academy of Sciences*, 943(1):131–147, 2001.
- [157] Shai S Shen-Orr, Ofir Goldberger, Yael Garten, Yael Rosenberg-Hasson, Patricia A Lovelace, David L Hirschberg, Russ B Altman, Mark M Davis, and Atul J Butte. Towards a cytokine-cell interaction knowledgebase of the adaptive immune system. *Pacific Symposium on Biocomputing. Pacific Symposium on Biocomputing*, pages 439–50, 2009.
- [158] Steven Simoens, Gerard Dunselman, Carmen Dirksen, Lone Hummelshoj, Attila Bokor, Iris Brandes, Valentin Brodzsky, Michel Canis, Giorgio Lorenzo Colombo, Thomas DeLeire, Tommaso Falcone, Barbara Graham, Gulden Halis, Andrew Horne, Omar Kanj, Jens Jørgen Kjer, Jens Kristensen, Dan Lebovic, Michael Mueller, Paola Vigano, Marcel Wullschleger, and Thomas D’Hooghe. The burden of endometriosis: costs and quality of life of women with endometriosis and treated in referral centres. *Human Reproduction*, 27(5):1292–1299, 2012.
- [159] K. H. Spencer, M. Y. Kim, C. C. W. Hughes, and E. E. Hui. A screen for short-range paracrine interactions. *Integr. Biol.*, 6:382–387, 2014.
- [160] Ulrich Stelzl, Uwe Worm, Maciej Lalowski, Christian Haenig, Felix H. Brembeck, Heike Goehler, Martin Stroedicke, Martina Zenkner, Anke Schoenherr, Susanne Koeppen, Jan Timm, Sascha Mintzlaff, Claudia Abraham, Nicole Bock, Silvia Kietzmann, Astrid Goedde, Engin Toksoz, Anja Droege, Sylvia Krobitsch, Bernhard Korn, Walter Birchmeier, Hans Lehrach, and Erich E. Wanker. A human protein-protein interaction network: A resource for annotating the proteome. *Cell*, 122(6):957 – 968, 2005.

- [161] Aravind Subramanian, Pablo Tamayo, Vamsi K Mootha, Sayan Mukherjee, and Benjamin L Ebert. Gene set enrichment analysis : A knowledge-based approach for interpreting genome-wide. *Proc Natl Acad Sci U S A*, 2005.
- [162] Damian Szklarczyk, Andrea Franceschini, Stefan Wyder, Kristoffer Forslund, Davide Heller, Jaime Huerta-Cepas, Milan Simonovic, Alexander Roth, Alberto Santos, Kalliopi P. Tsafou, Michael Kuhn, Peer Bork, Lars J. Jensen, and Christian von Mering. String v10: protein-protein interaction networks, integrated over the tree of life. *Nucleic Acids Research*, 43(D1):D447–D452, 2015.
- [163] Daolin Tang, Rui Kang, Carolyn B. Coyne, Herbert J. Zeh, and Michael T. Lotze. Pamps and damp: signal 0s that spur autophagy and immunity. *Immunological Reviews*, 249(1):158–175, 2012.
- [164] Christopher J. Tape, Stephanie Ling, Maria Dimitriadi, Kelly M. McMahon, Jonathan D. Worboys, Hui Sun Leong, Ida C. Norrie, Crispin J. Miller, George Poulgiannis, Douglas A. Lauffenburger, and Claus Jørgensen. Oncogenic KRAS Regulates Tumor Cell Signaling via Stromal Reciprocation. *Cell*, 165(4):910–920, 2016.
- [165] Christopher J. Tape, Ida C. Norrie, Jonathan D. Worboys, Lindsay Lim, Douglas A. Lauffenburger, and Claus Jørgensen. Cell-specific Labeling Enzymes for Analysis of Cell-Cell Communication in Continuous Co-culture. *Molecular & Cellular Proteomics*, 13(7):1866–1876, 2014.
- [166] Nadja Tariverdian, Theoharis C Theoharides, Friederike Siedentopf, Gabriela Gutiérrez, Udo Jeschke, Gabriel a Rabinovich, Sandra M Blois, and Petra C Arck. Neuroendocrine-immune disequilibrium and endometriosis: an interdisciplinary approach. *Seminars in immunopathology*, 29(2):193–210, Jun 2007.
- [167] P R Taylor, L Martinez-Pomares, M Stacey, H-H Lin, G D Brown, and S Gordon. Macrophage receptors and immune recognition. *Annual review of immunology*, 23:901–44, jan 2005.
- [168] U. Thiruchelvam, I. Dransfield, P. T. K. Saunders, and H. O. D. Critchley. The importance of the macrophage within the human endometrium. *Journal of Leukocyte Biology*, 93(2):217–225, 2013.
- [169] P Uetz, L Giot, Gerard Cagney, T a Mansfield, R S Judson, J R Knight, D Lockshon, V Narayan, M Srinivasan, P Pochart, a Qureshi-Emili, Y Li, B Godwin, D Conover, T Kalbfleisch, G Vijayadamodar, M Yang, M Johnston, S Fields, and J M Rothberg. A comprehensive analysis of protein-protein interactions in *Saccharomyces cerevisiae*. *Nature*, 403(6770):623–627, 2000.
- [170] Hendrik Ungefroren, Martina Voss, Martina Jansen, Christian Roeder, Doris Henne-Bruns, Bernd Kremer, and Holger Kalthoff. Human pancreatic adenocarcinomas express fas and fas ligand yet are resistant to fas-mediated apoptosis. *Cancer Research*, 58(8):1741–1749, 1998.

- [171] Jorge Valdez, Christi D. Cook, Caroline Chopko Ahrens, Alex J. Wang, Alexander Brown, Manu Kumar, Linda Stockdale, Daniel Rothenberg, Kasper Renggli, Elizabeth Gordon, Douglas A. Lauffenburger, Forest M. White, and Linda G. Griffith. On-demand dissolution of modular, synthetic extracellular matrix reveals local epithelial-stromal communication networks. *Biomaterials*, 130:90–103, 2017.
- [172] Koen Van der Borgh, Geert Verbeke, and Herman van Vlijmen. Multi-model inference using mixed effects from a linear regression based genetic algorithm. *BMC Bioinformatics*, 15(1):88, Mar 2014.
- [173] Fabio Vandin, Patrick Clay, Eli Upfal, and Benjamin J. Raphael. *Discovery of mutated subnetworks associated with clinical data in cancer*, pages 55–66. WORLD SCIENTIFIC, 2012.
- [174] Oron Vanunu, Oded Magger, Eytan Ruppin, Tomer Shlomi, and Roded Sharan. Associating genes and protein complexes with disease via network propagation. *PLOS Computational Biology*, 6(1):1–9, 01 2010.
- [175] P. Vercellini, L. Fedele, G. Aimi, G. Pietropaolo, D. Consonni, and P.G. Crosignani. Association between endometriosis stage, lesion type, patient characteristics and severity of pelvic pain symptoms: a multivariate analysis of over 1000 patients. *Human Reproduction*, 22(1):266–271, 2007.
- [176] Allison F. Vitonis, Katy Vincent, Nilufer Rahmioglu, Amelie Fassbender, Germaine M. Buck Louis, Lone Hummelshoj, Linda C. Giudice, Pamela Stratton, and G. David Adamson for the WERF EPHeC Working Group. World Endometriosis Research Foundation Endometriosis Phenome and Biobanking Harmonisation Project: II. Clinical and covariate phenotype data collection in endometriosis research. *Fertility and Sterility*, 102(5):1223–1232, 2014.
- [177] Christian von Mering, Martijn Huynen, Daniel Jaeggi, Steffen Schmidt, Peer Bork, and Berend Snel. STRING: A database of predicted functional associations between proteins. *Nucleic Acids Research*, 31(1):258–261, 2003.
- [178] Slobodan Vukicevic, Hynda K. Kleinman, Frank P. Luyten, Anita B. Roberts, Nanette S. Roche, and A.H. Reddi. Identification of multiple active growth factors in basement membrane matrigel suggests caution in interpretation of cellular activity related to extracellular matrix components. *Experimental Cell Research*, 202(1):1–8, 1992.
- [179] Albertha J. M. Walhout, Raffaella Sordella, Xiaowei Lu, James L. Hartley, Gary F. Temple, Michael A. Brasch, Nicolas Thierry-Mieg, and Marc Vidal. Protein interaction mapping in *c. elegans* using proteins involved in vulval development. *Science*, 287(5450):116–122, 2000.

- [180] Jack D. Wang, El-Sayed Khafagy, Khalil Khanafer, Shuichi Takayama, and Mohamed E. H. ElSayed. Organization of endothelial cells, pericytes, and astrocytes into a 3D microfluidic in vitro model of the blood-brain barrier. *Molecular Pharmaceutics*, 13(3):895–906, 2016.
- [181] Christer Wingren, Anna Sandström, Ralf Segersvärd, Anders Carlsson, Roland Andersson, Matthias Löhr, and Carl A. K. Borrebaeck. Identification of serum biomarker signatures associated with pancreatic cancer. *Cancer Research*, 72(10):2481–2490, 2012.
- [182] Alejandro Wolf-Yadlin, Neil Kumar, Yi Zhang, Sampsa Hautaniemi, Muhammad Zaman, Hyung-Do Kim, Viara Grantcharova, Douglas A Lauffenburger, and Forest M White. Effects of her2 overexpression on cell signaling networks governing proliferation and migration. *Molecular Systems Biology*, 2(1), 2006.
- [183] Helen L. Wright, Roger C. Bucknall, Robert J. Moots, and Steven W. Edwards. Analysis of sf and plasma cytokines provides insights into the mechanisms of inflammatory arthritis and may predict response to therapy. *Rheumatology*, 51(3):451–459, 2012.
- [184] Steven W. Yancey, Hector G. Ortega, Oliver N. Keene, Bhabita Mayer, Necdet B. Gunsoy, Christopher E. Brightling, Eugene R. Bleecker, Pranabashis Haldar, and Ian D. Pavord. Meta-analysis of asthma-related hospitalization in mepolizumab studies of severe eosinophilic asthma. *Journal of Allergy and Clinical Immunology*, 139(4):1167–1175.e2, 2017.
- [185] Xunqin Yin, Mary Ellen Pavone, Zhenxiao Lu, JianJun Wei, and J. Julie Kim. Increased activation of the pi3k/akt pathway compromises decidualization of stromal cells from endometriosis. *The Journal of Clinical Endocrinology & Metabolism*, 97(1):E35–E43, 2012.
- [186] Wei-Dong Zhou, Hui-Ming Yang, Qin Wang, Dong-Yin Su, Fu-An Liu, Min Zhao, Qiong-Hua Chen, and Qing-Xi Chen. Sb203580, a p38 mitogen-activated protein kinase inhibitor, suppresses the development of endometriosis by down-regulating proinflammatory cytokines and proteolytic factors in a mouse model. *Human Reproduction*, 25(12):3110–3116, 2010.
- [187] Junmin Zhu. Bioactive modification of poly(ethylene glycol) hydrogels for tissue engineering. *Biomaterials*, 31(17):4639 – 4656, 2010.
- [188] Annelien J.M. Zweemer, Cory B. French, Joshua Mesfin, Simon Gordonov, Aaron S. Meyer, and Douglas A. Lauffenburger. Apoptotic Bodies Elicit Gas6-Mediated Migration of AXL-Expressing Tumor Cells. *Molecular Cancer Research*, 15(December):1656–1667, 2017.